



# A review of gold nanoparticle synthesis: Transitioning from conventional techniques to plant-mediated green nanofabrication

Truong Dinh <sup>\*</sup>, Zsolt Dobó, Árpád Bence Palotás, Helga Kovács

Institute of Energy, Ceramics and Polymer Technology, University of Miskolc, 3515, Miskolc, Hungary



## ARTICLE INFO

**Keywords:**  
Gold nanoparticles  
Synthesis  
Biosynthesis  
Plant-mediated synthesis

## ABSTRACT

Nowadays, gold nanoscience and nanotechnology are receiving significant attention owing to their unique material properties and an increasing range of applications. The distinctive characteristics of gold nanoparticles (AuNPs), such as non-toxicity, biocompatibility, and inertness, along with unique physical and chemical properties, make them ideal for numerous implementations across scientific research and multiple industries. Additionally, the continuously rising demand for AuNPs and the increasing global market share have spurred researchers to develop techniques for large-scale production. This review summarizes the different AuNPs production methods and achievements provided by various approaches through scientific publications. Although physical and chemical methods are predominant in the AuNP production industry, specific attention is being paid to biological AuNP fabrication due to there has been increasing focus on creating eco-friendly and green processes for gold nanoparticle production. Specifically, the use of living plants for AuNP synthesis has emerged as an environmentally friendly approach, offering promising solutions for sustainable AuNP production. This review highlights the significance of this plant-mediated synthesis and explores its potential as a viable method for AuNP fabrication, paving the way for further innovations in green nanotechnology.

## 1. Introduction

All matter in the universe is composed of atoms, which serve as fundamental building blocks. Depending on their size and arrangement, particles made of these atoms are categorized into three main groups [1]: coarse particles ( $\leq 10000$  nm), fine particles ( $\leq 2500$  nm), and ultrafine particles ( $\leq 100$  nm) (Fig. 1). Ultrafine particles, the smallest category, are referred to as nanoparticles [2]. The study of nanoparticles falls under the field of nanotechnology, which has been rapidly advancing in technology, engineering, and science [3,4]. First introduced by Japanese scientist Norio Taniguchi in 1974 [5], nanotechnology derives its prefix “nano” from the Greek word “nanos”, meaning “small”, with a reference scale of  $10^{-9}$  m. Nanoparticles are characterized by many unique physical and chemical properties due to their high surface-area-to-volume ratio [6]. Among the various types of nanoparticles, metallic ones such as Au, Ag, Pt, and Pd have garnered significant attention due to their wide range of applications. These nanoparticles are commonly utilized in environmental remediation, biosensing, nanomedicine, and energy storage, owing to their unique physicochemical properties [7]. For instance, Au and Ag nanoparticles

are widely used in biosensors and medical diagnostics [8–10], while Pt and Pd nanoparticles serve as highly efficient catalysts in fuel cells and hydrogen storage systems [11,12]. Additionally, their tunable optical and electronic properties make them valuable in the development of high-performance sensors, conductive inks, and advanced nanocomposites for emerging technologies [13].

Gold nanoparticles are a prominent example of metallic nanoparticles in material science [10]. They can be categorized into various types based on their size and shape [14,15], which are influenced by the synthesis methods employed. Fig. 2 illustrates various AuNPs morphologies, including nanospheres, nanoshells, nanoclusters, nanocages, nanorods, nanostars, nanowires, and nanobelts. Nanospheres are the simplest and most symmetric gold nanoparticles, characterized by their spherical geometry and uniform surface. They are typically synthesized via reduction of gold salts (such as HAuCl<sub>4</sub>) using citrate or similar reducing agents in aqueous solution. The size and uniformity are controlled by reaction conditions and the type of capping agent used [16]. Nanoshells consist of a dielectric core, coated with a thin outer shell of gold. They are produced by attaching gold seeds to the core surface, followed by additional gold salt reduction, which completes the

\* Corresponding author.

E-mail address: [truong.dinh@uni-miskolc.hu](mailto:truong.dinh@uni-miskolc.hu) (T. Dinh).

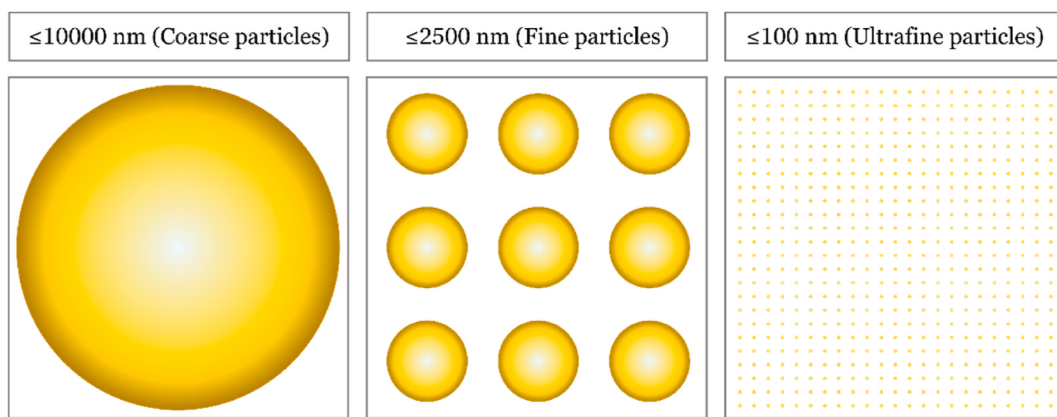


Fig. 1. Particle size classification, adapted from Ref. [1].

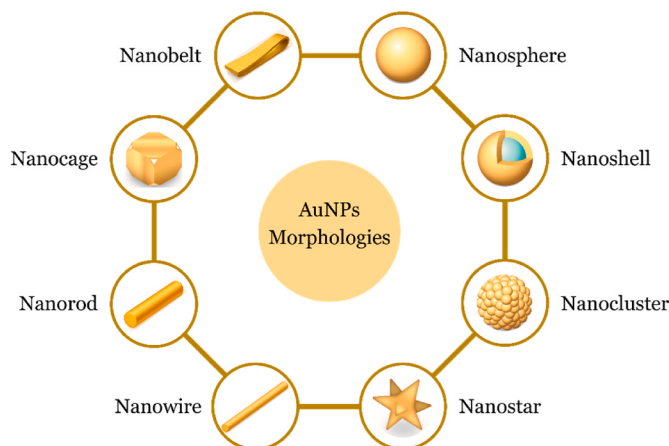


Fig. 2. Various morphologies of AuNPs, adapted from Ref. [28].

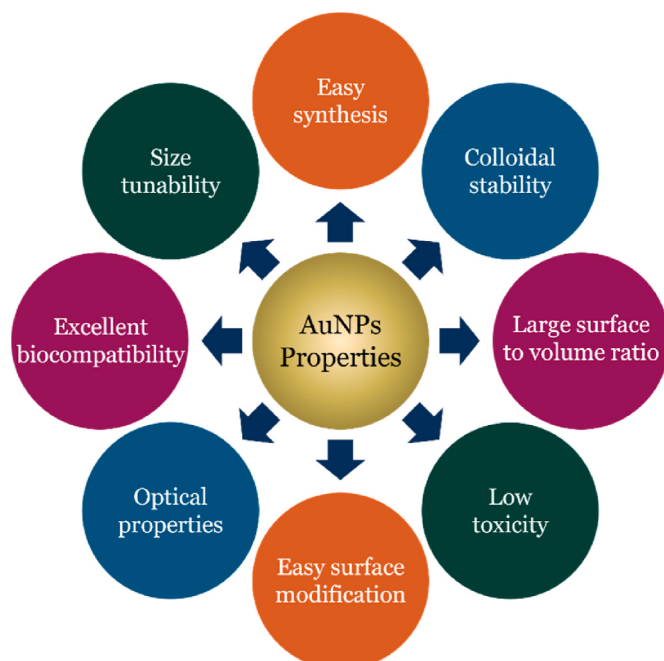
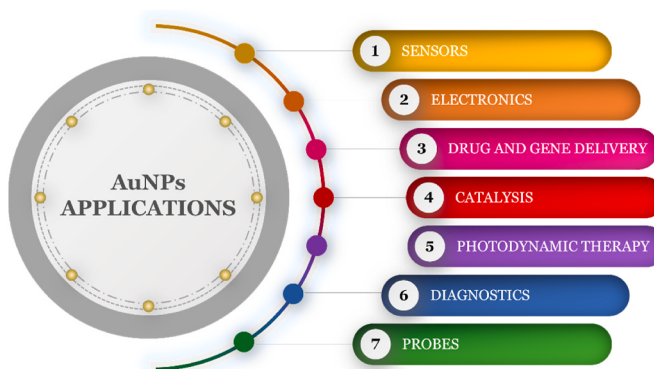


Fig. 3. Desirable properties of gold nanoparticles, adapted from Ref. [30].

shell [17,18]. Nanoclusters are ultrasmall assemblies, consisting of just a few to several tens of gold atoms, distinguished by their discrete electronic energy levels and unique quantum properties. They are synthesized by one-step reduction of gold salts in the presence of thiol ligands, which arrest further particle growth and stabilize the tiny clusters [19]. Nanocages are hollow, porous gold structures produced by galvanic replacement of silver nanocubes with gold ions. The wall thickness and porosity of the nanocages can be fine-tuned by manipulating the ratio of gold to silver reactants, giving these structures unique optical and drug delivery capabilities [20]. Nanorods are elongated particles whose length substantially exceeds their diameter, achieved using the seed-mediated growth method. This typically involves introducing gold seeds into a growth solution with a mild reducing agent and structure-directing surfactants, often with silver ions present to further promote elongation [21]. Nanostars, characterized by a central core with multiple sharp branches, are generated via seed-mediated growth with specific surfactants and additives. The branched structure significantly increases their surface area and enhances electromagnetic fields [22,23]. Nanowires are long, thin, one-dimensional gold structures ideal for catalysis and electronics. Their synthesis often involves chemical reduction of gold salts in deep eutectic solvents, which promote directional crystal growth [24,25]. Nanobelts are relatively rare among gold nanoparticle morphologies. They are formed through meticulous control of surfactant concentration, temperature, and reaction environment, yielding ultra-thin, belt-like structures with potential use in nanoelectronics and photonics [26,27].

The gold nanoparticles possess a set of physicochemical characteristics (Fig. 3) that make them highly versatile across various scientific and technological applications [29]. One of their significant advantages is their size adjustability, allowing precise control over their dimensions to fine-tune their optical and electronic properties for specific applications. Their exceptionally high surface-to-volume ratio enhances reactivity and adsorption capacity, making them ideal for catalysis, targeted drug delivery, and biosensing. Moreover, their intrinsic non-toxicity ensures safe use in biomedical applications without adverse effects on biological tissues, while their excellent biocompatibility further supports their role in drug delivery, imaging, and diagnostics. Another key attribute is their easy surface modification, as gold nanoparticles can be functionalized with a wide range of biomolecules, polymers, and ligands, thereby enhancing their specificity and performance in biosensors, targeted therapy, and molecular detection systems. Additionally, their easy synthesis enables large-scale production, supporting their widespread application across multiple disciplines. The essential physical properties of AuNPs, along with their surface plasmon resonance band, are dependent on their physiochemistry and morphology (temperature, core charge, surface ligands, solvent, and shape) [6]. The optical properties



**Fig. 4.** Applications of gold nanoparticles.

of AuNPs, influenced by these structural characteristics, offer the potential for their use as composite therapeutic agents in clinical applications. Adjusting nanoparticle size alters the color of colloidal AuNPs, a property used in colorimetric detection systems [6].

The applications of AuNPs are rapidly expanding across various fields [31–34], illustrated in Fig. 4 [35] and detailed as follows:

1. Sensors - Gold nanoparticles are widely used in sensor technology due to their unique optical and electronic properties. For instance, they are employed in colorimetric sensors for detecting food contaminants [36], such as pesticides, heavy metals, and bacterial toxins, through visible color shifts caused by AuNP aggregation [37]. Additionally, techniques such as surface-enhanced Raman spectroscopy utilize AuNPs as substrates to detect vibrational energies of chemical bonds, enabling the label-free detection of pollutants, proteins, and other molecules with high sensitivity [38].
2. Electronics - AuNPs play a crucial role in conductive materials, from printable inks to advanced electronic chip components [39]. As electronic devices become smaller, nanoparticles are essential in chip design, where AuNPs are utilized to connect resistors, conductors, and other electronic chip elements, improving electrical conductivity and device efficiency [40]. Furthermore, AuNP-based nanowires are being explored for use in flexible electronics, wearable devices, and high-performance sensors [41].
3. Drug and Gene Delivery - AuNPs are utilized in medicine for the delivery of drugs and genetic material [42,43]. AuNPs conjugated with therapeutic agents enhance the pharmacokinetics of free drugs, offering controlled and sustained release capabilities, making them valuable tools for drug and gene delivery [44]. Their high surface area-to-volume ratio allows conjugation with anti-fouling polymers, targeting agents, and therapeutics [45]. Notably, DNA-combined assembly AuNPs enhance gene transfection efficiency, advancing gene therapy while minimizing off-target effects [46].
4. Catalysis - AuNPs serve as catalysts in various chemical reactions due to their high surface reactivity [47]. They facilitate selective oxidation and reduction processes, such as nitrogen oxide reduction in environmental applications [48]. Their application in fuel cell technology offers promising solutions for enhancing energy conversion efficiency in clean energy development [49]. Additionally, AuNP-based catalysts have been used for organic synthesis, including carbon-carbon coupling reactions and oxidation processes [50].
5. Photodynamic Therapy - Gold nanoparticles, particularly those absorbing near-infrared light (such as nanorods and nanoshells), generate heat when exposed to light at wavelengths between 700 and 800 nm. This property is harnessed to target and destroy tumors in a process known as hyperthermia therapy [51]. When light is directed at a tumor containing AuNPs, they heat up rapidly, leading to localized destruction of tumor cells while minimizing damage to surrounding healthy tissues [52]. This method has shown promise in treating various types of cancer, including breast and prostate cancers [53].
6. Diagnostics - Gold nanoparticles are widely integrated into diagnostic tools for detecting infectious diseases, cancer biomarkers, and other medical conditions [54,55]. They are essential in lateral flow immunoassays, such as home pregnancy tests, providing high specificity and rapid results [56]. Additionally, AuNPs enhance biosensors for detecting viral infections, including SARS-CoV-2, improving diagnostic accuracy and speed [57].
7. Probes - AuNPs efficiently scatter light, producing distinct colors under dark-field microscopy. This property is exploited in biological imaging applications to visualize cells and molecular interactions in real-time [58,59]. Their high density also makes them effective contrast agents [60] in transmission electron microscopy, allowing for high-resolution imaging of cellular structures and biomolecules. Furthermore, AuNPs are utilized in fluorescence-based DNA and RNA detection, supporting advancements in molecular diagnostics [61].

The applications of AuNPs vary with their shape and size [62], as these physical characteristics influence their optical, electronic, and chemical properties. For instance, gold nanorods are widely employed in biosensors due to their unique optical properties, which enable the sensitive detection of biomolecules and disease markers [63]. In cancer therapy, gold nanorods play a crucial role in photothermal therapy, where they absorb near-infrared light and convert it into localized heat, effectively destroying cancer cells while minimizing damage to surrounding healthy tissues [64,65]. Additionally, gold nanorods are being explored for targeted drug delivery [66,67], serving as carriers for chemotherapeutic agents to facilitate controlled and site-specific release, thereby improving treatment efficacy and reducing systemic toxicity. Gold nanospheres are widely utilized in diagnostics, particularly in lateral flow assays such as pregnancy tests and rapid disease detection kits [68]. Their ability to enhance Raman signals also makes them valuable in surface-enhanced Raman spectroscopy (SERS)-based

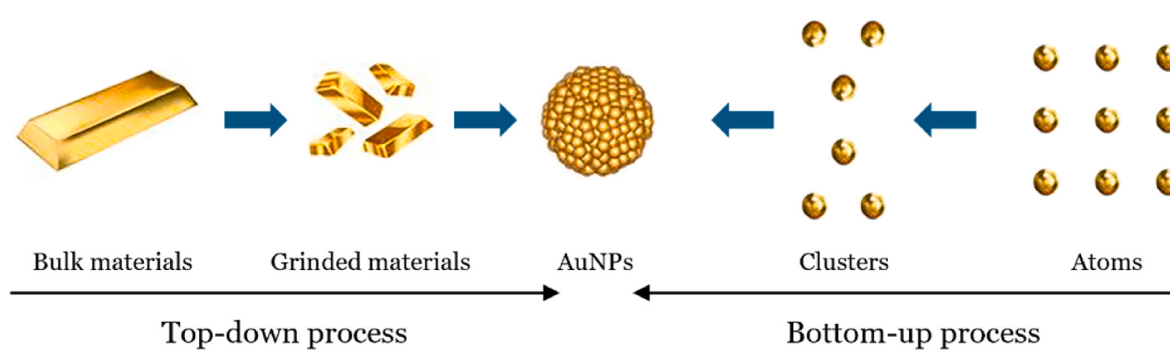


**Fig. 5.** Top-down and bottom-up approaches for the synthesis of AuNPs [5].

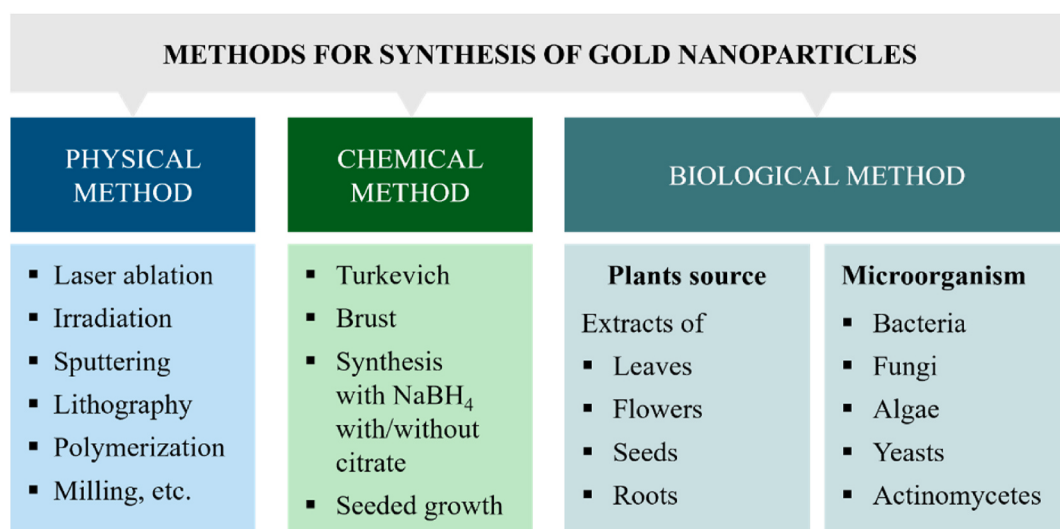


**Fig. 6.** Different methods for the synthesis of gold nanoparticles, adapted from Ref. [78].

biosensing, allowing for the detection of biomolecules at ultra-low concentrations [69]. Gold nanoshells are another type of AuNP shape with promising applications. Due to their tunable plasmonic resonance, they are extensively researched for use in photothermal therapy, where they generate heat upon near-infrared radiation to selectively destroy tumor cells [70]. Gold nanostars, with their sharp tips and branched structures, have gained attention for their use in surface-enhanced Raman spectroscopy applications, enabling highly sensitive molecular detection in medical diagnostics and environmental monitoring [71]. Gold nanoclusters consist of small, discrete groups of gold atoms with strong fluorescence properties. These nanoclusters are particularly beneficial in bioimaging and targeted drug delivery due to their small size and reduced cytotoxicity compared to larger nanoparticles [72]. Gold nanobubbles represent an innovative approach to targeted therapy. These hollow structures can be directed to specific areas, where they burst under laser or infrared-induced heat. They then gradually penetrate cancer cell walls, which helps inhibit cell growth [73].

## 2. General methods for synthesis of gold nanoparticles

AuNPs can be synthesized through physical, chemical, and biological methods, which are broadly classified into “bottom-up” and “top-down” synthesis [74]. In bottom-up methods, AuNPs are produced through the assembly of atoms or molecules, using techniques such as micro-emulsion synthesis, colloidal synthesis, sol-gel method, and chemical vapor deposition. Conversely, top-down approaches involve reducing the size of bulk materials using chemical and physical methods such as mechanical milling and laser ablation [75]. Fig. 5 illustrates the basic concepts of top-down and bottom-up approaches for AuNP synthesis.

The top-down method is known for its reliability, high controllability and consistency, and ease of use. However, it has drawbacks such as surface area defects, limited access in fabrication, high costs, and uncontrolled size distribution. On the other hand, the bottom-up approach is cost-effective, easy to handle, and provides high yield, though it faces challenges in controlling particle size, dispersity, and geometric shape. Compared to the top-down approach, bottom-up synthesis is more suitable for commercial production due to its high fabrication capacity and easier modifications to surface properties. Nonetheless, scaling up these two methods for industrial production presents several issues [76].

Various techniques within the two top-down and bottom-up approaches, including physical, chemical, and biological methods, are summarized in Fig. 6. Physical and chemical methods are predominant in AuNP synthesis; however, these processes utilize flammable chemicals and hazardous substances, consume high energy, and may deposit

**Table 1**

Comparison of physical, chemical, and biological methods for the synthesis of AuNPs [5].

Physical methods	Chemical methods	Biological methods
Less productivity	High productivity	High productivity
No use of toxic chemicals	Use of toxic chemicals	No use of toxic chemicals
Suitable for small-scale production	Suitable for small-scale production	Suitable for large-scale production
Difficult to control the size and shape	Controlled size and shape	Definite size and shape
Low stability	High stability	Low stability
High cost	Low cost	Effective cost

toxic materials on the nanoparticles, posing risks for pharmaceutical applications. In contrast, biological methods are more eco-friendly and easier to handle, as they do not use toxic chemicals, reducing agents, or stabilizers [5]. Each synthesis method has its own set of advantages and disadvantages [77], which are summarized in Table 1.

The properties of AuNPs, including size distribution, morphology, stability, purity, and biocompatibility, are significantly influenced by the synthesis method employed. AuNPs synthesized by physical methods are characterized by high purity because no chemical reagents or stabilizers are used in the process. These nanoparticles exhibit high crystallinity, stability, and clean surfaces, making them attractive for electronic applications sensitive to contamination. Nevertheless, physical methods often yield a wider size distribution and provide less precise control over nanoparticle shape and uniformity. Furthermore, these techniques are energy-intensive and costly, making them better suited for small-scale or specialized applications where high purity is critical [79–81]. In contrast, chemical methods offer better control over nanoparticle size and shape, and monodispersity. These approaches produce uniform spherical morphology AuNPs with narrow size distribution and high stability. Through careful adjustment of reagent concentrations and reaction conditions, it can produce nanoparticles with tailored optical and physicochemical properties. Nevertheless, these particles may contain residual reducing and capping agents, potentially affecting their biocompatibility and requiring further purification. This makes chemically synthesized nanoparticles ideal for catalysis and optical sensing, but less directly suited to clinical applications without additional processing [62,82,83]. On the other hand, biological methods are conducted under mild conditions without toxic chemicals, yielding AuNPs with diverse morphologies, good biocompatibility, and functionalized surfaces due to capping by biomolecules. These biosynthesized

**Table 2**  
Studies on the physical synthesis of AuNPs.

Method	Condition	AuNPs size (nm)	Morphology	Ref.
Sputter deposition	Sputtering gold into a liquid matrix containing thiolate ligand as a stabilizer	1.6–2.7	–	[86]
Sputter deposition	AuNPs were synthesized in a standard ionic liquid, 1-butyl-3-methylimidazolium tetrafluoroborate ( $[\text{C}_4\text{mim}]^+\text{BF}_4^-$ )	–	–	[87]
Sputter deposition	An argon pressure of 0.1 mbar, an electric current of 50 mA, a sputtering time of 60 s, and a target–substrate distance of 40 mm were applied	<2.5	Spherical	[88]
Laser ablation	Laser ablation in liquid method is utilized to synthesize AuNPs in water in a clean way.	5–35	Spherical	[89]
Laser ablation	AuNPs are fabricated employing pulsed laser ablation in water by varying the laser fluence.	10–15	Spherical	[90]
Laser ablation	AuNPs are prepared by pulsed laser ablation of a gold wire in liquid-flow and in the presence of highly diluted electrolytes.	6–30	–	[91]
Laser ablation	AuNPs are synthesized by laser ablation in organic solvents of acetonitrile ( $\text{CH}_3\text{CN}$ ), tetrahydrofuran (THF), and dimethylsulfoxide (DMSO)	1.8–2.5	–	[92]
Laser ablation	The formation of AuNPs is achieved via irradiation of the gold plate immersed in the liquid.	–	–	[93]
$\gamma$ -irradiation	AuNPs were fabricated by $\gamma$ -irradiation of HAuCl <sub>4</sub> using sodium alginate as a stabilizer.	5–40	–	[94]
$\gamma$ -irradiation	AuNPs were prepared by $\gamma$ -Co-60 irradiation using water-soluble chitosan as a stabilizer and size enlargement by the seed approach.	10–50	–	[95]
$\gamma$ -irradiation	AuNPs were synthesized by gamma Co-60 ray irradiation.	4–10	Spherical	[96]
$\gamma$ -irradiation	AuNPs were synthesized by irradiating the solution of HAuCl <sub>4</sub> and chitosan at 5, 10, and 15 kGy	27, 12, and 7	–	[97]
Microwave irradiation	Irradiation under 800 W of microwave, using quaternized carboxymethyl chitosan (QCMC) as a reducing and stabilizing reagent	10–50	Spheroidal	[98]
Microwave irradiation	Microwave radiation utilizing alkali-treated curdlan (CRD) as a reducing and stabilizing agent	1.5–2	Spherical	[99]
Microwave irradiation	HAuCl <sub>4</sub> in aqueous solution is irradiated	7.7	Spherical	[100]

**Table 2 (continued)**

Method	Condition	AuNPs size (nm)	Morphology	Ref.
Ultrasound irradiation	under 800 W of microwave.	–	–	
Ion implantation	Sonicating a mixture of AuCl <sub>3</sub> and dimethyl sulfoxide (DMSO)	15–40	Polyhedral	[101]
Lithography	Ion implantation combined with electron-beam irradiation	1.5–5	Crystalline	[102]
Polymerization	Optical lithography	30–40	Nanofilm	[103]
	Thermosensitive AuNPs were synthesized using plasma treatment and graft polymerization	15	Spherical	[104]
Milling	High-speed vibration milling, room temperature	6.3–27.8	Polyhedral	[105]
Thermal evaporation	Temperatures of 1523 and 1773 K	4–10	Nanofilm	[106]

nano particles are eco-friendly and non-toxic, making them attractive for drug delivery and diagnostic applications. However, they often exhibit greater size variability, less morphological control, and lower long-term stability compared to chemical methods because of the complex mixture of reductants present in biological extracts. Moreover, reproducibility remains a challenge in biosynthesis due to the complex and variable nature of biologically reducing agents [78,84,85]. Overall, physical methods produce exceptionally pure gold nanoparticles with high crystallinity but less size control; chemical methods provide excellent control over particle characteristics and offer stability, though with the risk of residual contaminants; and biological methods yield highly biocompatible nanoparticles, often with functionalized surfaces but less uniformity. The preferred synthesis method should be chosen according to the intended application, with trade-offs between precision, scalability, purity, and environmental safety.

### 3. Physical methods

The physical methods used for synthesizing AuNPs encompass a wide range of techniques, such as laser ablation, milling, thermal evaporation, irradiation ( $\gamma$ -irradiation, microwave irradiation, ultrasound irradiation), ion implantation, lithography, polymerization, sputter deposition, etc. (Table 2). Each physical method for synthesizing AuNPs has its own advantages and limitations, playing crucial roles in determining the most suitable synthesis technique for specific applications.

Sputtering involves depositing a thin nanoparticle layer followed by an annealing process. The effectiveness of this AuNPs synthesis method is influenced by various factors, including temperature, annealing duration, layer thickness, and type of substrate [79]. These variables significantly impact the size and morphology of the resulting nanoparticles [107].

Milling is another method that breaks down bulk materials into nanoscale structures through mechanical processes. In mechanical milling, the kinetic energy transferred from rollers or balls reduces the grain size of the bulk material. Factors such as the temperature, duration, intensity, milling media, and type of mill play pivotal roles in determining the shape and size of the nanoparticles produced [108].

Laser ablation involves irradiating a pure metal surface with a laser beam, generating a low-flux plasma plume that sublimates to form AuNPs. This technique offers rapid synthesis with precise control over particle size and shape, yielding high quantities and enhanced long-term stability [79]. By adjusting parameters such as laser pulse energy, wavelength, and ablation duration, the size of the AuNPs can be fine-tuned [109]. Moreover, laser ablation can be performed in both aqueous and organic solvents, facilitating its application in biomedical fields, such as the *in situ* conjugation of biomolecules with AuNPs [92].

**Table 3**  
Studies on the synthesis of AuNPs using the Turkevich method.

Gold precursor	Chemical used	AuNP size (nm)	Morphology	Ref.
95 mL of HAuCl <sub>4</sub> (containing 5 mg Au)	5 mL of 1 % sodium citrate	20	Spherical	[114]
50 mL of 0.2 % HAuCl <sub>4</sub>	0.5 mL of 1 % sodium citrate	16	Spherical	[115]
500 mL of 1 mM HAuCl <sub>4</sub>	50 mL of 38.8 mM sodium citrate	13	Spherical	[116]
500 mL of 0.01 % HAuCl <sub>4</sub>	7.5 mL of 1 % sodium citrate	18	Spherical	
240 mg of HAuCl <sub>4</sub> in 500 mL of water	50 mL of 1 % sodium citrate	12.6	–	[117]
500 mL of 1 mM HAuCl <sub>4</sub>	50 mL of a 38.8 mM sodium citrate	13	–	[118]
25 mL of 5.8 mM HAuCl <sub>4</sub>	25 cm <sup>3</sup> solution of the stabilizer sodium 3-mercaptopropionate and sodium citrate (2.0 %)	10	Spherical	[119]
100 mL of 0.01 % HAuCl <sub>4</sub>	4 mL of 1 % sodium citrate	10	Spherical	[120]
200 mL of 0.24 mM HAuCl <sub>4</sub>	0.94 mL of 0.34 M sodium citrate	15	–	[121]
40 mL of 0.5 M HAuCl <sub>4</sub>	160 mL of 0.5 M sodium citrate	40	Spherical	[122]
4 mL, 24.3 mM of HAuCl <sub>4</sub> -ethanol solution	100 mL of 1.0 mM tri-sodium citrate	4	Spherical	[123]
500 mL of 1 mM HAuCl <sub>4</sub>	50 mL of 38.8 mM sodium citrate	10	–	[124]
950 mL of 0.25 mM HAuCl <sub>4</sub>	50 mL of 1 % sodium citrate	18	Spherical	[125]
Solution of 0.165 mM HAuCl <sub>4</sub>	Sodium citrate	36.6	Spherical	[126]
Solution of 0.25 mM HAuCl <sub>4</sub>	Sodium citrate	17.8	Spherical	
20 mL of 1 mM HAuCl <sub>4</sub>	2 mL of 1 % trisodium citrate dehydrate	15	Spherical	[127]
50 mL of a 0.01 % solution of HAuCl <sub>4</sub> in deionized H <sub>2</sub> O	2 mL of 1 % sodium citrate	22.7	Spherical	[128]
HAuCl <sub>4</sub> (50 mL, 1 mg/mL)	Sodium citrate solution (2 mL, 1 mg/mL)	13	Spherical	[129]
100 mL of 5 mM HAuCl <sub>4</sub>	10 mL of 125 mM sodium citrate	5	Spherical	[130]
30 mL of 0.01 % HAuCl <sub>4</sub>	200 mL of 1 % sodium citrate	50	Spherical	[131]
0.1025 mL of 4 % HAuCl <sub>4</sub>	0.8484 mL of 1 % sodium citrate	16.4	Spherical	[132]
50 mL of 0.2 g of HAuCl <sub>4</sub>	4 mL of 10 g of sodium citrate	13	Spherical	[133]
50 mL of 1 mM HAuCl <sub>4</sub>	5 mL of 38.8 mM sodium citrate	21.61	Spherical	[134]
10 mg HAuCl <sub>4</sub> in 90 mL of deionized water	0.4–0.9 mL of 250 mM sodium citrate	50	–	[135]
25 mM HAuCl <sub>4</sub> added every 30 min for two cycles	2.18 mM sodium citrate	22, 105 and 186 nm for 1st, 13th, 16th	Spherical	[136]

In aqueous solutions, this method can efficiently modify the geometric shape, surface area, and biological and physical properties of AuNPs [110].

Radiation-induced synthesis approach utilizes ionizing radiation, such as X-rays and gamma to produce highly pure AuNPs. In this process, an aqueous solution undergoes radiolysis when exposed to radiation, leading to the formation of transient molecules that reduce metal ions to atoms, which subsequently aggregate into nanoparticles. Critical parameters for this method include system pH, solvent type, and radiation dose [79].

Microwave irradiation using citric acid as a reducing agent offers another efficient route for synthesizing AuNPs. This method accelerates the reduction process and promotes the formation of spherical gold nanoparticles [100].

Ion implantation is a potential technique for producing AuNPs. This has been widely used to produce nanocomposites with consistent and minimal impurities, along with desirable chemical and physical properties [111].

Thermal evaporation involves heating bulk gold to its evaporation point, allowing the vaporized atoms to condense onto a cooler substrate, forming nanoparticles. This method provides precise control over nanoparticle formation and distribution [112].

The summarized studies in this section (Table 2) demonstrate the versatility and range of physical techniques for synthesizing AuNPs. However, most reports focus on the procedural parameters without critically addressing limitations in scalability, reproducibility, and practical applicability. For example, while laser ablation provides fine control over particle properties, the studies often overlook its energy inefficiency and technical complexity, which may hinder its feasibility for broader application. Similarly, sputter deposition studies achieve ultra-small particles, but there is limited discussion on their high operational costs. Radiation methods offer cleaner synthesis, but the long-term stability of the produced nanoparticles remains poorly investigated. Studies using microwave and ultrasound irradiation report fast synthesis of AuNPs, while the consistency is inadequately discussed. Milling, lithography, and ion implantation can fabricate different forms

**Table 3 (continued)**

Gold precursor	Chemical used	AuNP size (nm)	Morphology	Ref.
50 mg HAuCl <sub>4</sub> in 510 mL water	45, 75, 90, or 180 mg of sodium citrate in 10 mL of water	32, 28, 22, and 17 nm, respectively	–	[137]
100 mL of 0.3 mM HAuCl <sub>4</sub>	706 mL of 0.17 M sodium citrate	14.6	Spherical	[138]
0.415 g of HAuCl <sub>4</sub> in 1 L of double-distilled nanopure water	100 mL of 1 % sodium citrate	13	–	[139]
3 mL of 5 mM HAuCl <sub>4</sub> in 54 mL of water	3 mL of 0.02 M sodium citrate	11.5	Spherical	[140]
25 mL of 1 mM HAuCl <sub>4</sub>	2.5 mL of 38.8 mM sodium citrate	15	–	[141]
25 mL of 1 mM HAuCl <sub>4</sub>	2.5 mL of 38.8 mM sodium citrate	30	Spherical	[142]
100 mL of 1 mM HAuCl <sub>4</sub>	5 mL of 1 wt% of trisodium citrate	21.75	Spherical	[143]
100 mL of 0.01 % (w/v) HAuCl <sub>4</sub>	4 mL of 1 % sodium citrate	15	Spherical	[144]
100 mL of 0.01 % (w/v) HAuCl <sub>4</sub>	1.5 mL of 1 % sodium citrate	25	Spherical	

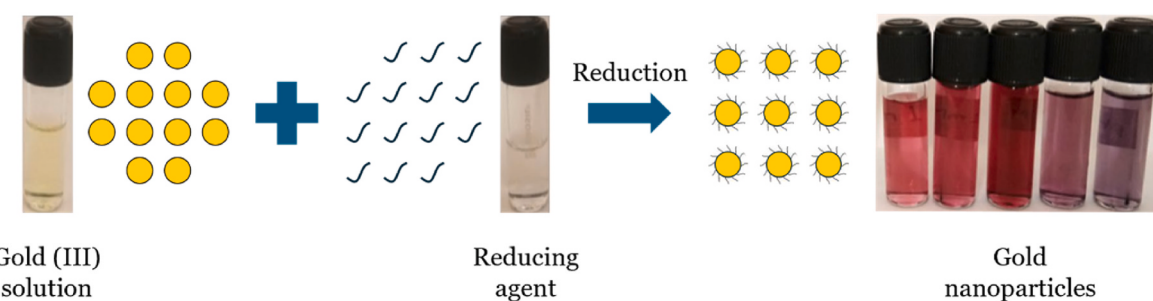


Fig. 7. Schematic diagram for chemical synthesis of AuNPs by the Turkevich method [30].

of AuNPs, but these methods lack precision in shape control and are unsuitable for biomedical applications due to contamination risks. Furthermore, comparisons between studies are hindered by the lack of standardized synthesis conditions and assessment metrics.

#### 4. Chemical methods

The chemical method involving the reduction of gold ions ( $\text{Au}^{3+}$ ) to neutral gold atoms ( $\text{Au}^0$ ) is widely employed for synthesizing gold nanoparticles. This synthesis process hinges on two critical factors of reduction and stabilization. Common reducing agents encompass acetylene, sulfites, formaldehyde, hydrogen peroxide, oxalic acids, polymers, sugars, sodium citrate, and sodium borohydride. Meanwhile, stabilizing agents typically include dendrimers, polymers, trisodium citrate, nitrogen/sulfur (thiolates)/oxygen-based ligands, and surfactants such as CTAB (cetyltrimethylammonium bromide) [113]. Similar to physical methods, several chemical approaches to AuNP synthesis have been developed, comprising the Turkevich method, synthesis with  $\text{NaBH}_4$  with/without citrate method, Brust method, and seeded growth method [2,62].

##### 4.1. Turkevich method

First introduced by Turkevich in 1951 [114], this method is one of the most prominent approaches for synthesizing spherical AuNPs ranging from 10 to 30 nm in size [30]. Turkevich's process relies on the reduction of a gold precursor using trisodium citrate as both a reducing and stabilizing agent. The synthesis involves heating the gold precursor solution to boiling, followed by the rapid addition of trisodium citrate solution under vigorous stirring. Factors such as incubation time, precursor concentration, reaction temperature, and pH also influence the AuNP size. Studies regarding this method are summarized in Table 3.

In the original Turkevich method, 95 mL of  $\text{HAuCl}_4$  solution containing 5 mg of gold was boiled [114]. Subsequently, 5 mL of 1 % sodium citrate solution was added under continuous mechanical stirring. The color of the solution changes from pale yellow to wine red, indicating the formation of AuNPs (Fig. 7), with an average size of approximately 20 nm.

After the fabrication disclosed by Turkevich, subsequent modifications refining the original method have been introduced. In 1973, Frens modified this method to control particle sizes by varying the concentration of reducing agents [115]. Higher citrate concentrations yield smaller AuNPs, while lower concentrations promote aggregation into larger particles. The author unveiled that 50 mL of 0.2 % boiling  $\text{HAuCl}_4$  mixed with 0.5 mL of 1 % sodium citrate for 5 min yielded 16 nm particles.

In 1997, Mayya et al. dissolved 240 mg of  $\text{HAuCl}_4$  (chloroauric acid) in 500 mL of water and brought the solution to a boil [117]. Afterward, 50 mL of 1 % sodium citrate was added, and boiling was maintained for 1 h, yielding particles with a size of 12.6 nm.

Yonezawa and Kunitake added 25 mL of 5.8 mM  $\text{HAuCl}_4$  to 250 mL of refluxing water, and the solution was boiled [119]. A 25 mL solution

**Table 4**  
Studies on the synthesis of AuNPs with  $\text{NaBH}_4$  with/without citrate.

Gold precursor	Chemical used	AuNP size (nm)	Morphology	Ref.
100 mL of 0.1 mM $\text{HAuCl}_4$	0.15 mM trisodium citrate; 1 mL of 0.05 M $\text{NaBH}_4$	6	Spherical	[145]
1 mL of 1 % $\text{HAuCl}_4$ in 90 mL of water	2 mL of 38.8 mM sodium citrate; 1.00 mL of 0.075 % $\text{NaBH}_4$ in 38.8 mM sodium citrate	15–60	–	[146]
100 mL of 0.1 mM $\text{HAuCl}_4$	0.01 g of $\text{NaBH}_4$	7	Spherical	[147]
1 mL of 1 % $\text{HAuCl}_4$ in 90 mL of water	2 mL of 38.8 mM sodium citrate; 1.00 mL of 0.075 % $\text{NaBH}_4$ in 38.8 mM sodium citrate	13	–	[148]
50 mL of 0.25 mM $\text{HAuCl}_4$ containing NaCl	2 mL of 1 % sodium citrate; 0.5 mL of 0.25 % $\text{NaBH}_4$ containing 1 % sodium citrate	19	Spherical	[149]
0.25 mL of 0.01 M $\text{HAuCl}_4$	0.25 mL of 0.01 M Na-citrate; 0.3 mL of 0.1 M $\text{NaBH}_4$	3.5	Spherical	[150]
10 mg of $\text{HAuCl}_4$ in 100 mL of deionized water	1.891 g of $\text{NaBH}_4$ in 500 mL of deionized water	30	Spherical	[151]
0.27 mM $\text{HAuCl}_4$	1.1 mL of 1 wt% tri-sodium citrate; 5.5 mL solution of 0.08 wt% $\text{NaBH}_4$ and 1 wt% sodium citrate	7.5	Spherical	[152]
100 mL of 1 mM $\text{HAuCl}_4$	8 mL of 38.8 mM sodium citrate; 3 mL of 100 mM $\text{NaBH}_4$	24.5	Spherical	[153]
100 mL of 0.01 % (w/v) $\text{HAuCl}_4$	0.645 mL of 1 % sodium citrate; 3 mL of 0.1 M $\text{NaBH}_4$	4	–	[154]

containing 2.0 % sodium citrate and stabilizer sodium 3-mercaptopropionate (with a stabilizer-to-gold ratio of 0.1) was then injected. The solution's color transitioned from yellow to red or brown, producing nanoparticles with an average size of 10 nm.

In 2003, Seitz et al. synthesized AuNPs by adding 40 mL of 0.5 M  $\text{HAuCl}_4$  to 10 mL of distilled water, resulting in a solution of 2 mM  $\text{HAuCl}_4$  [122]. Then, 10 mL of an 8 mM sodium citrate solution was added to the boiling  $\text{HAuCl}_4$  solution. The mixture, initially grey, slowly turned light red after 1 h of boiling and cooling to room temperature. The resulting particles measured 40 nm in diameter.

Yang et al. added 4 mL of 24.3 mM  $\text{HAuCl}_4$  in ethanol to a boiling solution of 100 mL of 1.0 mM trisodium citrate under vigorous stirring [123]. Within 30 s, the solution turned purple-red and was rapidly cooled in an ice bath and concentrated to 20 mL under vacuum. The synthesized gold nanoparticles were measured at 4 nm in size.

In 2003, Huang et al. synthesized AuNPs by boiling 500 mL of 1 mM

**Table 5**  
Studies on the synthesis of AuNPs using the Brust method.

Gold precursor	Chemical used	AuNP size (nm)	Morphology	Ref.
30 mL of 30 mM HAuCl <sub>4</sub>	TOAB (Tetraoctylammonium bromide) in toluene (80 mL, 50 mM); dodecanethiol (170 mg); NaBH <sub>4</sub> (25 mL, 0.4 mM)	1–3	Spherical	[155]
HAuCl <sub>4</sub> (120 mL, 4 mM)	TOAB (5.5 g, 10 mM) in 240 mL toluene; chlorobenzene-methanethiol (0.32 g, 2 mM); 0.8 g NaBH <sub>4</sub> in 50 mL water	3.2–3.4	Spherical	[156]
20:1 M ratio of n-Dodecanethiol/HAuCl <sub>4</sub> into ethanol (60 mL, 95 %); HAuCl <sub>4</sub> (1.5 mL, 0.103 M)	Dodecanethiol; NaBH <sub>4</sub> (2 mL, 2 %)	10	Polyhedral	[157]
HAuCl <sub>4</sub> (0.39 g, 1 mM) in 40 mL of nanopure water	TOAB (1.09 g, 2 mM) in 160 mL toluene; NaBH <sub>4</sub> (0.38 g, 10 mM)	5	Spherical	[158]
310 mg of HAuCl <sub>4</sub> in 25 mL nano-pure water	1.5 g of TOAB in 80 mL toluene; 17 L of 1-decanethiol; 0.38 g of NaBH <sub>4</sub> in 25 mL nano-pure water	3.76	Spherical	[159]
HAuCl <sub>4</sub> (1 mL, 10 mM)	20 mg of TOAB in 20 mL of toluene; 1 mg of NaBH <sub>4</sub>	10	Spherical	[160]
30 mM HAuCl <sub>4</sub>	25 mM TOAB in 80 mL of toluene; 0.4 M NaBH <sub>4</sub>	5–15	Spherical	[161]
34 mM HAuCl <sub>4</sub>	34 mM TOAB; NaBH <sub>4</sub>	1.7–1.9	Spherical	[162]
HAuCl <sub>4</sub> (30 mL, 30 mM)	TOAB (80 mL, 25 mM); NaBH <sub>4</sub> (25 mL, 0.4 M)	5.5	Spherical	[163]
HAuCl <sub>4</sub> (0.39 g, 1.0 M) in 40 mL of nanopure H <sub>2</sub> O	TOAB (1.09 g, 2 mM) in 160 mL of toluene; NaBH <sub>4</sub> (0.38 g, 10 mM)	3.4	Spherical	[164]
HAuCl <sub>4</sub> (30 mL, 30 mM)	TOAB (80 mL, 25 mM); NaBH <sub>4</sub> (25 mL, 0.4 M); DMAP (4-(N,N-dimethylamino pyridine))	20	Spherical	[165]
0.45 mM HAuCl <sub>4</sub> in 15 mL of purified water	1 mM TOAB in 40 mL of toluene; 0.45 mM dodecanethiol; 5 mM NaBH <sub>4</sub> in 12 mL of water	1.8	Spherical	[166]
HAuCl <sub>4</sub> (6 mL, 0.03 M)	Solution of TOAB in toluene (6 mL, 0.15 M); NaBH <sub>4</sub> (6 mL, 0.26 M)	5.2	Spherical	[167]
100 mL of 0.05 M HAuCl <sub>4</sub> in 1 M HCl was added to 10 mL of deionized water	0.1 mL of 0.05 M NaBH <sub>4</sub> in 1 M NaOH; 0.1 g dodecanethiol in 5 g n-hexane	3.75	Spherical	[168]
HAuCl <sub>4</sub> x 3H <sub>2</sub> O, 50 mg, 0.12 mM	TOAB (500 mg, 0.9 mM), NaBH <sub>4</sub> (50 mg, 1.3 mM)	2–3	–	[169]
HAuCl <sub>4</sub> (60 mL, 10 mM)	TOAB (160 mL, 7.5 mM); mercaptopropionic acid (20 mL, 30 mM); NaBH <sub>4</sub> (60 mL, 6 mM)	2	Spherical	[170]
HAuCl <sub>4</sub> (30 mL, 30 mM)	TOAB (80 mL, 50 mM); pentanethiol (170 mg, 0.84 mM); NaBH <sub>4</sub> (25 mL, 0.4 M)	5	Spherical	[171]
300 mg HAuCl <sub>4</sub> in 30 mL deionized water	2 g TOAB in 80 mL toluene; NaBH <sub>4</sub> (25 mL, 0.4 M); 2.4 L dodecanethiol	5	Spherical	[172]
HAuCl <sub>4</sub> (0.25 g, 0.64 mM) in 13 mL nitrogen-sparged water	TOAB (0.4 g, 0.73 mM) in 17 mL toluene; triphenylphosphine (0.58 g, 2.21 mM); NaBH <sub>4</sub> (0.35 g, 9.4 mM, 10 mL)	2.8	Spherical	[173]
HAuCl <sub>4</sub> (3 mL, 0.03 M)	Solution of TOAB in toluene (8 mL, 0.05 M); Dodecanethiol (17 mg); NaBH <sub>4</sub> (2.5 mL, 0.4 M)	3–4	Spherical	[174]
HAuCl <sub>4</sub> (160 mL; 5.18 mM)	Toluene solution of TOAB (160 mL, 0.02 M); 1-hexanethiol (0.016 M); NaBH <sub>4</sub> (160 mL, 0.0674 M)	2	Spherical	[175]

HAuCl<sub>4</sub> in a 1 L round-bottom flask with vigorous stirring [124]. After the rapid addition of 50 mL of 38.8 mM sodium citrate, the solution's color changed from pale yellow to wine-red. Boiling continued for 10 min, and stirring persisted as the solution cooled to room temperature, yielding 10 nm particles.

In another study, 950 mL of a 0.25 mM HAuCl<sub>4</sub> solution was boiled under reflux [125]. By adding 50 mL of 1 % sodium citrate into the boiling solution, AuNPs with a size of 18 nm were fabricated.

Ojea-Jiménez et al. investigated the effect of reagent addition sequence on synthesized AuNPs [126]. In the direct method, 149 mL of an aqueous HAuCl<sub>4</sub> solution (0.165 or 0.25 mM) was heated to 100 °C for 15 min, and 1 mL of sodium citrate (0.34 or 0.26 mM, respectively) was added. In the inverse method, the sodium citrate solution was heated for 15 min before adding 1 mL of HAuCl<sub>4</sub>. The direct method yielded particles of 36.6 nm and 17.8 nm for 13.6 and 6.8 SC/HAuCl<sub>4</sub> ratios, respectively. The inverse method produced particles of 9 nm and 14.9 nm for the same ratios. Other synthesis procedures using the Turkevich method are depicted in Table 3.

#### 4.2. Synthesis with NaBH<sub>4</sub> with/without citrate

To perform AuNP fabrication under milder circumstances, particularly without the need for heating, the Turkevich method was adapted by adding sodium borohydride (NaBH<sub>4</sub>) [79]. This approach allows control over the size and distribution of nanoparticles by modifying the gold-to-citrate molar ratio and reaction conditions. A summary of the relevant studies is presented in Table 4.

Wang et al. prepared an aqueous solution of HAuCl<sub>4</sub> (0.1 mM, 100 mL) and trisodium citrate (0.15 mM) [145]. Subsequently, 1 mL of 0.05 M sodium borohydride solution was rapidly added under constant stirring. The mixture was stirred for 2 h, yielding 6 nm particles.

In another experiment, Aryal et al. reduced 100 mL of 0.1 mM

HAuCl<sub>4</sub> solution with 0.01 g NaBH<sub>4</sub> at room temperature, producing ruby-red gold hydrosol with an average nanoparticle size of 7 nm [147].

Kalimuthu and John added HAuCl<sub>4</sub> (1 mL, 1 %) to 90 mL of water at room temperature [148]. Afterward, sodium citrate (2 mL, 38.8 mM) was injected into the chloroauric acid solution, followed by adding sodium borohydride (1 mL, 0.075 %) in 38.8 mM sodium citrate. The mixture was stirred for 5 min, producing 13 nm particles.

In the synthesis by Zhao et al., 50 mL of 0.25 mM HAuCl<sub>4</sub> in an aqueous solution containing NaCl was cooled and mixed with 2 mL of 1 % sodium citrate and 0.5 mL of 0.25 % NaBH<sub>4</sub> (with 1 % sodium citrate). The resulting AuNPs measured 19 nm in diameter [149].

Kesik et al. mixed 9.5 mL of deionized water, 0.25 mL of 0.01 M HAuCl<sub>4</sub>, and 0.25 mL of 0.01 M sodium citrate [150]. Next, 0.3 mL of 0.1 M ice-cold sodium borohydride was added, leading to a pink solution. The mixture was left undisturbed for 3 h, resulting in 3.5 nm spherical AuNPs.

Iqbal et al. dissolved 10 mg of HAuCl<sub>4</sub> in 100 mL of 0.25 mM deionized water. A 0.1 M NaBH<sub>4</sub> solution (prepared by dissolving 1.891 g in 500 mL deionized water) was added dropwise to the HAuCl<sub>4</sub> solution under 750 rpm stirring. After centrifugation, 30 nm particles were achieved [151].

Shajkumar et al. mixed HAuCl<sub>4</sub> (107.4 mg, 0.27 mM) with deionized water [152]. Subsequently, 11 mL of 1 % tri-sodium citrate was added, followed by the injection of 5.5 mL of 0.08 % NaBH<sub>4</sub> and 1 % sodium citrate. The solution was stirred for 10 min, producing 7.5 nm particles.

Chaudhary and Garg mixed 100 mL of 1 mM HAuCl<sub>4</sub> with 8 mL of 38.8 mM sodium citrate [153]. Following that, 3 mL of 100 mM ice-cold sodium borohydride was injected dropwise under constant stirring. The solution was stirred for 24 h and centrifuged at 2500 rpm for 5 min, yielding 24.5 nm particles.

Wang et al. synthesized 4 nm AuNPs by adding sodium citrate (0.645 mL, 1 %) to HAuCl<sub>4</sub> (100 mL, 0.01 %) under vigorous stirring. After 3

min, 3 mL of 0.1 M ice-cold NaBH<sub>4</sub> was added, and the solution was stirred for 30 min to obtain the nanoparticles [154]. Other synthesis approaches are presented in Table 4.

#### 4.3. Brust method

This technique was first disclosed by Brust in 1994 [155]. It is employed to produce small-sized AuNPs (1.5–5 nm), with narrow dispersity and thermal stability using organic solvents [30]. The two-phase process involves transferring an aqueous gold precursor to an organic solvent, such as toluene, by utilizing a phase-transfer agent like tetraoctylammonium bromide (TOAB). Following that, the reduction stage is conducted using sodium borohydride in the presence of alkanethiols. The transition of the organic phase color from orange to brown indicates the formation of AuNPs. By varying the ratio of thiol to gold, the particle size and dispersity can be finely controlled. A summary of the related studies is provided in Table 5.

In the original Brust method [155], a 30 mL aqueous solution of 30 mM HAuCl<sub>4</sub> was mixed with TOAB in toluene (80 mL, 50 mM). After vigorous stirring, the tetrachloroaurate was transferred to the organic layer. Dodecanethiol (170 mg) was then added, followed by the gradual addition of NaBH<sub>4</sub> (25 mL, 0.4 M) under continuous stirring. After 3 h, the organic phase was separated, evaporated to 10 mL, and mixed with 400 mL of ethanol to eliminate excess thiol. The mixture was kept at -18 °C for 4 h, leading to the precipitation of a dark brown solid, which was filtered and washed with ethanol. The crude product was redissolved in 10 mL of toluene and reprecipitated with 400 mL of ethanol, yielding AuNPs with an average size of 2.5 nm.

In an adaptation by Kim et al., 120 mL of HAuCl<sub>4</sub> solution (1.6 g, 4 mM) was mixed with TOAB (5.5 g, 10 mM) in 240 mL of toluene and stirred for 2 min [156]. Chlorobenzenemethanethiol (0.32 g, 2 mM) in toluene was then added, followed by 0.8 g NaBH<sub>4</sub> in 50 mL of water. After 3 h of stirring, the toluene phase was separated, and the volume was reduced to 30 mL. Precipitation in 500 mL of methanol and subsequent washing with 400 mL of methanol yielded AuNPs with a size range of 3–4 nm.

Prahraj et al. added 1 mL of 10 mM HAuCl<sub>4</sub> to 20 mg of TOAB in 20 mL of toluene [160]. After shaking, the AuCl<sub>4</sub><sup>-</sup> ions were transferred to the organic phase. The solution was divided into two vials containing cetyltrimethylammonium chloride and cetyltrimethylammonium bromide. After stirring, 1 mg of sodium borohydride was added to each, turning the solution wine red. The size of the gold nanoparticles synthesized was 10 nm.

Ghosh et al. synthesized AuNPs using sodium borohydride as a reducing agent and DMAP (4-(N, N-dimethylaminopyridine)) as a stabilizer [165]. A 30 mL of 30 mM HAuCl<sub>4</sub> solution was mixed with an 80 mL toluene solution of 25 mM TOAB, leading to the transition of the AuCl<sub>4</sub><sup>-</sup> ions to the organic phase. By adding 25 mL of 0.4 M NaBH<sub>4</sub> solution with vigorous stirring, the organic phase changed from light yellow to wine red. After 30 min, the organic phase was washed with sulfuric acid (0.1 M), sodium hydroxide (0.1 M), and water, then dried over anhydrous sodium sulfate. DMAP (0.98 g) was added to precipitate the AuNPs, which were washed and resuspended in water, yielding AuNPs with a particle size of 20 nm.

Wang et al. combined 6 mL of 0.03 M HAuCl<sub>4</sub> with 6 mL of TOAB in 0.15 M toluene [167]. The aqueous phase turned colorless, and the organic phase became orange. After 10 min of stirring, 6 mL of 0.26 M NaBH<sub>4</sub> was injected dropwise over 30 min. The organic phase was separated, washed with sulfuric acid (1 %) and water, dried with MgSO<sub>4</sub>, and filtered, producing 5.2 nm particles.

In another AuNP synthesis study, Kuroda et al. used 3-mercaptopropionic acid (MPA) instead of alkanethiols [170]. First, a solution of HAuCl<sub>4</sub> (60 mL, 10 mM) with 7.5 mM TOAB in 160 mL toluene was stirred for 10 min. Afterward, 20 mL of 30 mM MPA was added, followed by the addition of sodium borohydride (60 mL, 6 mM). The mixture was then stirred overnight, leading to the formation of MPA-protected

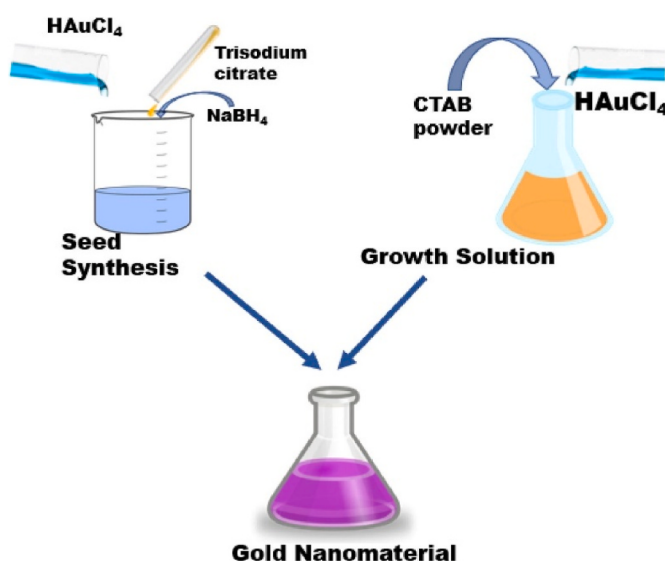


Fig. 8. Schematic representation of the seeded-growth method for synthesis of AuNPs [80].

AuNPs (2 nm). Other synthesis approaches modifying the Brust method are presented in Table 5.

#### 4.4. Seeded growth method

The seeded growth method enables the synthesis of narrowly sized gold nanoparticles (5–40 nm) in various shapes, including tubes, cubes, rods, and spheres [30]. This approach is characterized by its simplicity, cost-effectiveness, and rapidity, comprising two main steps: seed formation and seed growth. Initially, a strong reducing agent (e.g., NaBH<sub>4</sub>) is used to produce small seed particles from a gold precursor. These seed particles are subsequently introduced into a solution containing weak reducing agents (e.g., sodium citrate or ascorbic acid) and structure-directing agents. By adjusting the concentrations of seed particles, reducing agents, and structural additives, a wide variety of AuNP shapes and sizes can be synthesized.

The seeded-growth method was depicted in detail by Jana et al. [176] (Fig. 8). The process begins with preparing a 20 mL aqueous solution containing 0.25 mM HAuCl<sub>4</sub> and 0.25 mM trisodium citrate in a conical flask. Then, 0.6 mL of freshly prepared, ice-cold 0.1 M sodium borohydride is added while stirring. The solution turns pink instantly, indicating the formation of nanoparticles. The particles in this solution are utilized as seeds within 2–5 h post-preparation. In this step, citrate acts solely as a capping agent rather than a reducing agent, as it is not able to reduce gold salt at room temperature.

For the growth phase, 6 g of 0.08 M cetyltrimethylammonium bromide (CTAB) is added to 200 mL of 0.25 mM HAuCl<sub>4</sub> solution. The mixture is heated until it becomes a clear orange solution, which is then cooled to room temperature and employed as the stock growth solution.

Four sets of 50 mL conical flasks, labeled A, B, C, and D, are prepared as follows:

1. Set A: 7.5 mL of growth solution is combined with 0.05 mL of 0.1 M ascorbic acid. Subsequently, 2.5 mL of seed solution is added while stirring. The mixture is stirred for an additional 10 min after the solution turns wine red. The resulting particles are spherical, with a diameter of 5.5 nm.
2. Set B: 9 mL of growth solution is mixed with 0.05 mL of 0.1 M ascorbic acid, followed by the addition of 1 mL of seed solution under vigorous stirring. The mixture is stirred for 10 min, yielding a deep red solution. The particles formed are spherical, with a diameter of 8 nm. These particles are used as seeds for set C within 30 min.

**Table 6**

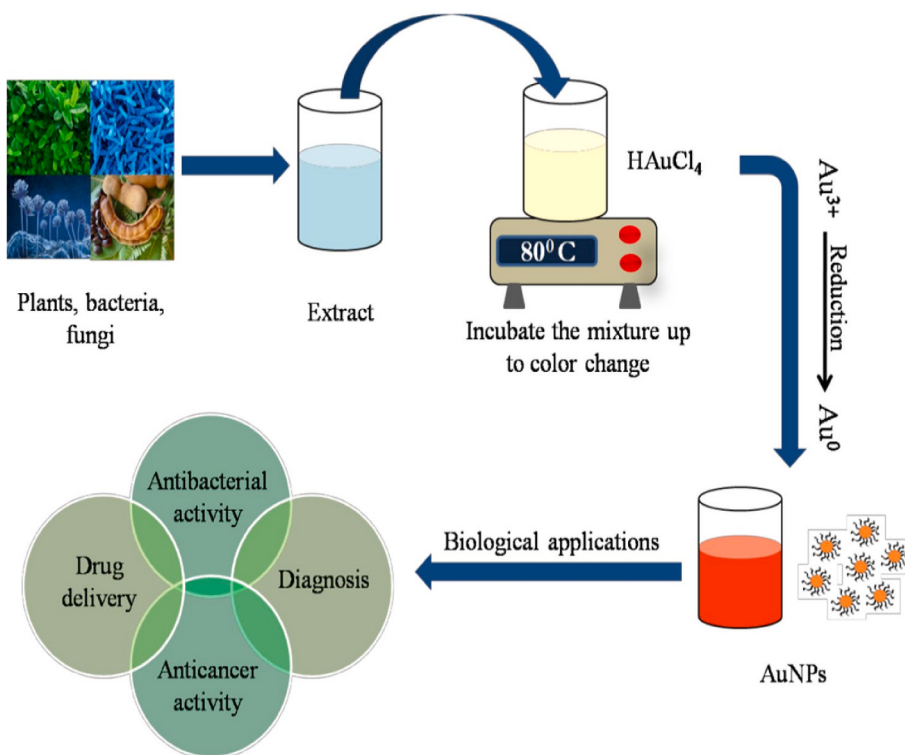
Studies on the chemical synthesis of AuNPs using the seeded growth method.

Seed solution	Growth solution	AuNP size (nm)	Morphology	Ref.
20 mL solution of 0.25 mM HAuCl <sub>4</sub> and 0.25 mM trisodium citrate; NaBH <sub>4</sub> (0.6 mL, 0.1 M)	HAuCl <sub>4</sub> (200 mL, 0.25 mM); cetyltrimethylammonium bromide CTAB (0.6 g, 0.08 M)	5.5–37	Spherical	[176]
20 mL solution containing HAuCl <sub>4</sub> (2 mg, 2.5 mM) and trisodium citrate (1.5 mg, 2.5 mM); NaBH <sub>4</sub> (0.6 mL, 0.1 M)	HAuCl <sub>4</sub> (5 mg, 50 mL, 0.25 mM); 1,2-Bis(10,12-tricosadiynoyl)-sn-glycero-3-phosphocholine (46 mg)	1.5–30	Spherical	[177]
Au <sup>4+</sup> ions and NaBH <sub>4</sub> (0.6 mL, 0.01 M) in CTAB (5 mL, 0.2 M)	CTAB (5 mL, 0.2 M), HAuCl <sub>4</sub> (5 mL, 1 mM), AgNO <sub>3</sub> (0.25 mL, 4 mM), and ascorbic acid (70 μL, 8 mM)	32.6	Nanorods	[178]
AgNO <sub>3</sub> (1 mL, 10 mM); HCl (2 mL, 1 M); ascorbic acid (0.8 mL, 0.1 M)	100 mL solution of 0.5 mM HAuCl <sub>4</sub> and 0.1 M CTAB	50	Nanobipyramids	[179]
AgNO <sub>3</sub> (0.02 mL, 0.1 mM); ascorbic acid (0.1 mL, 0.1 M)	20 mL solution of 0.25 mM HAuCl <sub>4</sub> , 0.1 M CTAB, 0.2 mL acetone, and 0.32 mL cyclohexane	10	Anisotropic	[180]
HAuCl <sub>4</sub> (0.05 mL, 50 mM); CTAB (10 mL, 0.1 M); NaBH <sub>4</sub> (0.60 mL, 10 mM)	CTAB (100 mL, 0.10 M); AgNO <sub>3</sub> (1 mL, 0.008 M); HAuCl <sub>4</sub> (1 mL, 50 mM); HNO <sub>3</sub> (1.0 mL, 2 M); ascorbic acid (0.6 mL, 0.1 M)	86	Nanodumbbells	[181]
HAuCl <sub>4</sub> (100 mL, 0.01 %); 1 % sodium citrate	Sodium citrate (0.22 mL, 1 %) and HAuCl <sub>4</sub> (100 mL, 0.01 %); hydroquinone (1 mL, 30 mM)	4–40	—	[154]
HAuCl <sub>4</sub> (1 mL, 0.023 M) in 99 mL water; trisodium citrate (10 mL, 0.014 M)	HAuCl <sub>4</sub> (24 mL, 2.3 mM)	18–60	Spherical	[182]
HAuCl <sub>4</sub> (50 mL, 0.015 mM); sodium citrate (20 mL, 0.1 M); NaBH <sub>4</sub> (0.6 mL, 0.01 M)	HAuCl <sub>4</sub> (200 mL, 0.05 mM); CTAB (40 mL, 0.1 mM); ascorbic acid (0.5 mL, 0.1 M)	31.41–47.86	Spherical	[183]

- Set C: 9 mL of growth solution and 0.05 mL of 0.1 M ascorbic acid are mixed, followed by the addition of 1 mL from set B under vigorous stirring. The solution is stirred for 10 min, resulting in a reddish-brown color solution containing roughly spherical nanoparticles with a diameter of 17 nm. This solution is utilized as a seed for set D within 30 min post-preparation.
- Set D: The growth solution (9 mL) is combined with ascorbic acid (0.05 mL, 0.1 M). Next, 1 mL from set C is added while stirring vigorously. The stirring continues for 10 min, resulting in a brown solution. The particles formed are a mixture of rods (with an average minor axis of 17 nm and a major axis of 200 nm) and spheres (37 nm in diameter). The solutions in sets A, B, C, and D remain stable for over a month due to the stabilizing effect of CTAB.

Other studies utilizing the seeded growth technique typically adopt the procedure proposed by Jana et al. [176], with minor modifications, as illustrated in Table 6.

While these chemical methods demonstrate effective control over nanoparticle morphology, most studies neglect to evaluate key aspects such as reproducibility, purity, and byproduct formation. For instance, although the Turkevich method (Table 3) is simple, scalable, and extensively cited, it typically yields spherical particles only and involves relatively high temperatures, limiting its versatility. In addition, the reproducibility of this technique under different laboratory conditions and scale-up feasibility remains unaddressed. The NaBH<sub>4</sub>-based reductions (Table 4) enable room temperature synthesis and smaller particle sizes, but they often result in broader size distributions and raise concerns over NaBH<sub>4</sub> toxicity. The Brust method (Table 5), though, is

**Fig. 9.** Synthesis of AuNPs using bioagents (microorganisms and plant extracts) [30].

**Table 7**  
Possible mechanisms of AuNPs synthesis from biogenic agents [5].

Biogenic agent	Possible mechanism
Plant derivatives (leaves, roots, flowers, barks, seeds)	Phytochemicals such as alkaloids, flavonoids, saponins, and steroids act as reducing and capping agents.
Algae (macro algae, micro algae)	Polysaccharides with hydroxyl groups and other functional groups accelerate the reduction and stabilization of AuNPs.
Fungi	Intracellularly or extracellularly enzymes reduce the metal ions.
Yeast	Oxidoreductases and quinones in the membrane act as reducing agents.
Bacteria	The microbial cell reduces gold ions in the presence of NADH-dependent reductase or nitrate-dependent reductase.

suitable for organic solvents and yields stable small AuNPs; the toxicity and environmental hazards of organic solvents and phase transfer agents like TOAB are insufficiently investigated in the referenced studies. While seeded growth methods (Table 6) are widely adopted for anisotropic AuNPs, the influence of seed quality on the final particle uniformity is insufficiently explored in these studies. Overall, the reviewed chemical methods are experimentally effective but require more scrutiny regarding purity, scalability, and applicability.

## 5. Biological methods

Traditional physical and chemical techniques for synthesizing AuNPs involve toxic chemicals and high temperatures, posing risks to both the environment and human health. In contrast, biological synthesis approaches are emerging as an eco-friendlier alternative. These methods are also simple, rapid, and cost-effective, making them ideal for large-scale production. Furthermore, biosynthesis is biocompatible, safe for clinical applications, and aligns with the growing demand for environmentally sustainable technologies in nanotechnology and biotechnology [184].

Biosynthesis can utilize either biological agents or living plants to produce gold nanoparticles [185,186]. Biological agents, including microorganisms and plant extracts, serve as both reducing and stabilizing agents, facilitating the reduction of gold salts, such as HAuCl<sub>4</sub>, into nanoparticles [6,187]. On the other hand, living plants accumulate gold from soils through a process known as phytomining [188,189]. In this process, plants absorb soluble gold salts and subsequently reduce metallic ions, leading to the biosynthesis of nanoparticles [190].

### 5.1. Synthesis of gold nanoparticles using biological agents

Biological agents used in AuNP synthesis include microorganisms (e.g., fungi, yeast, bacteria, and actinomycetes) and plant extracts derived from various sources such as flowers, peels, roots, bark, fruits, stems, and leaves. The solution of precursor gold salt is treated with either microorganisms or plant extracts, leading to its bioreduction and the formation of AuNPs. Fig. 9 illustrates the biogenic synthesis of AuNPs using microorganisms and plant extracts, while Table 7 outlines the mechanisms involved in their synthesis.

#### 5.1.1. Synthesis by microorganisms

The biosynthesis of gold nanoparticles through microorganisms, including actinomycetes, algae, fungi, bacteria, etc., has garnered significant attention in industrial microbiology due to its numerous advantages [184]. These microorganisms offer an eco-friendly, cost-effective, and easily manageable approach for AuNP production. Their ability to adsorb and bio-reduce metal ions into nanoparticles makes them highly attractive [191]. AuNP biosynthesis can occur either extracellularly or intracellularly, depending on the specific microbial processes. Typically, microbial cultures are introduced to gold

**Table 8**  
Studies regarding the synthesis of AuNPs using microorganisms.

Name	Genus	Size of AuNPs (nm)	Morphology	Ref.
<i>Escherichia coli</i>	Bacteria	5–20	—	[193]
<i>Escherichia coli DH5α</i>	Bacteria	10	—	[194]
<i>Escherichia coli</i> PTCC 1330	Bacteria	10	Spherical	[195]
<i>Escherichia coli</i> ATCC 8739, <i>Bacillus subtilis</i> ATCC 6633	Bacteria	13	Spherical	[196]
<i>Streptomyces</i> sp	Bacteria	5–50	Polygonal	[197]
<i>Streptomyces clavuligerus</i>	Bacteria	8.2	Spherical	[198]
<i>Streptomyces nopalater</i>	Bacteria	14.5	Spherical	[199]
<i>Rhodopseudomonas capsulata</i>	Bacteria	10–20	Spherical	[200]
<i>Rhodopseudomonas capsulata</i>	Bacteria	10–20	Spherical	[201]
<i>Rhodococcus</i> species	Bacteria	5–15	Spherical	[202]
<i>Stenotrophomonas maltophilia</i>	Bacteria	40	Oval	[203]
<i>Marinobacter pelagius</i>	Bacteria	10	Mostly spherical with nano triangles	[204]
<i>Geobacillus</i> sp. strain ID17	Bacteria	5–50	Quasi-hexagonal	[205]
<i>Sporosarcina Koreensis</i>	Bacteria	92.4	Spherical	[206]
<i>Deinococcus radiodurans</i>	Bacteria	43.75	Spherical, triangular, and irregular	[207]
<i>Leptothrix</i> (iron-oxidizing bacteria)	Bacteria	5	Spherical	[208]
<i>Bacillus marisflavi</i> YCIS MN 5	Bacteria	14	Spherical	[209]
<i>Vibrio alginolyticus</i>	Bacteria	100–150	Irregular	[210]
<i>Staphylococcus aureus</i>	Bacteria	6–30	Spherical	[211]
<i>Fusarium oxysporum</i>	Fungi	22–30	Spherical and hexagonal	[212]
<i>Fusarium solani</i>	Fungi	40–45	Spindle	[213]
<i>Candida albicans</i>	Fungi	20–80	Spherical, non-spherical	[214]
<i>Candida albicans</i>	Fungi	4–10	Spherical	[215]
<i>Penicillium</i> sp.	Fungi	45–50	Spherical	[216]
<i>Penicillium brevicompactum</i>	Fungi	25–60	Spherical	[217]
<i>Trichoderma viride</i>	Fungi	2–500	Spherical, triangular, hexagonal, pentagonal, and nanosheet	[218]
<i>Trichoderma hamatum</i> SU136	Fungi	5–30	Spherical, pentagonal, and hexagonal	[219]
<i>Aspergillus clavatus</i>	Fungi	20–35	Triangular	[220]
<i>Aspergillus terreus</i> IF0	Fungi	10–19	Spherical	[221]
<i>Verticillium</i> sp.	Fungi	2–20	—	[222]
<i>Fusarium oxysporum</i>	Fungi	2–50	—	[222]
<i>Rhizopus oryzae</i>	Fungi	10	Spherical	[223]
<i>Cladosporium oxysporum</i>	Fungi	72.32	Quasi-spherical	[224]
<i>Alternaria</i> sp.	Fungi	7–93	Spherical, quasi-spherical, rod, square, pentagonal, and hexagonal	[225]
<i>Ganoderma lucidum</i>	Fungi	15–40	Multi-shaped structures	[226]
<i>Shewanella</i> algaee	Algae	9.6 100–200	Nanoplates	[227]
<i>Dunaliella salina</i>	Algae	22.4	Spherical	[228]
<i>Ecklonia cava</i>	Algae	30	Spherical and triangular	[229]
<i>Gracilaria verrucosa</i>	Algae	20–80	Spherical, oval, octahedral, rhombus, pentagonal, and triangular	[230]
<i>Candida guilliermondii</i>	Yeast	50–70	Spherical	[231]

(continued on next page)

**Table 8** (continued)

Name	Genus	Size of AuNPs (nm)	Morphology	Ref.
<i>Magnusiomyces ingens</i> LH-F1	Yeast		Spherical, triangular, and hexagonal	[232]
<i>Saccharomyces cerevisiae</i>	Yeast	9.18	Spherical	[134]

precursors, facilitating nanoparticle synthesis, after which the nanoparticles are isolated and purified through downstream processing techniques. The characteristics of the synthesized AuNPs, such as size and morphology, can be fine-tuned by adjusting key microbial growth parameters [192]. Table 8 summarizes various studies on AuNP biosynthesis using microorganisms.

**5.1.1.1. Synthesis by bacteria.** Bacteria are promising candidates for nanoparticle biosynthesis owing to their resilience in extreme conditions, rapid proliferation, and widespread availability. Both actinomycetes and prokaryotic bacteria have been extensively employed for AuNP synthesis, occurring either extracellularly or intracellularly. The presence of biomolecules such as sugars, fatty acids, and enzymes in bacterial cells facilitates the reduction of metal ions into stable nanoparticles. Numerous studies have reported the biosynthesis of AuNPs using different bacteria such as *Pseudomonas aeruginosa* [233], *Lactobacillus* [234], *Escherichia coli* [235], etc.

He et al. explored the extracellular biosynthesis of AuNPs utilizing the bacterium *Rhodopseudomonas capsulata*. Their study revealed that pH plays a crucial role in determining nanoparticle morphology. When the bacterial biomass was incubated with an aqueous HAuCl<sub>4</sub> solution at different pH levels (ranging from 7 to 4), spherical AuNPs ranging from 10 to 20 nm were formed at pH 7, while numerous nanoplates appeared at pH 4 [201]. Similarly, Nadaf and Kanase reported extracellular AuNP synthesis using *Bacillus marisflavi* YCIS MN 5. When gold chloride solution was introduced into a cell-free extract of the bacterium, crystalline spherical AuNPs approximately 14 nm in size were produced at room temperature within 96 h. The bacterial extract functioned as both a reducing and stabilizing agent, eliminating the need for additional capping or stabilizing agents [209].

Ahmad et al. investigated the intracellular biosynthesis of gold nanoparticles employing *Rhodococcus* species, which is a novel alkali-tolerant actinomycete. Upon exposure to chloroauric acid, the bacterial cells rapidly reduced gold ions, resulting in highly monodisperse AuNPs (5–15 nm) on the cytoplasmic membrane, as confirmed by TEM imaging. The biosynthesized AuNPs exhibited no effects on the cells, allowing microbial growth to continue despite nanoparticle production [202]. Correa-Llantén et al. studied intracellular AuNP biosynthesis utilizing *Geobacillus* sp. strain ID17, a thermophilic bacterium. When bacterial cells were introduced to Au<sup>3+</sup> ions, the bacterial culture transitioned from a colorless to a deep purple, indicating intracellular gold nanoparticle formation. TEM analysis confirmed the presence of quasi-hexagonal gold nanoparticles ranging from 5 to 50 nm in size [205]. Sharma et al. employed *Marinobacter pelagius*, a marine bacterium with high salt tolerance and resistance to metal ion toxicity, for AuNP biosynthesis. The TEM analysis revealed the formation of mono-disperse, stable AuNPs (~10 nm) upon exposure to chloroauric acid [204].

While bacteria present a promising approach for AuNP biosynthesis, several challenges hinder their large-scale application. Maintaining bacterial cultures can be labor-intensive, requiring careful handling to prevent contamination. Additionally, the biosynthesis process is relatively slow, often taking hours to days to yield nanoparticles. These limitations make bacteria not a preferable option for industrial-scale AuNP production.

**5.1.1.2. Synthesis by fungi.** In recent decades, a wide range of fungi has been explored for their potential role in the biosynthesis of nanoparticles, including gold nanoparticles. Fungi are commonly used in this process due to their ability to secrete large quantities of enzymes, which have numerous beneficial applications [191]. Their ease of cultivation, cost-effectiveness, scalability, and straightforward downstream processing make them ideal for both laboratory and industrial scales [78]. The biosynthesis of AuNPs using fungi is influenced by several factors, including the presence of bioactive molecules produced by the fungi, the concentration of gold precursor salts, and the optimization of experimental conditions. All of these play a crucial role in controlling nanoparticle size, shape, and biochemical properties of the AuNPs synthesized. Various fungal species, including *Penicillium* sp [216], *Aspergillus clavatus* [220], *Aspergillus niger* [236], and *Candida albicans* [214], have been widely utilized in AuNP synthesis.

Sastray et al. investigated the synthesis of gold nanoparticles employing *Verticillium* sp. and *Fusarium oxysporum*. In the presence of aqueous gold and silver ions, *Verticillium* sp. facilitated intracellular reduction, forming nanoparticles in the 2–20 nm range. Conversely, *Fusarium oxysporum* reduced gold and silver ions extracellularly, resulting in nanoparticles between 2 and 50 nm in size [222].

Mishra et al. reported the fungal-mediated AuNP biosynthesis employing *Penicillium rugulosum*, an industrially significant fungus. Transmission electron microscopy (TEM) analysis confirmed that the nanoparticles formed ranged in size from 25 to 60 nm [217].

Priyadarshini et al. developed an environmentally friendly method for the size-controlled fabrication of AuNPs at ambient temperature using *Aspergillus terreus* IF0. The addition of chloroauric acid to an aqueous fungal extract immediately triggered nanoparticle formation. The particle size was adjusted by modifying the pH of the fungal extract, with an average particle size of 10–19 nm observed at pH 10 [221].

Dhanasekar et al. investigated the biological synthesis of AuNPs utilizing culture filtrate from *Alternaria* sp. Exposure of the filtrate to three different concentrations of chloroaurate ions resulted in the reduction of gold ions to Au(0), leading to the formation of stable nanoparticles of varying sizes and shapes. For 1 mM chloroaurate solutions, diverse morphologies of AuNPs, including hexagonal, pentagonal, square, rod, and spherical structures with particle sizes of 69–93 nm, were observed. While at lower concentrations (0.3 and 0.5 mM), quasi-spherical and spherical nanoparticles were obtained, measuring 7–13 nm and 15–18 nm, respectively [225].

Kumari et al. explored the potential of *Trichoderma viride* filtrate in generating gold nanoparticles of diverse shapes and sizes. The synthesized AuNPs ranged between 2 and 500 nm, exhibiting morphologies such as nano-sheets, nano-hexagons, nano-pentagons, nanotriangles, and nanospheres. Experimental findings demonstrated that factors like culture filtrate concentration, reaction time, temperature, and pH significantly influence the final morphology of the nanoparticles [218].

Molnar et al. examined 29 thermophilic filamentous fungal strains to compare AuNP biosynthesis through intracellular fractions, fungal autolysates, and extracellular fractions. Their study found that nanoparticle sizes varied from 6 to 40 nm, with standard deviations between 30 % and 70 %, depending on fungal strain and environmental conditions [237].

Nguyen et al. successfully synthesized gold nanoparticles using an extract from *Ganoderma lucidum*, obtaining multi-shaped nanoparticles with sizes ranging between 15 and 40 nm [226].

The biosynthesis of gold nanoparticles using fungi presents a promising, eco-friendly alternative to traditional chemical synthesis methods. The ability to control nanoparticle characteristics through fungal species selection and environmental parameter adjustments highlights the potential for scalable industrial applications.

**5.1.1.3. Synthesis by algae.** Gold nanoparticles can be biosynthesized using various species of algae as natural reducing agents [238]. Several

**Table 9**  
Studies regarding the synthesis of AuNPs using plant extracts.

Name	Plant part	Size of AuNPs (nm)	Morphology	Ref.
<i>Pelargonium graveolens</i> (geranium)	Leaf	20–40	Decahedral, icosahedral	[241]
<i>Cymbopogon flexuosus</i> (lemongrass)	Leaf	50–1800	Triangle	[242]
<i>Azadirachta indica</i> (Neem)	Leaf	–	Triangular	[243]
<i>Tamarind</i>	Leaf	20–40	Triangular and hexagonal	[244]
<i>Aloe vera</i>	Leaf	50–350	Triangle	[245]
<i>Cinnamomum camphora</i>	Leaf	55–80	Triangle	[246]
<i>Coriandrum sativum</i> (Coriander)	Leaf	20.65	Spherical, triangular, truncated triangles, and decahedral	[247]
<i>Camellia sinensis</i> (green tea)	Leaf	40	Nanotriangle	[248]
<i>Eucalyptus camaldulensis</i>	Leaf	5.5	–	[249]
<i>Pelargonium roseum</i>	Leaf	7.5	–	[249]
<i>Cape aloe</i>	Leaf	4–50	Spherical, triangular	[250]
<i>Psidium guajava</i> (guava)	Leaf	27	Predominantly spherical	[251]
<i>Cinnamomum zeylanicum</i>	Leaf	25	Nanoprisms and spheres	[252]
<i>Magnolia Kobus</i> (magnolia)	Leaf	5–300	Spherical, triangles, pentagons, and hexagons	[253]
<i>Diospyros kaki</i> (Persimmon)	Leaf	5–300	Spherical, triangles, pentagons, and hexagons	[253]
<i>Phyllanthus amarus</i>	Leaf	18–38	Spherical, triangular, hexagonal, and rod-shaped	[254]
<i>Henna</i>	Leaf	21	Spherical, triangular	[255]
<i>Coleus amboinicus</i> (Indian borage)	Leaf	4.6–55.1	Spherical, truncated triangle, triangle, hexagonal, and decahedral	[256]
<i>Centella asiatica</i>	Leaf	9.3–10.9	Triangular, hexagonal	[257]
Green tea	Leaf	20	Mostly spherical	[258]
<i>Terminalia catappa</i> (almond)	Leaf	21.9	Predominantly spherical	[259]
<i>Stevia rebaudiana</i> (zero-calorie sweetener herb)	Leaf	8–20	Octahedral	[260]
<i>Mangifera indica</i>	Leaf	17–20	Spherical	[261]
<i>Sorbus aucuparia</i> (European rowan)	Leaf	18	Spherical, triangular, hexagonal	[262]
<i>Rosa rugosa</i> (Japanese rosa)	Leaf	11	Triangular and hexagonal	[263]
<i>Chenopodium album</i> (obnoxious weed)	Leaf	10	Quasi-spherical	[264]
<i>Callistemon viminalis</i>	Leaf	90	Nanotriangles and spherical	[265]
<i>Ocimum sanctum</i> (Krishna tulsi)	Leaf	30	Hexagonal	[266]
<i>Murraya koenigii</i> (curry tree)	Leaf	20	Spherical	[267]
<i>Anacardium occidentale</i> (cashew)	Leaf	6.5, 17	Spherical	[268]

**Table 9 (continued)**

Name	Plant part	Size of AuNPs (nm)	Morphology	Ref.
<i>Semecarpus anacardium</i> L.	Leaf	13–55	–	[269]
Olive	Leaf	50–100	Triangular, hexagonal, and spherical	[270]
<i>Camellia Sinensis</i> (tea)	Leaf and leaf bud	13.14	Irregular spherical, hexagonal, triangular, and elongated	[271]
<i>Olax Scandens</i>	Leaf	5–15	Spherical	[272]
<i>Podophyllum hexandrum</i>	Leaf	5–35	Spherical	[273]
<i>Mentha piperita</i>	Leaf	10–300	Spherical, triangular, and hexagonal	[274]
<i>Lantana montevidensis</i>	Leaf	10–20	Spherical	[275]
<i>Nerium oleander</i>	Leaf	2–10	Almost spherical	[276]
<i>Momordica cochinchinensis</i>	Leaf	10–80	Spherical, oval, and triangular	[277]
<i>Naregamia alata</i>	Leaf	27.92	Poly-shaped	[278]
<i>Syzygium jambos</i>	Leaf	5.24	Spherical	[279]
<i>Artemisia vulgaris</i>	Leaf	50–100	Spherical, triangular, and hexagonal	[280]
<i>Nigella arvensis</i>	Leaf	3–37	Predominantly spherical	[281]
<i>Alpinia nigra</i>	Leaf	21.52	Predominantly spherical	[282]
<i>Salix alba</i> L. (white willow)	Leaf	50–80	–	[283]
<i>Alcea rosea</i>	Leaf	4–95	Triangular, pentagonal, hexagonal, and spherical	[284]
<i>Simarouba glauca</i>	Leaf	10	Prism and spherical	[285]
<i>Jasminum auriculatum</i>	Leaf	8–37	Spherical	[286]
<i>Petroselinum crispum</i>	Leaf	17	Spherical	[287]
<i>Curcumae kwangsiensis</i>	Leaf	8–25	Spherical	[288]
<i>Mentha longifolia</i>	Leaf	13.45	Poly-dispersed and round oval	[289]
<i>Populus alba</i>	Leaf	16.3	Spherical and rod	[290]
<i>Embla officinalis</i> (Indian gooseberry)	Fruit	15–25	–	[291]
Pear	Fruit	200–500 (edges), 12–20 (thickness)	Triangular and hexagonal nanoplates	[292]
<i>Tanacetum vulgare</i> (common tansy)	Fruit	11	Spherical and triangular	[293]
<i>Couroupita guianensis</i>	Fruit	26	Anisotropic	[294]
<i>Dillenia indica</i>	Fruit	5–50	Spherical, triangular, tetragonal, and pentagonal	[295]
<i>Garcinia indica</i>	Fruit	20–30	Spherical	[296]
<i>Muntingia calabura</i>	Fruit	27	Spherical and oval	[297]
<i>Garcinia mangostana</i>	Fruit	20–40	Spherical	[298]
<i>Cornus mas</i>	Fruit	19	Spherical and pseudo-spherical	[299]
<i>Hylocereus undatus</i>	Fruit	35–100	Spherical	[300]
<i>Cicer arietinum</i> L. (Bengal gram beans)	Seed	25	Triangular prism	[301]
<i>Mucuna pruriens</i>	Seed	6–17.7	Spherical	[302]
<i>Vitis vinifera</i>	Seed	50	Spherical	[303]
<i>Oryza sativa</i>	Seed	80–150	Spherical	[304]
<i>Mangifera indica</i>	Seed	46.8	Spherical	[305]
<i>Coffea arabica</i>	Seed	28–69	Spherical and irregular shapes	[240]
<i>Trachyspermum ammi</i>	Seed	16.63	Spherical and spheroidal	[306]

(continued on next page)

**Table 9 (continued)**

Name	Plant part	Size of AuNPs (nm)	Morphology	Ref.
<i>Tamarindus indica</i>	Seed	10–15	Irregular	[307]
<i>Panax ginseng</i> (Korean red ginseng)	Root	16.2	Mostly spherical	[308]
<i>Coleus forskohlii</i>	Root	10–30	Spherical	[309]
<i>Dalbergia coronandiana</i>	Root	10.5	Spherical	[310]
<i>Glycyrrhiza glabra</i> L	Root	26.47–63.25	Circular	[311]
<i>Musa paradisiaca</i> (banana)	Peel	300	Microcubes and microwires	[312]
<i>Garcinia mangostana</i>	Peel	32.96	Mostly spherical	[313]
<i>Annona squamosa</i>	Peel	5	Spherical	[314]
Willow tree	Bark	15	Spherical	[315]
<i>Syzygium jambos</i>	Bark	10.34	Spherical	[279]
<i>Salacia chinensis</i>	Bark	30–50	Predominantly spherical	[316]
<i>Mimosa tenuiflora</i>	Bark	2–200	Multiple shapes	[317]
Cinnamon	Bark	35	Spherical	[318]
<i>Medicago sativa</i> (alfalfa)	Shoot	30–60	Decahedra and icosahedra	[319]
<i>Alvia officinalis</i> , <i>Lippia citriodora</i> , <i>Pelargonium graveolens</i> , and <i>Punica granatum</i>	Shoot	10	Spherical, triangular	[320]
		150	Triangles, truncated triangles, pentagons, and hexagons	
<i>Adiantum philippense</i>	Shoot	33.9	Spherical and triangular	[321]
<i>Salvia officinalis</i>	Shoot	6–27	Spherical	[239]
<i>Beta vulgaris</i> (sugar beet)	Pulp	160	Triangular	[322]
		20	Spherical	
		25	Nanorods	
<i>Beta vulgaris</i> (sugar beet)	Pulp	15–50	Nanowires	[323]
<i>Rosa hybrida</i> (rose)	Petal	10	Spherical, triangular, hexagonal	[324]
<i>Cassia auriculata</i>	Flower	12–41	Spherical	[325]
<i>Platycodon grandiflorum</i>	Flower	15	Spherical	[326]
<i>Syzygium aromaticum</i> (clove)	Flower and bud	100–300	Triangular, polygonal	[327]
<i>Acanthopanax sessiliflorus</i>	Root and stem bark	30–60	Nanoflower	[328]
<i>Allium cepa</i> (onion)	–	100	Spherical and cubic	[329]
<i>Abelmoschus esculentus</i>	–	13.96	Mostly spherical	[330]
<i>Sargentodoxa cuneata</i>	–	15–30	Hexagonal	[331]
<i>Fagonia indica</i>	–	20	Hexagonal	[332]
<i>Taxus baccata</i>	–	<20	Spherical, semi-spherical, hexagonal, and triangular	[333]
<i>Terminalia chebula</i>	–	10	Spherical	[334]
<i>Turbinaria ornata</i>	–	20–30	Spherical and triangular	[335]

algae, including *Shewanella algae*, *Galaxaura elongata*, *Spirulina platensis*, and *Turbinaria conoides*, have been used for the production of AuNPs [78].

Venkatesan et al. successfully achieved the rapid biosynthesis of AuNPs using *Ecklonia cava*, a marine brown alga belonging to the family Lessoniaceae, through the reduction of chloroauric acid. Microscopic analysis revealed that the nanoparticles were predominantly spherical and triangular, with an average diameter of  $30 \pm 0.25$  nm [229].

In another study, Singh et al. synthesized AuNPs utilizing an aqueous extract of a unicellular, halotolerant microalga named *Dunaliella salina*. The optimized synthesis parameters are as follows: 75 min of sunlight

exposure, a 30 % *Dunaliella* extract concentration, and 1 mM HAuCl<sub>4</sub>·xH<sub>2</sub>O. TEM analysis confirmed the formation of nearly spherical AuNPs with an average diameter of 22.4 nm [228].

Furthermore, Chellapandian et al. developed a simple, one-step synthesis method for AuNPs employing an aqueous extract of *Gracilaria verrucosa*, a marine red seaweed. The study disclosed the presence of both anisotropic and isotropic nanoparticles with varied morphologies, ranging in size from 20 to 80 nm [230].

**5.1.1.4. Synthesis by yeast.** Yeast-derived biomolecules can serve as reducing agents in the synthesis of gold nanoparticles [191]. Nevertheless, only a limited number of yeast strains have been investigated for AuNP production.

In one study, Mishra et al. studied the extracellular biosynthesis of Au and Ag NPs utilizing *Candida guilliermondii*. TEM analysis revealed the formation of well-dispersed, nearly spherical nanoparticles, with gold nanoparticles measuring between 50 and 70 nm, while silver nanoparticles were significantly smaller, ranging from 10 to 20 nm [231].

Zhang et al. employed *Magnusiomyces ingens* LH-F1 yeast cells to synthesize AuNPs, yielding nanoparticles with diverse geometries, including hexagonal, triangular, and spherical structures, with an average size of 80.1 nm [232].

Uthaman et al. investigated an environmentally friendly approach for the biosynthesis of AuNPs using mannan, a polysaccharide derived from *Saccharomyces cerevisiae*, as both a reducing and stabilizing agent. The resulting gold nanoparticles exhibited a spherical shape, with an average diameter of  $9.18 \pm 0.71$  nm [134].

### 5.1.2. Synthesis by plant extracts

In recent years, plant extracts have emerged as an efficient and eco-friendly alternative for synthesizing metal nanoparticles, replacing traditional physical and chemical techniques. Biosynthesis of AuNPs using plant extracts involves extracting phytochemicals from different plant parts (root, seed, peel, flower, bark, fruit, leaf, etc.) to reduce gold salts and stabilize the resulting nanoparticles. The process typically begins by washing the plant material, cutting it into small pieces, and boiling it in distilled water to prepare the extract. The extract is then purified via filtration or centrifugation and subsequently mixed with different concentrations of gold salt solution. Within minutes to a few hours, gold ions in the gold salt solution are reduced to form AuNPs, and the transformation is visually monitored by color change. To ensure complete reduction, the reaction mixture is incubated further, and the synthesized AuNPs are subsequently purified by centrifugation and washed thoroughly in water for further use.

This biosynthetic approach is simple, sustainable, and highly scalable. Phytochemicals present in the plant extracts serve as both reducing and stabilizing agents, eliminating the need for additional stabilizers or capping agents. The size of AuNPs can be controlled by adjusting the ratio of reducing agents in the reaction mixture [184]. The variability in metabolite composition across different plant parts and species plays a vital role in defining nanoparticle morphology [78]. Additionally, factors such as pH and temperature significantly influence the final characteristics of the AuNPs [239,240]. Numerous plant species have been explored for AuNP biosynthesis, with leaves being the most widely utilized plant component. A summary of studies on AuNP synthesis using plant extracts is provided in Table 9.

**5.1.2.1. Synthesis of AuNPs using extracts of leaves.** Narayanan and Sakthivel demonstrated the extracellular biosynthesis of gold nanoparticles utilizing coriander leaf extract. When exposed to aqueous gold ions, the extract facilitated the reduction, yielding nanoparticles with diverse morphologies, including decahedral, truncated triangles, triangular, and spherical shapes, with sizes ranging from 6.75 to 57.91 nm [247].

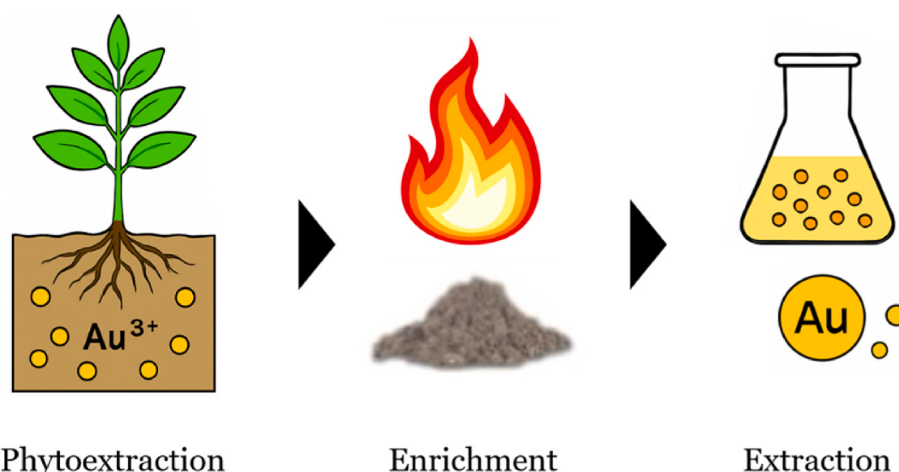


**Fig. 10.** Illustration of the entire gold phytomining approach.

Similarly, Boruah et al. developed a rapid, cost-effective, and eco-friendly method to produce AuNPs employing leaf buds and fresh young leaves of *Camellia sinensis* (tea plant). Upon interaction with chloroauric acid at room temperature, the extract's polyphenols reduced  $\text{Au}^{3+}$  to  $\text{Au}^0$ , resulting in nanoparticles with an average size of 13.14 nm, within a range of  $\sim 2.94\text{--}45.58\text{ nm}$  [271].

Chahardoli et al. reported a one-step green synthesis of spherical gold nanoparticles (3–37 nm in size) utilizing the extract of *Nigella arvensis* leaves [281]. Meanwhile, Islam et al. introduced a reproducible method for synthesizing stable AuNPs from white willow (*Salix alba* L.) leaf extract. The synthesized nanoparticles, predominantly sized between 50 and 80 nm, exhibited high colloidal stability across various pH and salt concentrations and demonstrated significant antifungal, analgesic, and muscle-relaxant properties, highlighting their biomedical potential [283].

Chen et al. synthesized AuNPs by reacting the leaf aqueous extract of *Curcumae Kwangsiensis* Folium with chloroauric acid under *in vitro* conditions. TEM analysis revealed spherical nanoparticles measuring 8–25 nm. Notably, these AuNPs demonstrated dose-dependent anti-ovarian cancer potential owing to their antioxidant properties [288].

**5.1.2.2. Synthesis of AuNPs using extracts of other plant parts.** Besides leaves, various other plant parts, including peels, seeds, fruits, flowers, and barks, have been successfully employed in AuNP biosynthesis. Rao et al. synthesized gold nanoparticles with a size of 20–30 nm using extracts from the peel of *Citrus sinensis*, leaves of *Mentha spicata* and *Azadirachta indica*, and flowers and leaves of *Ocimum tenuiflorum* [336].

Elia et al. investigated AuNP synthesis using extracts from *Punica granatum*, *Pelargonium graveolens*, *Lippia citriodora*, and *Salvia officinalis*. TEM imaging showed the formation of nanoparticles with diverse morphologies, including spherical, triangular, pentagonal, and hexagonal shapes, with sizes ranging from 10 nm to 150 nm. These nanoparticles demonstrated potential for biomedical applications [320]. Oueslati et al. further explored the role of polyphenols from *Salvia officinalis* in an eco-friendly synthesis process. Their study also demonstrated that pH significantly influenced nanoparticle size: smaller (~6 nm) monodisperse nanoparticles formed in an alkaline medium (pH ~11), whereas larger (~27 nm) particles were generated in an acidic environment (pH ~5) [239].

Bahram and Mohammadzadeh utilized willow bark extract to generate spherical AuNPs (<15 nm), which showed promising applications in colorimetric sensing for cysteine detection [315]. Rodríguez-León et al. employed *Mimosa tenuiflora* bark extract, rich in polyphenols, to synthesize AuNPs ranging from 20 to 200 nm via a one-pot method [317]. ElMiitwalli et al. used cinnamon bark extract as both a reducing and stabilizing agent to generate spherical AuNPs (~35

nm) [318].

Parida et al. employed *Allium cepa* (onion) extract to synthesize AuNPs (~100 nm) with spherical and cubic morphologies [329]. Sett et al. reported the synthesis of AuNPs (5–50 nm) using aqueous fruit extract of *Dillenia indica*, where phytochemicals acted as effective reducing and capping agents [295]. Lee et al. synthesized AuNPs by reducing gold ions with the peel extract of *Garcinia mangostana*. TEM analysis confirmed mostly spherical nanoparticles with an average size of  $32.96 \pm 5.25$  nm. The presence of anthocyanins, benzophenones, flavonoids, and phenols suggested their role as reducing agents [313]. Bogireddy et al. investigated a size-controlled synthesis of crystalline AuNPs utilizing the extract of sun-dried *Coffea arabica* seeds at room temperature. By altering the reaction pH (pH 5 to pH 10.5), they observed that lower pH led to larger nanoparticles (~69 nm), whereas higher pH yielded smaller quasi-spherical particles (~28 nm) [240]. Anbu et al. used balloon flower (*Platycodon grandiflorum*) extract to synthesize spherical AuNPs (~15 nm), which exhibited significant antibacterial effects against *Escherichia coli* and *Bacillus subtilis*, highlighting their antimicrobial applications [326].

On the whole, the biosynthesis of AuNPs using plant extracts represents a sustainable, cost-effective, and scalable alternative to conventional synthesis methods. The phytochemicals within plant materials act as natural reducing and stabilizing agents, facilitating nanoparticle formation without hazardous chemicals. The variability in plant species, extract composition, and reaction conditions influences the size, shape, and stability of AuNPs, broadening their potential applications in biomedicine, sensing, and environmental remediation.

### *5.2. Synthesis of gold nanoparticles using living plants*

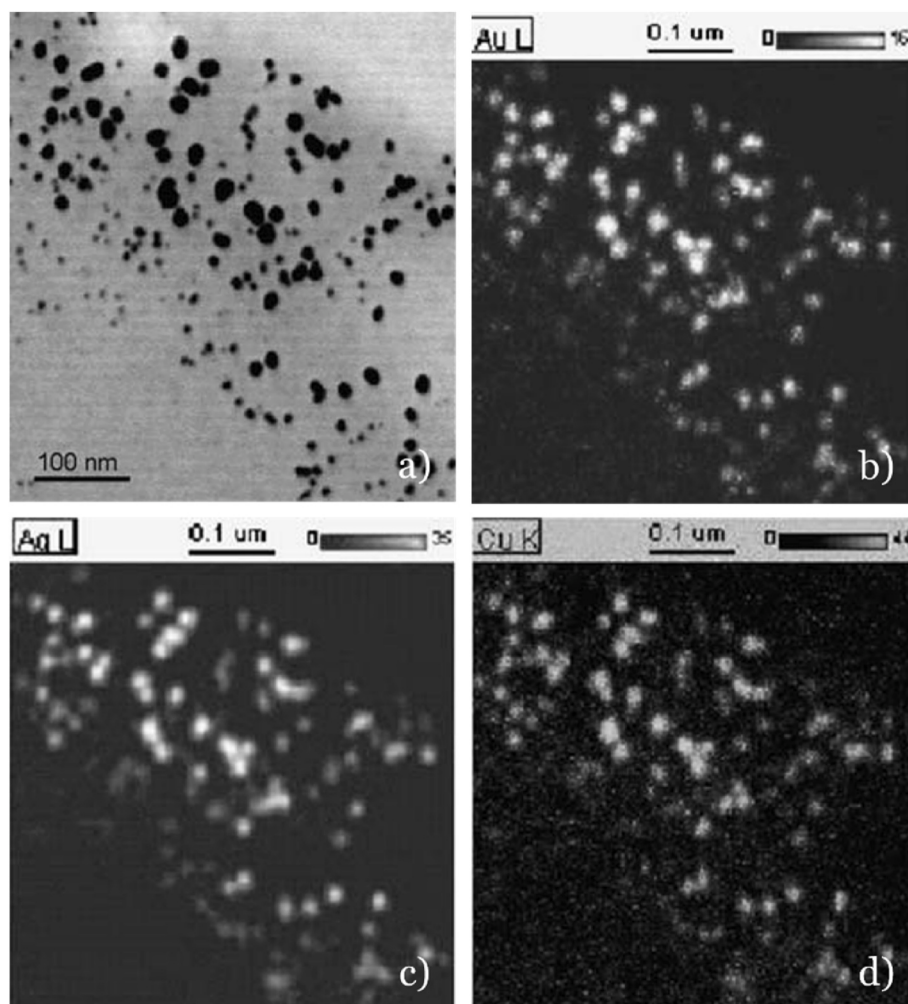
The synthesis of AuNPs using biological methods has attracted growing interest with several review articles recently published [5,29, 78,184,187,191]. However, to our knowledge, none of these reviews provides a comprehensive overview of AuNP synthesis specifically using living plants. The present study is the first to focus in depth on the use of living plants for AuNP synthesis, highlighting this emerging and promising area of green nanotechnology.

Plants are used to accumulate and synthesize AuNPs from soils through a process called phytomining. Phytomining is an innovative, plant-based technique for extracting gold from ores, mining runoff, and polluted soils. The entire process involves 3 stages: (i) Phytoextraction, the initial phase, utilizes plants to accumulate gold from soils; (ii) Enrichment, during which the plants are combusted to concentrate gold in ashes; (iii) Extraction, in which gold is recovered from the ashes, completing the phytomining chain [337,338]. The overall phytomining pathway is depicted in Fig. 10.

**Table 10**

Studies regarding the synthesis of AuNPs using living plants.

Plant	Part	NP	Size (nm)	Morphology	Ref.
<i>Brassica juncea</i> (Indian mustard)	Above-ground part	Au/Ag/Cu	5–50	Spherical	[340]
<i>Brassica juncea</i> (Indian mustard)	Shoot and leaf	Au/Ag	<50	—	[343]
<i>Brassica juncea</i> (Indian mustard)	Shoot	Au	5–50	Spherical	[344]
<i>Brassica juncea</i> (Indian mustard)	Leaf and stem	Au	2–100	Mostly spherical	[345]
	Root	Au	2–40	Mostly spherical	
<i>Brassica juncea</i> (Indian mustard)	Root	Au	43	Varying shapes	[346]
	Shoot	Au	61	Varying shapes	
<i>Medicago sativa</i> (Alfalfa)	Root	Au	44	Varying shapes	
	Shoot	Au	38	Varying shapes	
<i>Medicago sativa</i> (Alfalfa)	Shoot	Au	6–10 4	Twinned structures Icosahedron	[347]
<i>Medicago Sativa</i> (Alfalfa)	Root	Au	10–30	Spherical, triangular, hexagonal, and rectangular	[348]
Alfalfa	—	Au	2–40	—	[189]
<i>Medicago sativa</i> L. (Alfalfa)	—	Au	5–100	—	[349]
<i>Arabidopsis thaliana</i> L. (Arabidopsis)	Shoot, root	Au	5–30	Differently shaped	
<i>Arabidopsis thaliana</i> (Thale cress)	Root	Au	20–50	Predominately spherical	[350]
<i>Chilopis linearis</i> (desert willow)	Stem, leaf	Au	1.1	—	[351]
<i>Chilopis linearis</i> (desert willow)	Root	Au	0.8	—	[352]
	Leaf	Au	1.5	—	
	Stem	Au	3.8	—	
<i>Sesbania drummondii</i> (Rattlebush)	Shoot, root	Au	6–20	Spherical	[353]
<i>Erigeron canadensis</i> (Shrub)	Stem	Au-bearing nanoparticle	20–50	Irregular	[354]
<i>Boehmeria nivea</i> (Weed)	Stem	Au-bearing nanoparticle	5–15	Circular, elliptical, or bone-rod	
<i>Arachis hypogaea</i> (Peanut)	—	Au	5–50	Oval	[355]
<i>Ulva armoricana</i> (Seaweed)	—	Au	10	Predominately spherical	[356]

**Fig. 11.** a) TEM of metallic nanoparticles in *Brassica juncea*; TEM-EDX maps of b) Au, c) Ag, and d) Cu [340].

The synthesis of gold nanoparticles from biomass not only offers an environmentally friendly approach to metal extraction but also opens a potential era for producing nanoparticles with applications in catalysis, materials science, and environmental remediation. The phytomining approach offers distinctive ecological and economic advantages compared to traditional chemical and even other biological methods. Plants possess the unique ability to absorb trace levels of gold from low-grade ores, mine tailings, contaminated soils, or aqueous solutions and reduce them to elemental Au within their tissues under ambient conditions, eliminating the need for hazardous chemical reducing agents and energy-intensive conditions [339]. They naturally can yield nanoparticles with diverse morphologies, including mixed-metal nanoalloys such as Au–Ag–Cu, which are often difficult to produce via standard chemical syntheses [340]. In addition, the use of living plants for nanoparticle synthesis can aid land remediation by removing contaminants, contributing to ecological rehabilitation, and potentially enhancing biodiversity [341]. The metal accumulation process can be improved by applying non-toxic chelating agents, such as thiosulfate, thiocyanate, iodide, bromide, cyanide, and thiourea, which help solubilize metals from their substrates for plant uptake. *Berkheyacoddii* and *Brassica juncea* treated with thiocyanate solutions were found to hyperaccumulate gold. Meanwhile, gold hyperaccumulation in chicory and *Brassica juncea* occurs in the presence of thiocyanate, thiosulfate, iodide, bromide, and cyanide solubilizing agents [342].

Despite these advantages, AuNPs synthesis using living plants presents significant limitations and operational challenges. The process is slow because plant growth takes time, and it requires large areas to produce sufficient biomass for profitable yields. Gold uptake can impose physiological stress on plants, limiting biomass productivity. The yields are highly variable and influenced by factors such as metal speciation, plant species, age, environmental conditions, and gold bioavailability, making reproducibility more difficult compared to controlled microbial or chemical systems. The nanoparticles produced in plants typically exhibit broad size distributions and variable morphologies, posing challenges for applications that require monodispersity, such as biomedical and plasmonic technologies. Recovery of AuNPs from biomass requires additional processing steps like combustion and extraction, which may diminish the “green” advantage if not optimized (energy, emissions, and reagent use must be considered). Moreover, plant health, metal toxicity, and the need for metal-mobilizing agents (chelators) can introduce ecological risks or require careful management.

Compared with other biological routes, microbial and plant extract-based syntheses offer faster production rates, better size control, and easier scalability, though these approaches require processed feedstocks and controlled conditions. Meanwhile, living-plant synthesis enables the production of complex nanoalloys and extracting gold from low-grade substrates in which other biological and chemical approaches are often inefficient, but it requires more complex downstream processing and lags in precision control and production speed. Traditional chemical synthesis remains superior for generating high-purity, uniform AuNPs tailored for specialized applications, although it uses harsher reagents and lacks the sustainability benefits and environmental remediation potential of the living-plant system.

Looking ahead, overcoming the current challenges in living-plant AuNP synthesis will require further research in plant biotechnology and process engineering. Careful selection and genetic modification of plant species can enhance metal uptake and improve control over nanoparticle formation. Optimizing growth and exposure conditions is essential for maximizing both metal accumulation and biomass production, which directly influence the efficiency of the phytomining process. The development of green, low-energy downstream processes, such as combustion and extraction, is important to complete the entire synthesis route in an environmentally responsible way. Designing processes tailored to applications that tolerate size variability, such as heterogeneous catalysis, will be critical for making the living-plant

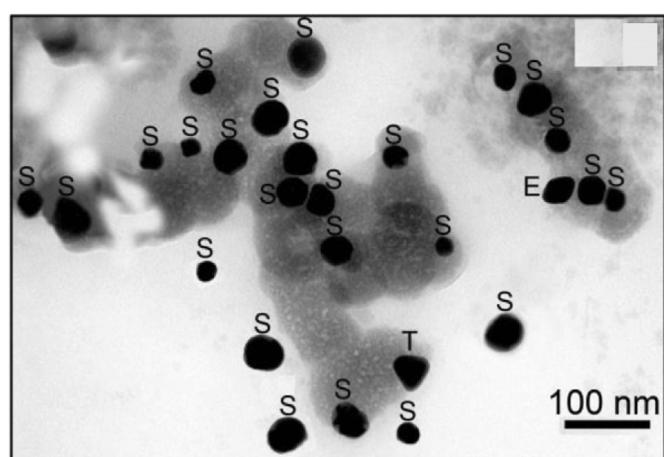


**Fig. 12.** TEM of AuNPs in *Arabidopsis thaliana* (S = spherical, T = triangular, E = exotic) [350].

AuNP synthesis a viable and competitive nanomanufacturing strategy. Additionally, comprehensive techno-economic analyses will be essential to evaluate feasibility, scalability, and help position this innovative pathway as a truly sustainable alternative in the nanomaterials industry. Table 10 summarizes the studies regarding the synthesis of gold nanoparticles using living plants.

Haverkamp et al. revealed the first synthesis of mixed metal nanoparticles in living *Brassica juncea*, highlighting its potential for developing complex catalysts that are otherwise challenging to produce through traditional chemical techniques [340]. The resulting nanoalloys comprised Au, Ag, and Cu, with their composition and structure validated via STEM (scanning transmission electron microscopy) and EDX (energy-dispersive X-ray spectroscopy). High-resolution STEM micrographs showed well-dispersed nanoparticles distributed within plant tissues, while EDX elemental mapping confirmed the alloy composition (Fig. 11). The study demonstrated that nanoparticle alloys can be controlled by adjusting the metal components in the plant's growth medium. This work marked a milestone in employing living plants for synthesizing mixed-metal nanoparticles that are difficult to obtain by conventional routes, underscoring the role of plants as both reducing and templating environments for alloy formation. Similarly, Anderson et al. observed that *Brassica juncea* grown on mine waste could accumulate over 3500 mg/kg dry weight of gold, producing discrete nanoparticles in shoot and leaf tissues [343]. The addition of Ag<sup>+</sup> ions was found to facilitate the formation of Au–Ag nanoalloys but simultaneously reduce both the AuNP size and the extent of Au reduction within plant tissues. While Cu at similar concentrations did not incorporate into the alloy, but still suppressed particle growth. The authors proposed that plants “build” nanoparticles during metal accumulation, with particle size increasing over time. However, Cu- or Ag-induced physiological stress could slow accumulation, yielding smaller nanoparticles.

Bali and Harris evaluated the metallophytes *Brassica juncea* and *Medicago sativa* for their ability to sequester gold from aqueous solutions of KAuCl<sub>4</sub> [346]. The gold nanoparticles formed in the epidermis, cortex, and vascular tissues, notably within the xylem parenchyma cells of both species. In *Medicago sativa*, particles ranged in size from 2 nm to 1 μm, whereas in *Brassica juncea*, they ranged from 2 nm to 2 μm. Interestingly, the root parts of both plants showed similar particle distributions, while aboveground tissues in *Brassica juncea* exhibited a wider range of nanoparticle sizes. Comparable root size distributions in both species suggest a common root-based reduction pathway, while the broader spread in *B. juncea* shoots points to species-specific differences in transport efficiency or local biochemistry. The wide range of gold nanoparticle sizes across tissues also reveals that growth conditions and sampling time strongly influence size distributions in whole-plant

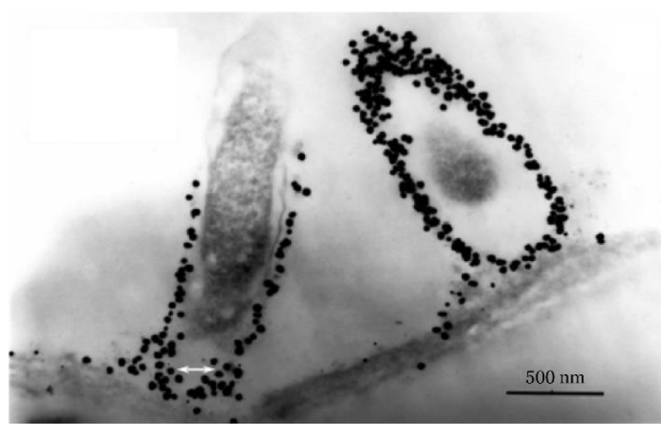


**Fig. 13.** TEM of AuNPs in *Sesbania drummondii* root [353].

systems.

Rodriguez et al. investigated gold accumulation in *Chilopsis linearis* (desert willow), focusing on different developmental stages [352]. Plants were grown in gold-enriched agar media containing 20, 40, 80, 160, and 320 mg/L of Au for periods of 13, 18, 23, and 35 d. The amount and oxidation state of gold within the plant tissues were measured utilizing ICP-OES (inductively coupled plasma optical emission spectroscopy) and XAS (X-ray absorption spectroscopy). Leaf Au concentrations for the 20, 40, 80, and 160 mg/L treatments reached 32, 60, 62, and 179 mg/kg dry weight, respectively, confirming efficient uptake. Gold concentrations of 20–80 mg/L did not significantly affect growth, and gold uptake increased with plant age, supporting the feasibility for controlled phytomining and nanomaterial formation. Whereas, after exposing the plants to 160 mg/L Au media, AuNPs formed in the roots, stems, and leaves, with average particle sizes of 0.8 nm, 1.8 nm, and 3.5 nm, respectively. The study also unveiled that nanoparticle size correlated directly with both the gold concentration and tissue type.

In a study on *Arabidopsis thaliana*, Jain et al. observed monodispersed gold nanoparticles in the root biomatrix after treating seedlings with 10 mg/L  $\text{KAuCl}_4$  for 7 d [350]. The TEM image (Fig. 12) depicted the occurrence of monodisperse gold nanoparticles with different sizes and morphologies in the root biomatrix. The various shapes of these nanoparticles include irregular, triangular, and spherical, with sizes ranging between 20 and 50 nm. Taylor et al. further investigated the physiological and genetic response of *Arabidopsis thaliana* L. to gold exposure, showing that approximately 10–15 % of absorbed  $\text{Au}^{3+}$  was translocated to shoot tissues, where it accumulated as AuNPs [349]. This accumulation process was passive, with gold primarily retained and reduced in the roots. In contrast, *M. sativa* showed limited nanoparticle accumulation in hydroponic cultures, with particle sizes ranging from 5 to 100 nm, emphasizing species-specific differences in uptake, reduction, and

intracellular stabilization under comparable ionic gold exposures.

The ability of *Sesbania* seedlings to accumulate gold from  $\text{KAuCl}_4$  solutions was demonstrated by Sharma et al., resulting in the formation of stable gold nanoparticles within plant tissues [353]. TEM (Fig. 13) showed uniformly distributed spherical nanoparticles, likely through the reduction of the metal ions by secondary metabolites present in cells. Additionally, marine green algae (*Ulva armoricana*) were reported to synthesize AuNPs rapidly when exposed to dilute  $\text{Au}^{3+}$  solutions under illumination. Mukhoro et al. observed that light-assisted synthesis occurred within just 15 min, a significant improvement compared to the slow, two-week formation process under non-illuminated conditions [356], indicating light as a powerful acceleration lever for Au (III) reduction in living photosynthetic systems. TEM confirmed that the algae retained their cell structure and nanoparticle formation along the cell walls and within chloroplasts. These biosynthesized AuNPs demonstrated excellent catalytic activity in reducing aqueous 4-nitrophenol.

Starnes et al. examined gold accumulation across various plant species, including alfalfa, ryegrass, sunflower, red clover, oregano, and cucumber [348]. Gold concentrations in root tissues ranged from 500 mg/kg in ryegrass to 2500 mg/kg in alfalfa. Due to its high accumulation potential, alfalfa was selected for further studies, which revealed that most AuNPs were generated within the first 6 h of treatment. The nanoparticles primarily fell within the 10–30 nm size range. Spherical gold nanoparticles in the size range 1–50 nm were observed commonly across different treatments, but altering growth conditions shifted the proportion of spherical, triangular, hexagonal, and rectangular forms (Fig. 14), enabling in-planta control over nanoparticle size and shape.

The eco-friendliness and simplicity are emphasized in biological studies. However, the nanoparticle yield and control, process standardization, and the stability and scalability of biologically produced AuNPs are rarely analyzed in the cited works. For instance, while bacterial and fungal systems demonstrate biosynthesis capabilities, many yield polydisperse particles and require longer reaction times. Algal methods report multiple shapes and particle sizes but lack reproducible protocols and face challenges with batch-to-batch variability. Studies using yeast are potential but underexplored, offering little comparative advantage over bacterial approaches. Furthermore, controlling nanoparticle uniformity and optimizing growth parameters remains a major hurdle, particularly in microbial approaches (Table 8). The plant extracts synthesis (Table 9) is a sustainable option, but its reproducibility of phytochemical-mediated reduction is under-examined. While the synthesis of AuNPs utilizing living plants (Table 10) is innovative and promising, presently, this approach is discussed on a rather theoretical basis. Hence, while biologically derived AuNPs offer sustainability and reduced toxicity, further standardization, mechanistic understanding, and scalability assessments are essential before industrial application.

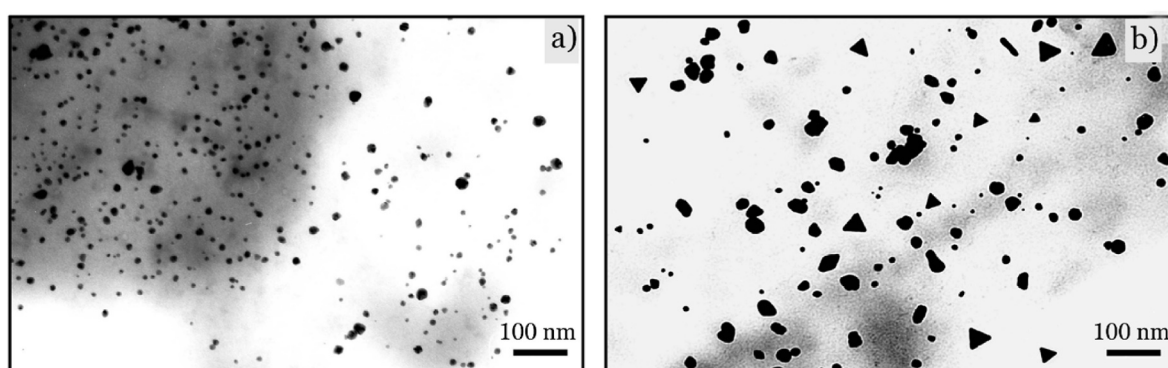


**Fig. 14.** TEM of AuNPs in Alfalfa under different conditions: a) pH 5.8, b) pH 3.8 [348].

## 6. Conclusion

Nanotechnology is advancing rapidly, driven by its wide array of implementations across various technological and scientific domains. Among the nanomaterials, AuNPs are highly valued in diverse areas like biology, sensing, optics, catalysis, and electronics due to their unique properties. Various synthesis techniques, including physical, chemical, and biological methods, have been developed to fabricate AuNPs, each offering distinct advantages and challenges. Among these, nanoparticle synthesis using living plants, also known as phytomining, is an innovative approach over conventional pathways as it eliminates the need for elevated pressure, temperature, energy consumption, and toxic chemicals. To our knowledge, this study provides the first comprehensive review of literature based on the synthesis of gold nanoparticles using living plants, shedding light on an emerging area of green nanotechnology. While significant progress has been made, research in this domain remains in the exploratory stage. Deeper insight into its basic principles and further investigation efforts are essential to better understand and advance this promising field.

## CRediT authorship contribution statement

**Truong Dinh:** Writing – original draft, Visualization, Methodology, Investigation. **Zsolt Dobó:** Writing – original draft, Validation, Supervision, Conceptualization. **Árpád Bence Palotás:** Writing – review & editing, Validation, Resources. **Helga Kovács:** Writing – review & editing, Validation, Supervision, Conceptualization.

## Declaration of competing interest

The authors declare that they have no known competing financial interests or personal relationships that could have appeared to influence the work reported in this paper.

## Acknowledgements

Supported by the University Research Scholarship Program of the Ministry for Culture and Innovation from the source of the National Research, Development and Innovation Fund.

## Data availability

No data was used for the research described in the article.

## References

- [1] H.-S. Kwon, M.H. Ryu, C. Carlsten, Ultrafine particles: unique physicochemical properties relevant to health and disease, *Exp. Mol. Med.* 52 (2020) 318–328, <https://doi.org/10.1038/s12276-020-0405-1>.
- [2] M. Shah, Gold nanoparticles: various methods of synthesis and antibacterial applications, *Front. Biosci.* 19 (2014) 1320, <https://doi.org/10.2741/4284>.
- [3] C.M. Niemeyer, C.A. Mirkin (Eds.), *Nanobiotechnology*, Wiley, 2004, <https://doi.org/10.1002/3527602453>.
- [4] D. Astruc (Ed.), *Nanoparticles and Catalysis*, Wiley, 2007, <https://doi.org/10.1002/9783527621323>.
- [5] M.A.R. Khan, M.S. Al Mamun, M.A. Habib, A.B.M.N. Islam, M. Mahiuddin, K.M. R. Karim, J. Naimee, P. Saha, S.K. Dey, M.H. Ara, A review on gold nanoparticles: biological synthesis, characterizations, and analytical applications, *Results, Chem* 4 (2022) 100478, <https://doi.org/10.1016/j.rechem.2022.100478>.
- [6] N. Elahi, M. Kamali, M.H. Baghersad, Recent biomedical applications of gold nanoparticles: a review, *Talanta* 184 (2018) 537–556, <https://doi.org/10.1016/j.talanta.2018.02.088>.
- [7] K.N. Thakkar, S.S. Mhatre, R.Y. Parikh, Biological synthesis of metallic nanoparticles, *Nanomed. Nanotechnol. Biol. Med.* 6 (2010) 257–262, <https://doi.org/10.1016/j.nano.2009.07.002>.
- [8] A. Khosla, I.A. Wani, M.N. Lone, Gold and silver nanoparticles for biomedical applications, in: *Met. Magn. Carbon-Based Nanomater.*, Wiley, 2025, pp. 120–170, <https://doi.org/10.1002/9781119870685.ch2>.
- [9] E. Boisselier, D. Astruc, Gold nanoparticles in nanomedicine: preparations, imaging, diagnostics, therapies and toxicity, *Chem. Soc. Rev.* 38 (2009) 1759, <https://doi.org/10.1039/b806051g>.
- [10] N. Li, P. Zhao, D. Astruc, Anisotropic gold nanoparticles: synthesis, properties, applications, and toxicity, *Angew. Chem. Int. Ed.* 53 (2014) 1756–1789, <https://doi.org/10.1002/anie.201300441>.
- [11] K.S. Siddiqi, A. Husen, Green synthesis, characterization and Uses of Palladium/platinum nanoparticles, *Nanoscale Res. Lett.* 11 (2016) 482, <https://doi.org/10.1186/s11671-016-1695-z>.
- [12] M.A.R. Khan, M.S. Al Mamun, M.H. Ara, Review on platinum nanoparticles: synthesis, characterization, and applications, *Microchem. J.* 171 (2021) 106840, <https://doi.org/10.1016/j.microc.2021.106840>.
- [13] H.W. Tan, J. An, C.K. Chua, T. Tran, Metallic nanoparticle inks for 3D printing of electronics, *Adv. Electron. Mater.* 5 (2019) 1–20, <https://doi.org/10.1002/aelm.201800831>.
- [14] M.R. Langille, M.L. Personick, J. Zhang, C.A. Mirkin, Defining Rules for the shape Evolution of gold nanoparticles, *J. Am. Chem. Soc.* 134 (2012) 14542–14554, <https://doi.org/10.1021/ja305245g>.
- [15] M.L. Personick, C.A. Mirkin, Making Sense of the Mayhem behind shape control in the synthesis of gold nanoparticles, *J. Am. Chem. Soc.* 135 (2013) 18238–18247, <https://doi.org/10.1021/ja408645b>.
- [16] S.S. Shankar, S. Bhargava, M. Sastry, Synthesis of gold nanospheres and nanotriangles by the Turkovich approach, *J. Nanosci. Nanotechnol.* 5 (2005) 1721–1727, <https://doi.org/10.1166/jnn.2005.192>.
- [17] B.G. Prevo, S.A. Esakoff, A. Mikhailovsky, J.A. Zasadzinski, Scalable routes to gold nanoshells with tunable sizes and response to near-infrared Pulsed-laser irradiation, *Small* 4 (2008) 1183–1195, <https://doi.org/10.1002/smll.200701290>.
- [18] Y.-C. Wang, É. Rhéaume, F. Lesage, A. Kakkar, Synthetic methodologies to gold nanoshells: an overview, *Molecules* 23 (2018) 2851, <https://doi.org/10.3390/molecules23112851>.
- [19] Y. Bin Rus, M. Bosni, S. Maisonneuve, V. Guérineau, V. Noël, A. Courty, F. Miolandre, Versatile one-pot synthesis of gold nanoclusters and nanoparticles using 3,6-(dipyridin-2-yl)-(1,2,4,5)-tetrazine, *RSC Adv.* 11 (2021) 7043–7050, <https://doi.org/10.1039/DORA10961D>.
- [20] S.E. Skrabalak, J. Chen, Y. Sun, X. Lu, L. Au, C.M. Cobley, Y. Xia, Gold nanocages: synthesis, properties, and applications, *Acc. Chem. Res.* 41 (2008) 1587–1595, <https://doi.org/10.1021/ar800018v>.
- [21] J. Pérez-Juste, I. Pastoriza-Santos, L.M. Liz-Marzáñ, P. Mulvaney, Gold nanorods: synthesis, characterization and applications, *Coord. Chem. Rev.* 249 (2005) 1870–1901, <https://doi.org/10.1016/j.ccr.2005.01.030>.
- [22] F. Liebig, R. Henning, R.M. Sarhan, C. Prietzel, C.N.Z. Schmitt, M. Bargheer, J. Koetz, A simple one-step procedure to synthesise gold nanostars in concentrated aqueous surfactant solutions, *RSC Adv.* 9 (2019) 23633–23641, <https://doi.org/10.1039/C9RA02384D>.
- [23] I.B. Becerril-Castro, I. Calderon, N. Pazos-Perez, L. Guerrini, F. Schulz, N. Feliu, I. Chakraborty, V. Giannini, W.J. Parak, R.A. Alvarez-Puebla, Gold nanostars: synthesis, optical and SERS analytical properties, *Anal. Sens.* 2 (2022) 1–16, <https://doi.org/10.1002/anse.202200005>.
- [24] M. Chirea, A. Freitas, B.S. Vasile, C. Ghitulica, C.M. Pereira, F. Silva, Gold nanowire Networks: synthesis, characterization, and catalytic activity, *Langmuir* 27 (2011) 3906–3913, <https://doi.org/10.1021/la104092b>.
- [25] X. Jiang, X. Qiu, G. Fu, J. Sun, Z. Huang, D. Sun, L. Xu, J. Zhou, Y. Tang, Highly simple and rapid synthesis of ultrathin gold nanowires with (111)-dominant facets and enhanced electrocatalytic properties, *J. Mater. Chem. A* 6 (2018) 17682–17687, <https://doi.org/10.1039/C8TA06676K>.
- [26] N. Zhao, Y. Wei, N. Sun, Q. Chen, J. Bai, L. Zhou, Y. Qin, M. Li, L. Qi, Controlled synthesis of gold Nanobelts and Nanocombs in aqueous mixed surfactant solutions, *Langmuir* 24 (2008) 991–998, <https://doi.org/10.1021/la702848x>.
- [27] C.M. Payne, D.E. Tsentalovich, D.N. Benoit, L.J.E. Anderson, W. Guo, V.L. Colvin, M. Pasquale, J.H. Hafner, Synthesis and crystal structure of gold Nanobelts, *Chem. Mater.* 26 (2014) 1999–2004, <https://doi.org/10.1021/cm402506e>.
- [28] L. Freitas de Freitas, G.H.C. Varca, J.G. Dos Santos Batista, A. Benévolo Lugão, An overview of the synthesis of gold nanoparticles using radiation technologies, *Nanomaterials* 8 (2018) 939, <https://doi.org/10.3390/nano8110939>.
- [29] I. Hammami, N.M. Alabdullah, A. Al Jomaa, M. Kamoun, Gold nanoparticles: synthesis properties and applications, *J. King Saud Univ. Sci.* 33 (2021) 101560, <https://doi.org/10.1016/j.jksus.2021.101560>.
- [30] T. Patil, R. Gambhir, A.P. Vibhute, A.P. Tiwari, Gold nanoparticles: synthesis methods, functionalization and biological applications, *J. Cluster Sci.* 34 (2023) 705–725, <https://doi.org/10.1007/s10876-022-02287-6>.
- [31] M. Das, K.H. Shim, S.S.A. An, D.K. Yi, Review on gold nanoparticles and their applications, *Toxicol. Environ. Health Sci.* 3 (2011) 193–205, <https://doi.org/10.1007/s13530-011-0109-y>.
- [32] C. Louis, O. Pluchery, *Gold Nanoparticles for Physics, Chemistry and Biology*, IMPERIAL COLLEGE PRESS, 2012, <https://doi.org/10.1142/p815>.
- [33] A.I. Usman, A. Abdul Aziz, O. Abu Noqta, Application of green synthesis of gold nanoparticles: a review, *J. Teknol.* 81 (2018), <https://doi.org/10.11113/jt.v81.111409>.
- [34] M.-C. Daniel, D. Astruc, *Gold nanoparticles: assembly, supramolecular chemistry, quantum-size-related properties, and applications toward biology, catalysis, and nanotechnology*, *Chem. Rev.* 104 (2004) 293–346.
- [35] Gold Nanoparticles: Properties and Applications, (n.d.). <https://www.sigmaldrich.com/HU/en/technical-documents/technical-article/materials-science-and-engineering/biosensors-and-imaging/gold-nanoparticles#ref> (accessed May 3, 2024).
- [36] M.E. Ali, S. Mustafa, U. Hashim, Y.B. Che Man, K.L. Foo, Nanobioprobe for the determination of Pork Adulteration in Burger Formulations, *J. Nanomater.* 2012 (2012) 1–7, <https://doi.org/10.1155/2012/832387>.

- [37] G. Liu, M. Lu, X. Huang, T. Li, D. Xu, Application of gold-nanoparticle colorimetric sensing to rapid food safety Screening, Sensors 18 (2018) 4166, <https://doi.org/10.3390/s18124166>.
- [38] F. Tian, F. Bonnier, A. Casey, A.E. Shanahan, H.J. Byrne, Surface enhanced Raman scattering with gold nanoparticles: effect of particle shape, Anal. Methods 6 (2014) 9116–9123, <https://doi.org/10.1039/C4AY02112F>.
- [39] D. Huang, F. Liao, S. Molesa, D. Redinger, V. Subramanian, Plastic-compatible low resistance printable gold nanoparticle conductors for flexible electronics, J. Electrochem. Soc. 150 (2003) G412, <https://doi.org/10.1149/1.1582466>.
- [40] M.M. Ghobashy, S.A. Alkhursani, H.A. Alqahtani, T.K. El-damhougy, M. Madani, Gold nanoparticles in microelectronics advancements and biomedical applications, Mater. Sci. Eng. B 301 (2024) 117191, <https://doi.org/10.1016/j.mseb.2024.117191>.
- [41] H. Assad, I. Fatma, P.K. Sharma, E. Berdimurodov, A. Kumar, A. Kumar, Gold nanoparticles in electronic and photonic applications, in: Gold Nanoparticles, Nanomater. Nanocomposites, Elsevier, 2025, pp. 415–448, <https://doi.org/10.1016/B978-0-443-15897-1.00005-4>.
- [42] D.A. Giljohann, D.S. Seferos, W.L. Daniel, M.D. Massich, P.C. Patel, C.A. Mirkin, Gold nanoparticles for biology and medicine, Angew. Chem. Int. Ed. 49 (2010) 3280–3294, <https://doi.org/10.1002/anie.200904359>.
- [43] S.A. Akintelu, B. Yao, A.S. Folorunso, Bioremediation and pharmacological applications of gold nanoparticles synthesized from plant materials, Heliyon 7 (2021) e06591, <https://doi.org/10.1016/j.heliyon.2021.e06591>.
- [44] L. Dykman, B. Khlebtsov, N. Khlebtsov, Drug delivery using gold nanoparticles, Adv. Drug Deliv. Rev. 216 (2025) 115481, <https://doi.org/10.1016/j.addr.2024.115481>.
- [45] S.D. Brown, P. Nativo, J.-A. Smith, D. Stirling, P.R. Edwards, B. Venugopal, D. J. Flint, J.A. Plumb, D. Graham, N.J. Wheate, Gold nanoparticles for the improved anticancer drug delivery of the active component of Oxaliplatin, J. Am. Chem. Soc. 132 (2010) 4678–4684, <https://doi.org/10.1021/ja908117a>.
- [46] A. Jahangiri-Manesh, M. Mousazadeh, S. Taji, A. Bahmani, A. Zarepour, A. Zarrafi, E. Sharifi, M. Azimzadeh, Gold nanorods for drug and gene delivery: an overview of recent advancements, Pharmaceutics 14 (2022) 664, <https://doi.org/10.3390/pharmaceutics14030664>.
- [47] D.T. Thompson, Using gold nanoparticles for catalysis, Nano Today 2 (2007) 40–43, [https://doi.org/10.1016/S1748-0132\(07\)70116-0](https://doi.org/10.1016/S1748-0132(07)70116-0).
- [48] B. Hvolbæk, T.V.W. Janssens, B.S. Clausen, H. Falsig, C.H. Christensen, J. K. Nørskov, Catalytic activity of Au nanoparticles, Nano Today 2 (2007) 14–18, [https://doi.org/10.1016/S1748-0132\(07\)70113-5](https://doi.org/10.1016/S1748-0132(07)70113-5).
- [49] Z. Ali Sandhu, U. Farwa, M. Danish, M. Asam Raza, H. Ashraf, M. Hamayun, M. Elahi, A. Manzoor, S. Toor, A.G. Al-Shehmi, Gold nanoparticles as a promising catalyst for efficient oxygen reduction in fuel cells: Perils and prospects, Inorg. Chem. Commun. 160 (2024) 111961, <https://doi.org/10.1016/j.inoche.2023.111961>.
- [50] D. Mandal, A. Kumar, N.T. Patil, Gold catalysis in organic synthesis: fifteen years of research in India, Proc. Indian Natl. Sci. Acad. 88 (2022) 501–527, <https://doi.org/10.1007/s43538-022-00106-0>.
- [51] T. Stuchinskaya, M. Moreno, M.J. Cook, D.R. Edwards, D.A. Russell, Targeted photodynamic therapy of breast cancer cells using antibody-phthalocyanine-gold nanoparticle conjugates, Photochem. Photobiol. Sci. 10 (2011) 822–831, <https://doi.org/10.1039/c1pp05014a>.
- [52] P. Kesharwani, R. Ma, L. Sang, M. Fatima, A. Sheikh, M.A.S. Abourehab, N. Gupta, Z.-S. Chen, Y. Zhou, Gold nanoparticles and gold nanorods in the landscape of cancer therapy, Mol. Cancer 22 (2023) 98, <https://doi.org/10.1186/s12943-023-01798-8>.
- [53] A. Hossain, M.T. Rayhan, M.H. Mobarak, M.I.H. Rimon, N. Hossain, S. Islam, S.M. A. Al Kafi, Advances and significances of gold nanoparticles in cancer treatment: a comprehensive review, Results, Chem 8 (2024) 101559, <https://doi.org/10.1016/j.rechem.2024.101559>.
- [54] G. Peng, U. Tisch, O. Adams, M. Hakim, N. Shehada, Y.Y. Broza, S. Billan, R. Abdah-Bortnyak, A. Kuten, H. Haick, Diagnosing lung cancer in exhaled breath using gold nanoparticles, Nat. Nanotechnol. 4 (2009) 669–673, <https://doi.org/10.1038/nano.2009.235>.
- [55] C.A. Mirkin, The Polyvalent gold nanoparticle Conjugate—materials synthesis, Biodiagnostics, and intracellular gene Regulation, MRS Bull. 35 (2010) 532–539, <https://doi.org/10.1557/mrs2010.602>.
- [56] R. Wilson, The use of gold nanoparticles in diagnostics and detection, Chem. Soc. Rev. 37 (2008) 2028, <https://doi.org/10.1039/b712179m>.
- [57] J. Khan, Y. Rasmi, K.K. Kirboğa, A. Ali, M. Rudrapal, R.R. Patekar, Development of gold nanoparticle-based biosensors for COVID-19 diagnosis, Beni-Suef Univ. J. Basic Appl. Sci. 11 (2022) 111, <https://doi.org/10.1186/s43088-022-00293-1>.
- [58] J. Ma, Y. Liu, P.F. Gao, H.Y. Zou, C.Z. Huang, Precision improvement in dark-field microscopy imaging by using gold nanoparticles as an internal reference: a combined theoretical and experimental study, Nanoscale 8 (2016) 8729–8736, <https://doi.org/10.1039/C5NR08837B>.
- [59] S.D. Perrault, W.C.W. Chan, In vivo assembly of nanoparticle components to improve targeted cancer imaging, Proc. Natl. Acad. Sci. 107 (2010) 11194–11199, <https://doi.org/10.1073/pnas.1001367107>.
- [60] D. Luo, X. Wang, C. Burda, J.P. Basilion, Recent development of gold nanoparticles as contrast agents for cancer diagnosis, Cancers (Basel) 13 (2021) 1825, <https://doi.org/10.3390/cancers13081825>.
- [61] T.E. Pylaev, E.K. Volkova, V.I. Kochubey, V.A. Bogatyrev, N.G. Khlebtsov, DNA detection assay based on fluorescence quenching of rhodamine B by gold nanoparticles: the optical mechanisms, J. Quant. Spectrosc. Radiat. Transf. 131 (2013) 34–42, <https://doi.org/10.1016/j.jqsrt.2013.04.026>.
- [62] C. Daruich De Souza, B. Ribeiro Nogueira, M.E.C.M. Rostelato, Review of the methodologies used in the synthesis gold nanoparticles by chemical reduction, J. Alloys Compd. 798 (2019) 714–740, <https://doi.org/10.1016/j.jallcom.2019.05.153>.
- [63] J. Cao, T. Sun, K.T.V. Grattan, Gold nanorod-based localized surface plasmon resonance biosensors: a review, Sensors Actuators B Chem. 195 (2014) 332–351, <https://doi.org/10.1016/j.snb.2014.01.056>.
- [64] T.B. Huff, L. Tong, Y. Zhao, M.N. Hansen, J.-X. Cheng, A. Wei, Hyperthermic effects of gold nanorods on tumor cells, Nanomedicine 2 (2007) 125–132, <https://doi.org/10.2217/17435889.2.1.125>.
- [65] X. Huang, I.H. El-Sayed, W. Qian, M.A. El-Sayed, Cancer cell imaging and photothermal therapy in the near-infrared region by using gold nanorods, J. Am. Chem. Soc. 128 (2006) 2115–2120, <https://doi.org/10.1021/ja057254a>.
- [66] J.M. Stern, J. Stanfield, Y. Lotan, S. Park, J.-T. Hsieh, J.A. Cadeddu, Efficacy of laser-Activated gold nanoshells in ablating prostate cancer cells in vitro, J. Endourol. 21 (2007) 939–943, <https://doi.org/10.1089/end.2007.0437>.
- [67] P.K. Jain, K.S. Lee, I.H. El-Sayed, M.A. El-Sayed, Calculated absorption and scattering properties of gold nanoparticles of different size, shape, and composition: applications in biological imaging and biomedicine, J. Phys. Chem. B 110 (2006) 7238–7248, <https://doi.org/10.1021/jp0571700>.
- [68] N.A. Byzova, A.V. Zherdev, B.N. Khlebtsov, A.M. Burov, N.G. Khlebtsov, B. B. Dzantiev, Advantages of highly spherical gold nanoparticles as labels for lateral flow immunoassay, Sensors 20 (2020) 3608, <https://doi.org/10.3390/s20123608>.
- [69] M.S. Alam, S.F.U. Farhad, N.I. Tanvir, M.N.A. Bitu, M. Moniruzzaman, M. Hakim, M.A.A. Shaikh, Spherical and rod-shaped gold nanoparticles for surface enhanced Raman spectroscopy, in: 2022 4th Int. Conf. Sustain. Technol. Ind. 4.0, IEEE, 2022, pp. 1–4, <https://doi.org/10.1109/STI56238.2022.10103260>.
- [70] S. Pp, I. V, S. T, Gold nanoshells: a ray of hope in cancer diagnosis and treatment, Nucl. Med. Biomed. Imaging 2 (2017), <https://doi.org/10.15761/NMBI.1000122>.
- [71] C.G. Khoury, T. Vo-Dinh, Gold nanostars for surface-enhanced Raman scattering: synthesis, characterization and optimization, J. Phys. Chem. C 112 (2008) 18849–18859, <https://doi.org/10.1021/jp8054747>.
- [72] S.M. van de Looij, E.R. Hebel, M. Viola, M. Hembury, S. Oliveira, T. Vermonden, Gold nanoclusters: imaging, therapy, and Theranostic roles in biomedical applications, Bioconjug. Chem. 33 (2022) 4–23, <https://doi.org/10.1021/acs.bioconjchem.1c00475>.
- [73] K.S. Siddiqi, A. Husen, Recent advances in plant-mediated engineered gold nanoparticles and their application in biological system, J. Trace Elem. Med. Biol. 40 (2017) 10–23, <https://doi.org/10.1016/j.jtemb.2016.11.012>.
- [74] P. Zhao, N. Li, D. Astruc, State of the art in gold nanoparticle synthesis, Coord. Chem. Rev. 257 (2013) 638–665, <https://doi.org/10.1016/j.ccr.2012.09.002>.
- [75] C. Dhand, N. Dwivedi, X.J. Loh, A.N. Jie Ying, N.K. Verma, R.W. Beuerman, R. Lakshminarayanan, S. Ramakrishna, Methods and strategies for the synthesis of diverse nanoparticles and their applications: a comprehensive overview, RSC Adv. 5 (2015) 105003–105037, <https://doi.org/10.1039/C5RA19388E>.
- [76] X. Hu, Y. Zhang, T. Ding, J. Liu, H. Zhao, Multifunctional gold nanoparticles: a novel nanomaterial for various medical applications and biological activities, Front. Bioeng. Biotechnol. 8 (2020), <https://doi.org/10.3389/fbioe.2020.00990>.
- [77] K.P. Tyas, P. Maratussolihah, S. Rahmadianti, G.C.S. Girsang, A.B.D. Nandiyanto, Comparison of gold nanoparticle (AuNP) synthesis method, Arab. J. Chem. Environ. Res. 8 (2021) 436–454.
- [78] P.B. Santhosh, J. Genova, H. Chamati, Green synthesis of gold nanoparticles: an eco-friendly approach, Chemistry (Easton). 4 (2022) 345–369, <https://doi.org/10.3390/chemistry4020026>.
- [79] I. Ielo, G. Rando, F. Giacobello, S. Sfameli, A. Castellano, M. Galletta, D. Drommi, G. Rosace, M.R. Plutino, Synthesis, chemical–physical characterization, and biomedical applications of functional gold nanoparticles: a review, Molecules 26 (2021) 5823, <https://doi.org/10.3390/molecules26195823>.
- [80] H. Hassan, P. Sharma, M.R. Hasan, S. Singh, D. Thakur, J. Narang, Gold nanomaterials – the golden approach from synthesis to applications, Mater. Sci. Energy Technol. 5 (2022) 375–390, <https://doi.org/10.1016/j.mset.2022.09.004>.
- [81] M. Gul, M. Kashif, S. Muhammad, S. Azizi, H. Sun, Various methods of synthesis and applications of gold-based nanomaterials: a detailed review, Cryst. Growth Des. 25 (2025) 2227–2266, <https://doi.org/10.1021/acs.cgd.4c01687>.
- [82] Y.-C. Yeh, B. Creran, V.M. Rotello, Gold nanoparticles: preparation, properties, and applications in bionanotechnology, Nanoscale 4 (2012) 1871–1880, <https://doi.org/10.1039/CINR11188D>.
- [83] J. Georgeous, N. AlSawaftah, W.H. Abuwatfa, G.A. Husseini, Review of gold nanoparticles: synthesis, properties, shapes, cellular uptake, targeting, release mechanisms and applications in drug delivery and therapy, Pharmaceutics 16 (2024) 1332, <https://doi.org/10.3390/pharmaceutics16101332>.
- [84] E.O. Mikhailova, Gold nanoparticles: biosynthesis and potential of biomedical application, J. Funct. Biomater. 12 (2021) 70, <https://doi.org/10.3390/jfb12040070>.
- [85] H. Kalantar, R.J. Turner, Structural and antimicrobial properties of synthesized gold nanoparticles using biological and chemical approaches, Front. Chem. 12 (2024), <https://doi.org/10.3389/fchem.2024.1482102>.
- [86] Y. Ishida, I. Akita, T. Sumi, M. Matsubara, T. Yonezawa, Thiolate-protected gold nanoparticles via physical approach: Unusual structural and Photophysical characteristics, Sci. Rep. 6 (2016) 29928, <https://doi.org/10.1038/srep29928>.
- [87] Y. Hatakeyama, K. Onishi, K. Nishikawa, Effects of sputtering conditions on formation of gold nanoparticles in sputter deposition technique, RSC Adv. 1 (2011) 1815, <https://doi.org/10.1039/c1ra00688f>.

- [88] E. Vanecht, K. Binnemanns, J.W. Seo, L. Stappers, J. Fransaer, Growth of sputter-deposited gold nanoparticles in ionic liquids, *Phys. Chem. Chem. Phys.* 13 (2011) 13565, <https://doi.org/10.1039/c1cp20552h>.
- [89] X. Xu, G. Duan, Y. Li, G. Liu, J. Wang, H. Zhang, Z. Dai, W. Cai, Fabrication of gold nanoparticles by laser ablation in liquid and their application for simultaneous electrochemical detection of Cd 2+, Pb 2+, Cu 2+, Hg 2+, *ACS Appl. Mater. Interfaces* 6 (2014) 65–71, <https://doi.org/10.1021/am404816e>.
- [90] M. Vinod, R.S. Jayasree, K.G. Gopchandran, Synthesis of pure and biocompatible gold nanoparticles using laser ablation method for SERS and photothermal applications, *Curr. Appl. Phys.* 17 (2017) 1430–1438, <https://doi.org/10.1016/j.cap.2017.08.004>.
- [91] C. Rehbock, V. Merk, L. Gamrad, R. Streubel, S. Barcikowski, Size control of laser-fabricated surfactant-free gold nanoparticles with highly diluted electrolytes and their subsequent bioconjugation, *Phys. Chem. Chem. Phys.* 15 (2013) 3057–3067, <https://doi.org/10.1039/C2CP42641B>.
- [92] V. Amendola, S. Polizzi, M. Meneghetti, Laser ablation synthesis of gold nanoparticles in organic solvents, *J. Phys. Chem. B* 110 (2006) 7232–7237, <https://doi.org/10.1021/jp0605092>.
- [93] S.I. Dolgaev, A.V. Simakin, V.V. Voronov, G.A. Shafeev, F. Bozon-Verduraz, Nanoparticles produced by laser ablation of solids in liquid environment, *Appl. Surf. Sci.* 186 (2002) 546–551, [https://doi.org/10.1016/S0169-4332\(01\)00634-1](https://doi.org/10.1016/S0169-4332(01)00634-1).
- [94] N. Tue Anh, D. Van Phu, N. Ngoc Duy, B. Duy Du, N. Quoc Hien, Synthesis of alginate stabilized gold nanoparticles by  $\gamma$ -irradiation with controllable size using different Au<sup>3+</sup> concentration and seed particles enlargement, *Radiat. Phys. Chem.* 79 (2010) 405–408, <https://doi.org/10.1016/j.radphyschem.2009.11.013>.
- [95] N.N. Duy, D.X. Du, D. Van Phu, L.A. Quoc, B.D. Du, N.Q. Hien, Synthesis of gold nanoparticles with seed enlargement size by  $\gamma$ -irradiation and investigation of antioxidant activity, *Colloids Surfaces A Physicochem. Eng. Asp.* 436 (2013) 633–638, <https://doi.org/10.1016/j.colsurfa.2013.07.038>.
- [96] N.Q. Hien, D. Van Phu, N.N. Duy, L.A. Quoc, Radiation synthesis and characterization of hyaluronan capped gold nanoparticles, *Carbohydr. Polym.* 89 (2012) 537–541, <https://doi.org/10.1016/j.carbpol.2012.03.041>.
- [97] K.D.N. Vo, C. Kowandy, L. Dupont, X. Coqueret, N.Q. Hien, Radiation synthesis of chitosan stabilized gold nanoparticles comparison between e- beam and  $\gamma$  irradiation, *Radiat. Phys. Chem.* 94 (2014) 84–87, <https://doi.org/10.1016/j.radphyschem.2013.04.015>.
- [98] J. Luo, W. Deng, F. Yang, Z. Wu, M. Huang, M. Gu, Gold nanoparticles decorated graphene oxide/nanocellulose paper for NIR laser-induced photothermal ablation of pathogenic bacteria, *Carbohydr. Polym.* 198 (2018) 206–214, <https://doi.org/10.1016/j.carbpol.2018.06.074>.
- [99] T.I. Shaheen, M.E. El-Naggar, J.S. Hussein, M. El-Bana, E. Emara, Z. El-Khayat, M. M.G. Fouda, H. Ebaid, A. Hebeish, Antidiabetic assessment; in vivo study of gold and core-shell silver-gold nanoparticles on streptozotocin-induced diabetic rats, *Biomed. Pharmacother.* 83 (2016) 865–875, <https://doi.org/10.1016/j.biopharm.2016.07.052>.
- [100] A.K. Augustine, V.P.N. Nampoori, M. Kailasnath, Rapid synthesize of gold nanoparticles by microwave irradiation method and its application as an optical limiting material, *Optik* 125 (2014) 6696–6699, <https://doi.org/10.1016/j.jleo.2014.08.075>.
- [101] M.A. Bhosale, D.R. Chenna, B.M. Bhanage, Ultrasound assisted synthesis of gold nanoparticles as an efficient catalyst for reduction of various Nitro compounds, *ChemistrySelect* 2 (2017) 1225–1231, <https://doi.org/10.1002/slct.201601851>.
- [102] M. Morita, T. Tachikawa, S. Seino, K. Tanaka, T. Majima, Controlled synthesis of gold nanoparticles on fluorescent Nanodiamond via electron-beam-induced reduction method for Dual-Modal optical and electron bioimaging, *ACS Appl. Nano Mater.* 1 (2018) 355–363, <https://doi.org/10.1021/acsnano.7b00213>.
- [103] S.R. Ahmed, J. Kim, V.T. Tran, T. Suzuki, S. Neethirajan, J. Lee, E.Y. Park, In situ self-assembly of gold nanoparticles on hydrophilic and hydrophobic substrates for influenza virus-sensing platform, *Sci. Rep.* 7 (2017) 44495, <https://doi.org/10.1038/srep44495>.
- [104] K.-S. Chen, T.-S. Hung, H.-M. Wu, J.-Y. Wu, M.-T. Lin, C.-K. Feng, Preparation of thermosensitive gold nanoparticles by plasma pretreatment and UV grafted polymerization, *Thin Solid Films* 518 (2010) 7557–7562, <https://doi.org/10.1016/j.tsf.2010.05.043>.
- [105] D. Debnath, S.H. Kim, K.E. Geckeler, The first solid-phase route to fabricate and size-tune gold nanoparticles at room temperature, *J. Mater. Chem.* 19 (2009) 8810, <https://doi.org/10.1039/b905260g>.
- [106] M.C. Barnes, D.-Y. Kim, N.M. Hwang, The mechanism of gold deposition by thermal evaporation, in: *Proc. Korea Assoc. Cryst. Growth Conf., the Korea Association of Crystal Growth, 2000*, pp. 127–142.
- [107] M.T. Nguyen, T. Yonezawa, Sputtering onto a liquid: interesting physical preparation method for multi-metall nanoparticles, *Sci. Technol. Adv. Mater.* 19 (2018) 883–898, <https://doi.org/10.1080/14686996.2018.1542926>.
- [108] H. Schreyer, R. Eckert, S. Immohr, J. de Bellis, M. Felderhoff, F. Schüth, Milling down to Nanometers: a general process for the direct dry synthesis of supported metal catalysts, *Angew. Chem. Int. Ed.* 58 (2019) 11262–11265, <https://doi.org/10.1002/anie.201903545>.
- [109] T. Ahmad, J. Iqbal, M.A. Bustam, M. Irfan, H.M. Anwaar Asghar, A critical review on phytosynthesis of gold nanoparticles: issues, challenges and future perspectives, *J. Clean. Prod.* 309 (2021) 127460, <https://doi.org/10.1016/j.jclepro.2021.127460>.
- [110] F. Correador, K. Maximova, M.-A. Estève, C. Villard, M. Roy, A. Al-Kattan, M. Sentis, M. Gingras, A. V Kabashin, D. Braguier, Gold nanoparticles prepared by laser ablation in aqueous biocompatible solutions: assessment of safety and biological identity for nanomedicine applications, *Int. J. Nanomedicine* (2014) 5415–5430.
- [111] W.J. Nie, Y.X. Zhang, H.H. Yu, R. Li, R.Y. He, N.N. Dong, J. Wang, R. Hübner, R. Böttger, S.Q. Zhou, H. Amekura, F. Chen, Plasmonic nanoparticles embedded in single crystals synthesized by gold ion implantation for enhanced optical nonlinearity and efficient Q-switched lasing, *Nanoscale* 10 (2018) 4228–4236, <https://doi.org/10.1039/C7NR07304F>.
- [112] M.C. Barnes, D.-Y. Kim, H.S. Ahn, C.O. Lee, N.M. Hwang, Deposition mechanism of gold by thermal evaporation: approach by charged cluster model, *J. Cryst. Growth* 213 (2000) 83–92, [https://doi.org/10.1016/S0022-0248\(00\)00359-6](https://doi.org/10.1016/S0022-0248(00)00359-6).
- [113] R. Herizchi, E. Abbasi, M. Milani, A. Akbarzadeh, Current methods for synthesis of gold nanoparticles, *Artif. Cells, Nanomedicine, Biotechnol.* 44 (2016) 596–602, <https://doi.org/10.3109/21691401.2014.971807>.
- [114] J. Turkevich, P.C. Stevenson, J. Hillier, A study of the nucleation and growth processes in the synthesis of colloidal gold, *Discuss. Faraday Soc.* 11 (1951) 55, <https://doi.org/10.1039/df9511100055>.
- [115] G. Frens, Controlled nucleation for the Regulation of the particle size in monodisperse gold Suspensions, *Nat. Phys. Sci. (Lond.)* 241 (1973) 20–22, <https://doi.org/10.1038/physci241020a0>.
- [116] K.C. Grabar, R.G. Freeman, M.B. Hommer, M.J. Natan, Preparation and characterization of Au colloid Monolayers, *Anal. Chem.* 67 (1995) 735–743, <https://doi.org/10.1021/ac00100a008>.
- [117] K.S. Mayya, V. Patil, M. Sastry, Lamellar multilayer gold cluster films deposited by the Langmuir–Blodgett technique, *Langmuir* 13 (1997) 2575–2577, <https://doi.org/10.1021/la962057y>.
- [118] J.J. Storhoff, R. Elghanian, R.C. Mucic, C.A. Mirkin, R.L. Letsinger, One-pot colorimetric Differentiation of Polynucleotides with single Base Imperfections using gold nanoparticle Probes, *J. Am. Chem. Soc.* 120 (1998) 1959–1964, <https://doi.org/10.1021/ja972332i>.
- [119] T. Yonezawa, T. Kunitake, Practical preparation of anionic mercapto ligand-stabilized gold nanoparticles and their immobilization, *Colloids Surfaces A Physicochem. Eng. Asp.* 149 (1999) 193–199, [https://doi.org/10.1016/S0927-7757\(98\)0309-4](https://doi.org/10.1016/S0927-7757(98)0309-4).
- [120] C.X. Zhang, Y. Zhang, X. Wang, Z.M. Tang, Z.H. Lu, Hyper-Rayleigh scattering of protein-modified gold nanoparticles, *Anal. Biochem.* 320 (2003) 136–140, [https://doi.org/10.1016/S0003-2697\(03\)00353-1](https://doi.org/10.1016/S0003-2697(03)00353-1).
- [121] E. Mine, A. Yamada, Y. Kobayashi, M. Konno, L.M. Liz-Marzán, Direct coating of gold nanoparticles with silica by a seeded polymerization technique, *J. Colloid Interface Sci.* 264 (2003) 385–390, [https://doi.org/10.1016/S0021-9797\(03\)0022-3](https://doi.org/10.1016/S0021-9797(03)0022-3).
- [122] O. Seitz, M.M. Chehim, E. Cabet-Deliry, S. Truong, N. Felidj, C. Perruchot, S. J. Greaves, J.F. Watts, Preparation and characterisation of gold nanoparticle assemblies on silanised glass plates, *Colloids Surfaces A Physicochem. Eng. Asp.* 218 (2003) 225–239, [https://doi.org/10.1016/S0927-7757\(02\)00594-0](https://doi.org/10.1016/S0927-7757(02)00594-0).
- [123] Y. Yang, J. Shi, H. Chen, S. Dai, Y. Liu, Enhanced off-resonance optical nonlinearities of Au@CdS core-shell nanoparticles embedded in BaTiO<sub>3</sub> thin films, *Chem. Phys. Lett.* 370 (2003) 1–6, [https://doi.org/10.1016/S0009-2614\(02\)01863-8](https://doi.org/10.1016/S0009-2614(02)01863-8).
- [124] H. Huang, X. Yang, Chitosan mediated assembly of gold nanoparticles multilayer, *Colloids Surfaces A Physicochem. Eng. Asp.* 226 (2003) 77–86, [https://doi.org/10.1016/S0927-7757\(03\)00382-0](https://doi.org/10.1016/S0927-7757(03)00382-0).
- [125] T. Akiyama, K. Inoue, Y. Kuwahara, N. Terasaki, Y. Niidome, S. Yamada, Particle-size effects on the photocurrent efficiency of nanostructured assemblies consisting of gold nanoparticles and a ruthenium complex–viologen linked thiol, *J. Electroanal. Chem.* 550–551 (2003) 303–307, [https://doi.org/10.1016/S0022-0728\(03\)00152-9](https://doi.org/10.1016/S0022-0728(03)00152-9).
- [126] I. Ojea-Jiménez, N.G. Bastús, V. Puntes, Influence of the sequence of the reagents addition in the citrate-mediated synthesis of gold nanoparticles, *J. Phys. Chem. C* 115 (2011) 15752–15757, <https://doi.org/10.1021/jp2017242>.
- [127] N.R. Nirala, P.S. Saxena, A. Srivastava, Colorimetric detection of cholesterol based on enzyme modified gold nanoparticles, *Spectrochim. Acta Part A Mol. Biomol. Spectrosc.* 190 (2018) 506–512, <https://doi.org/10.1016/j.saa.2017.09.058>.
- [128] K. Mintz, E. Waideley, Y. Zhou, Z. Peng, A.O. Al-Youbi, A.S. Bashammakh, M.S. El-Shahawi, R.M. Leblanc, Carbon dots and gold nanoparticles based immunoassay for detection of alpha-L-fucosidase, *Anal. Chim. Acta* 1041 (2018) 114–121, <https://doi.org/10.1016/j.aca.2018.08.055>.
- [129] D. Shi, F. Sheng, X. Zhang, G. Wang, Gold nanoparticle aggregation: colorimetric detection of the interactions between avidin and biotin, *Talanta* 185 (2018) 106–112, <https://doi.org/10.1016/j.talanta.2018.02.102>.
- [130] D. Sangamithirai, S. Munusamy, V. Narayanan, A. Stephen, A voltammetric biosensor based on poly(o-methoxyaniline)-gold nanocomposite modified electrode for the simultaneous determination of dopamine and folic acid, *Mater. Sci. Eng. C* 91 (2018) 512–523, <https://doi.org/10.1016/j.msec.2018.05.070>.
- [131] J. Li, Y. Jiao, Q. Liu, Z. Chen, The aptamer-thrombin-aptamer sandwich complex-bridged gold nanoparticle oligomers for high-precision profiling of thrombin by dark field microscopy, *Anal. Chim. Acta* 1028 (2018) 66–76, <https://doi.org/10.1016/j.aca.2018.04.043>.
- [132] N. Hanžić, A. Horvat, J. Bibić, K. Unfried, T. Jurkin, G. Dražić, I. Marijanović, N. Slade, M. Gotić, Syntheses of gold nanoparticles and their impact on the cell cycle in breast cancer cells subjected to megavoltage X-ray irradiation, *Mater. Sci. Eng. C* 91 (2018) 486–495, <https://doi.org/10.1016/j.msec.2018.05.066>.
- [133] L.M. Niu, Y. Liu, K.Q. Lian, L. Ma, W.J. Kang, Characterization of a sensitive biosensor based on unmodified DNA and gold nanoparticle composite and its application in diquat determination, *Arab. J. Chem.* 11 (2018) 655–661, <https://doi.org/10.1016/j.arabjc.2015.03.009>.

- [134] S. Uthaman, H.S. Kim, V. Revuri, J.-J. Min, Y. Lee, K.M. Huh, I.-K. Park, Green synthesis of bioactive polysaccharide-capped gold nanoparticles for lymph node CT imaging, *Carbohydr. Polym.* 181 (2018) 27–33, <https://doi.org/10.1016/j.carbpol.2017.10.042>.
- [135] B.B. Karakocak, J. Liang, P. Biswas, N. Ravi, Hyaluronate coating enhances the delivery and biocompatibility of gold nanoparticles, *Carbohydr. Polym.* 186 (2018) 243–251, <https://doi.org/10.1016/j.carbpol.2018.01.046>.
- [136] R. Panday, A.J. Poudel, X. Li, M. Adhikari, M.W. Ullah, G. Yang, Amphiphilic core-shell nanoparticles: synthesis, biophysical properties, and applications, *Colloids Surfaces B Biointerfaces* 172 (2018) 68–81, <https://doi.org/10.1016/j.colsurfb.2018.08.019>.
- [137] L. Hong, M. Lu, M.-P. Dinel, P. Blain, W. Peng, H. Gu, J.-F. Masson, Hybridization conditions of oligonucleotide-capped gold nanoparticles for SPR sensing of microRNA, *Biosens. Bioelectron.* 109 (2018) 230–236, <https://doi.org/10.1016/j.bios.2018.03.032>.
- [138] R.L. Karpel, M. da Silva Liberato, J.D. Campeiro, L. Bergeon, B. Szchowski, A. Butler, G. Marino, J.F. Cusick, L.C.G. de Oliveira, E.B. Oliveira, M.A. de Farias, R.V. Portugal, W.A. Alves, M.-C. Daniel, M.A.F. Hayashi, Design and characterization of crotamine-functionalized gold nanoparticles, *Colloids Surfaces B Biointerfaces* 163 (2018) 1–8, <https://doi.org/10.1016/j.colsurfb.2017.12.013>.
- [139] G.S. Perera, S.A. Athukorale, F. Perez, C.U. Pittman, D. Zhang, Facile displacement of citrate residues from gold nanoparticle surfaces, *J. Colloid Interface Sci.* 511 (2018) 335–343, <https://doi.org/10.1016/j.jcis.2017.10.014>.
- [140] B. Bartosewicz, K. Bujno, M. Liszewska, B. Budner, P. Bazarnik, T. Płociński, B. Jankiewicz, Effect of citrate substitution by various  $\alpha$ -hydroxycarboxylate anions on properties of gold nanoparticles synthesized by Turkevich method, *Colloids Surfaces A Physicochem. Eng. Asp.* 549 (2018) 25–33, <https://doi.org/10.1016/j.colsurfa.2018.03.073>.
- [141] J. Wang, S. Mao, H.-F. Li, J.-M. Lin, Multi-DNAzymes-functionalized gold nanoparticles for ultrasensitive chemiluminescence detection of thrombin on microchip, *Anal. Chim. Acta* 1027 (2018) 76–82, <https://doi.org/10.1016/j.aca.2018.04.028>.
- [142] J. Nebu, J.S. Anjali Devi, R.S. Aparna, B. Aswathy, G.M. Lekha, G. Sony, Fluorescence turn-on detection of fenitrothion using gold nanoparticle quenched fluorescein and its separation using superparamagnetic iron oxide nanoparticle, *Sensors Actuators B Chem.* 277 (2018) 271–280, <https://doi.org/10.1016/j.snb.2018.08.153>.
- [143] S. Thambiraj, S. Hema, D. Ravi Shankaran, Functionalized gold nanoparticles for drug delivery applications, *Mater. Today Proc.* 5 (2018) 16763–16773, <https://doi.org/10.1016/j.matpr.2018.06.030>.
- [144] F. Takahashi, N. Yamamoto, M. Todoriki, J. Jin, Sonochemical preparation of gold nanoparticles for sensitive colorimetric determination of nereistoxin insecticides in environmental samples, *Talanta* 188 (2018) 651–657, <https://doi.org/10.1016/j.talanta.2018.06.042>.
- [145] M. Wang, C. Sun, L. Wang, X. Ji, Y. Bai, T. Li, J. Li, Electrochemical detection of DNA immobilized on gold colloid particles modified self-assembled monolayer electrode with silver nanoparticle label, *J. Pharm. Biomed. Anal.* 33 (2003) 1117–1125, [https://doi.org/10.1016/S0731-7085\(03\)00411-4](https://doi.org/10.1016/S0731-7085(03)00411-4).
- [146] C.R. Raj, T. Okajima, T. Ohsaka, Gold nanoparticle arrays for the voltammetric sensing of dopamine, *J. Electroanal. Chem.* 543 (2003) 127–133, [https://doi.org/10.1016/S0022-0728\(02\)01481-X](https://doi.org/10.1016/S0022-0728(02)01481-X).
- [147] S. Aryal, R.B. K.C., N. Dharmaraj, N. Bhattacharai, C.H. Kim, H.Y. Kim, Spectroscopic identification of S Au interaction in cysteine capped gold nanoparticles, *Spectrochim. Acta Part A Mol. Biomol. Spectrosc.* 63 (2006) 160–163, <https://doi.org/10.1016/j.saa.2005.04.048>.
- [148] P. Kalimuthu, S.A. John, Studies on ligand exchange reaction of functionalized mercaptothiadiazole compounds onto citrate capped gold nanoparticles, *Mater. Chem. Phys.* 122 (2010) 380–385, <https://doi.org/10.1016/j.matchemphys.2010.03.009>.
- [149] L. Zhao, D. Jiang, Y. Cai, X. Ji, R. Xie, W. Yang, Tuning the size of gold nanoparticles in the citrate reduction by chloride ions, *Nanoscale* 4 (2012) 5071, <https://doi.org/10.1039/C2nr30957b>.
- [150] M. Kesik, F.E. Kanik, G. Hizalan, D. Kozaoglu, E.N. Esenturk, S. Timur, L. Toppare, A functional immobilization matrix based on a conducting polymer and functionalized gold nanoparticles: synthesis and its application as an amperometric glucose biosensor, *Polymer (Guildf.)*, 54 (2013) 4463–4471, <https://doi.org/10.1016/j.polymer.2013.06.050>.
- [151] M. Iqbal, G. Usanase, K. Oulmi, F. Aberkane, T. Bendaikha, H. Fessi, N. Zine, G. Agusti, E.-S. Errachid, A. Elaissari, Preparation of gold nanoparticles and determination of their particle sizes via different methods, *Mater. Res. Bull.* 79 (2016) 97–104, <https://doi.org/10.1016/j.materresbull.2015.12.026>.
- [152] A. Shajkumar, B. Nandan, S. Sanwaria, V. Albrecht, M. Libera, M.-H. Lee, G. Auffermann, M. Stamm, A. Horechy, Silica-supported Au@hollow-SiO<sub>2</sub> particles with outstanding catalytic activity prepared via block copolymer template approach, *J. Colloid Interface Sci.* 491 (2017) 246–254, <https://doi.org/10.1016/j.jcis.2016.12.051>.
- [153] A. Chaudhary, S. Garg, siRNA delivery using polyelectrolyte-gold nanocomplexes in neuronal cells for BACE1 gene silencing, *Mater. Sci. Eng. C* 80 (2017) 18–28, <https://doi.org/10.1016/j.msec.2017.05.101>.
- [154] Y. Wang, M. Wang, L. Han, Y. Zhao, A. Fan, Enhancement effect of p-iodophenol on gold nanoparticle-catalyzed chemiluminescence and its applications in detection of thiols and guanidine, *Talanta* 182 (2018) 523–528, <https://doi.org/10.1016/j.talanta.2018.01.093>.
- [155] M. Brust, M. Walker, D. Bethell, D.J. Schiff, R. Whyman, Synthesis of thiol-derivatised gold nanoparticles in a two-phase Liquid-Liquid system, *J. Chem. Soc., Chem. Commun.* (1994) 801–802, <https://doi.org/10.1039/C39940000801>.
- [156] Y.J. Kim, Y.S. Yang, S.-C. Ha, S.M. Cho, Y.S. Kim, H.Y. Kim, H. Yang, Y.T. Kim, Mixed-ligand nanoparticles of chlorobenzenemethanethiol and n-octanethiol as chemical sensors, *Sensors Actuators B Chem.* 106 (2005) 189–198, <https://doi.org/10.1016/j.snb.2004.05.056>.
- [157] Y.K. Du, J.Z. Xu, M. Shen, P. Yang, L. Jiang, Alkanethiol-stabilized decahedron of gold nanoparticles, *Colloids Surfaces A Physicochem. Eng. Asp.* 257–258 (2005) 535–537, <https://doi.org/10.1016/j.colsurfa.2004.10.044>.
- [158] S.R. Isaacs, E.C. Cutler, J.-S. Park, T.R. Lee, Y.-S. Shon, Synthesis of tetraoctylammonium-protected gold nanoparticles with improved stability, *Langmuir* 21 (2005) 5689–5692, <https://doi.org/10.1021/la050656b>.
- [159] X. Liu, M. Atwater, J. Wang, Q. Huo, Extinction coefficient of gold nanoparticles with different sizes and different capping ligands, *Colloids Surfaces B Biointerfaces* 58 (2007) 3–7, <https://doi.org/10.1016/j.colsurfb.2006.08.005>.
- [160] S. Praharaj, S. Panigrahi, S. Basu, S. Pande, S. Jana, S.K. Ghosh, T. Pal, Effect of bromide and chloride ions for the dissolution of colloidal gold, *J. Photochem. Photobiol. Chem.* 187 (2007) 196–201, <https://doi.org/10.1016/j.jphotochem.2006.10.019>.
- [161] L. Zhang, R. Yuan, Y. Choi, X. Li, Investigation of the electrochemical and electrocatalytic behavior of positively charged gold nanoparticle and l-cysteine film on an Au electrode, *Anal. Chim. Acta* 596 (2007) 99–105, <https://doi.org/10.1016/j.aca.2007.05.050>.
- [162] N.M. Vörös, R. Patákfalvi, J. Dékány, Alkythiol-functionalized gold nanoparticles for sensing organic vapours: the connection between the adsorption isotherm and the sensor resistance, *Colloids Surfaces A Physicochem. Eng. Asp.* 329 (2008) 205–210, <https://doi.org/10.1016/j.colsurfa.2008.07.011>.
- [163] S.W. Kang, J. Hong, J.H. Park, S.H. Mun, J.H. Kim, J. Cho, K. Char, Y.S. Kang, Nanocomposite membranes containing positively polarized gold nanoparticles for facilitated olefin transport, *J. Memb. Sci.* 321 (2008) 90–93, <https://doi.org/10.1016/j.memsci.2008.04.047>.
- [164] Y.-S. Shon, S. Chuc, P. Voundsi, Stability of tetraoctylammonium bromide-protected gold nanoparticles: effects of anion treatments, *Colloids Surfaces A Physicochem. Eng. Asp.* 352 (2009) 12–17, <https://doi.org/10.1016/j.colsurfa.2009.09.037>.
- [165] S.K. Ghosh, Spectroscopic evaluation of 4-(dimethylamino)pyridine versus citrate as stabilizing ligand for gold nanoparticles, *Colloids Surfaces A Physicochem. Eng. Asp.* 371 (2010) 98–103, <https://doi.org/10.1016/j.colsurfa.2010.09.010>.
- [166] C. Quintana, P. Atienzar, G. Budroni, L. Mora, L. Hernández, H. García, A. Corma, Development and characterization of fluorine thin oxide electrodes modified with high area porous thin films containing gold nanoparticles, *Thin Solid Films* 519 (2010) 487–493, <https://doi.org/10.1016/j.tsf.2010.07.126>.
- [167] Y.Q. Wang, W.S. Liang, A. Satti, K. Nikitin, Fabrication and microstructure of Cu<sub>2</sub>O nanocubes, *J. Cryst. Growth* 312 (2010) 1605–1609, <https://doi.org/10.1016/j.jcrysgro.2010.01.019>.
- [168] A. Kyrychenko, G.V. Karpushina, S.I. Bogatyrenko, A.P. Krysthal, A.O. Doroshenko, Preparation, structure, and a coarse-grained molecular dynamics model for dodecanethiol-stabilized gold nanoparticles, *Comput. Theor. Chem.* 977 (2011) 34–39, <https://doi.org/10.1016/j.comptc.2011.09.003>.
- [169] M. Brust, G.J. Gordillo, Electrocatalytic hydrogen redox chemistry on gold nanoparticles, *J. Am. Chem. Soc.* 134 (2012) 3318–3321, <https://doi.org/10.1021/ja2096514>.
- [170] Y. Kuroda, K. Fukumoto, K. Kuroda, Uniform and high dispersion of gold nanoparticles on imogolite nanotubes and assembly into morphologically controlled materials, *Appl. Clay Sci.* 55 (2012) 10–17, <https://doi.org/10.1016/j.clay.2011.07.004>.
- [171] R.P. Briñas, M. Maetani, J.J. Barchi, A survey of place-exchange reaction for the preparation of water-soluble gold nanoparticles, *J. Colloid Interface Sci.* 392 (2013) 415–421, <https://doi.org/10.1016/j.jcis.2012.06.042>.
- [172] J.M. Lee, Y.S. Youn, E.S. Lee, Development of light-driven gas-forming liposomes for efficient tumor treatment, *Int. J. Pharm.* 525 (2017) 218–225, <https://doi.org/10.1016/j.ijpharm.2017.04.046>.
- [173] G.A. Dicheilo, T. Fukuda, T. Maekawa, R.L.D. Whitby, S.V. Mikhalovsky, M. Alavijeh, A.S. Pannala, D.K. Sarker, Preparation of liposomes containing small gold nanoparticles using electrostatic interactions, *Eur. J. Pharm. Sci.* 105 (2017) 55–63, <https://doi.org/10.1016/j.ejps.2017.05.001>.
- [174] S. Tianimoghadam, A. Salabat, A microemulsion method for preparation of thiol-functionalized gold nanoparticles, *Particuology* 37 (2018) 33–36, <https://doi.org/10.1016/j.partic.2017.05.007>.
- [175] H. Razzaq, R. Qureshi, L. Cabo-Fernandez, D.J. Schiff, Synthesis of Au clusters-redox centre hybrids by diazonium chemistry employing double layer charged gold nanoparticles, *J. Electroanal. Chem.* 819 (2018) 9–15, <https://doi.org/10.1016/j.jelechem.2017.05.016>.
- [176] N.R. Jana, L. Gearheart, C.J. Murphy, Seeding growth for size control of 5–40 nm diameter gold nanoparticles, *Langmuir* 17 (2001) 6782–6786, <https://doi.org/10.1021/la0104323>.
- [177] P. He, X. Zhu, Phospholipid-assisted synthesis of size-controlled gold nanoparticles, *Mater. Res. Bull.* 42 (2007) 1310–1315, <https://doi.org/10.1016/j.materresbull.2006.10.014>.
- [178] J. Spadavecchia, S. Casale, S. Boujday, C.-M. Pradier, Bioconjugated gold nanorods to enhance the sensitivity of FT-SPR-based biosensors, *Colloids Surfaces B Biointerfaces* 100 (2012) 1–8, <https://doi.org/10.1016/j.colsurfb.2012.03.035>.
- [179] Z. Guo, Y. Wan, M. Wang, L. Xu, X. Lu, G. Yang, K. Fang, N. Gu, High-purity gold nanopyramids can be obtained by an electrolyte-assisted and functionalization-

- free separation route, *Colloids Surfaces A Physicochem. Eng. Asp.* 414 (2012) 492–497, <https://doi.org/10.1016/j.colsurfa.2012.07.034>.
- [180] G.P. Sahoo, D. Kumar Bhui, D. Das, A. Misra, Synthesis of anisotropic gold nanoparticles and their catalytic activities of breaking azo bond in Sudan-1, *J. Mol. Liq.* 198 (2014) 215–222, <https://doi.org/10.1016/j.molliq.2014.06.032>.
- [181] J. Meng, S. Qin, L. Zhang, L. Yang, Designing of a novel gold nanodumbbells SERS substrate for detection of prohibited colorants in drinks, *Appl. Surf. Sci.* 366 (2016) 181–186, <https://doi.org/10.1016/j.apsusc.2016.01.078>.
- [182] A. Pan, M. Zhong, H. Wu, Y. Peng, H. Xia, Q. Tang, Q. Huang, L. Wei, L. Xiao, C. Peng, Topical application of Keratinocyte growth factor conjugated gold nanoparticles accelerate wound healing, *Nanomed. Nanotechnol. Biol. Med.* 14 (2018) 1619–1628, <https://doi.org/10.1016/j.nano.2018.04.007>.
- [183] U.M. Nayef, I.M. Khudhair, Synthesis of gold nanoparticles chemically doped with porous silicon for organic vapor sensor by using photoluminescence, *Optik* 154 (2018) 398–404, <https://doi.org/10.1016/j.jilgeo.2017.10.061>.
- [184] S. Ahmed, S. Annu, S. Yudha S. Ikram, Biosynthesis of gold nanoparticles: a green approach, *J. Photochem. Photobiol. B Biol.* 161 (2016) 141–153, <https://doi.org/10.1016/j.jphotobiol.2016.04.034>.
- [185] K.X. Lee, K. Shameli, Y.P. Yew, S.-Y. Teow, H. Jahangirian, R. Rafiee-Moghaddam, T. Webster, Recent developments in the facile bio-synthesis of gold nanoparticles (AuNPs) and their biomedical applications, *Int. J. Nanomedicine* 15 (2020) 275–300, <https://doi.org/10.2147/IJN.S233789>.
- [186] K.B. Narayanan, N. Sakthivel, Green synthesis of biogenic metal nanoparticles by terrestrial and aquatic phototrophic and heterotrophic eukaryotes and biocompatible agents, *Adv. Colloid Interface Sci.* 169 (2011) 59–79, <https://doi.org/10.1016/j.cis.2011.08.004>.
- [187] V. Ramalingam, Multifunctionality of gold nanoparticles: Plausible and convincing properties, *Adv. Colloid Interface Sci.* 271 (2019) 101989, <https://doi.org/10.1016/j.cis.2019.101989>.
- [188] T. Dinh, Z. Dobo, H. Kovacs, Phytomining of noble metals – a review, *Chemosphere* 286 (2022) 131805, <https://doi.org/10.1016/j.chemosphere.2021.131805>.
- [189] C.W.N. Anderson, R.B. Stewart, F.N. Moreno, J.L. Gardea-torresdey, B. H. Robinson, J. a Meech, Gold phytomining . Novel developments in a plant-based mining system, *Proc. Gold 2003 Conf. New Ind. Appl. Gold* (2003) 35–45.
- [190] A.K. Saim, F.N. Kumah, M.N. Opong, Extracellular and intracellular synthesis of gold and silver nanoparticles by living plants: a review, *Nanotechnol. Environ. Eng.* 6 (2020) 1, <https://doi.org/10.1007/s41204-020-00095-9>.
- [191] S. Menon, R. S. K.S. V, A review on biogenic synthesis of gold nanoparticles, characterization, and its applications, *Resour. Technol.* 3 (2017) 516–527, <https://doi.org/10.1016/j.refit.2017.08.002>.
- [192] T.S. Santra, F.-G. (Kevin, Tseng, T.K. Barik, Biosynthesis of silver and gold nanoparticles for potential biomedical applications—a Brief review, *J. Nanopharmaceutics Drug Deliv.* 2 (2014) 249–265, <https://doi.org/10.1166/jnd.2014.1065>.
- [193] S. Mazdeh, H. Motamed, A. Khiavi, M. Mehrabi, Gold nanoparticle biosynthesis by *E. coli* and conjugation with Streptomycin and evaluation of its antibacterial effect, *Curr. Nanosci.* 10 (2014) 553–561, <https://doi.org/10.2174/157341370966131203231344>.
- [194] H. Motamed, S. Khademi Mazdeh, A. Akbarzadeh Khiavi, M.R. Mehrabi, Optimization of gold nanoparticle biosynthesis by *Escherichia coli* DH5 $\alpha$  and its conjugation with Gentamicin, *J. Nano Res.* 32 (2015) 93–105. <https://dx.doi.org/10.4028/www.scientific.net/JNanR.32.93>.
- [195] M. Gholami-Shabani, M. Shams-Ghafarokhi, Z. Gholami-Shabani, A. Akbarzadeh, G. Riazi, S. Ajdari, A. Amani, M. Razaghi-Abyaneh, Enzymatic synthesis of gold nanoparticles using sulfite reductase purified from *Escherichia coli*: a green eco-friendly approach, *Process Biochem* 50 (2015) 1076–1085, <https://doi.org/10.1016/j.procbio.2015.04.004>.
- [196] Abd El-Aleem, R. El-Shanshoury, El-Zeiny E. Ebeid, Sobhy E. Elsilk, Samia F. Mohamed, Mohamed E. Ebeid, Biogenic synthesis of gold nanoparticles by bacteria and Utilization of the chemical fabricated for diagnostic performance of viral Hepatitis C virus-NS4, *Lett. Appl. NanoBioScience* 9 (2020) 1395–1408, <https://doi.org/10.33263/LIANBS93.13951408>.
- [197] L. Karthik, G. Kumar, T. Keswani, A. Bhattacharyya, B.P. Reddy, K.V.B. Rao, Marine actinobacterial mediated gold nanoparticles synthesis and their antimicrobial activity, *Nanomed. Nanotechnol. Biol. Med.* 9 (2013) 951–960, <https://doi.org/10.1016/j.nano.2013.02.002>.
- [198] C. Ganesh Kumar, Y. Poornachandra, C. Chandrasekhar, Green synthesis of bacterial mediated anti-proliferative gold nanoparticles: inducing mitotic arrest (G2/M phase) and apoptosis (intrinsic pathway), *Nanoscale* 7 (2015) 18738–18750, <https://doi.org/10.1039/C5NR04577K>.
- [199] T. Shanmugasundaram, M. Radhakrishnan, V. Gopikrishnan, K. Kadirvelu, R. Balagurunathan, Biocompatible silver, gold and silver/gold alloy nanoparticles for enhanced cancer therapy: in vitro and in vivo perspectives, *Nanoscale* 9 (2017) 16773–16790, <https://doi.org/10.1039/C7NR04979J>.
- [200] P.K. Singh, S. Kundu, Biosynthesis of gold nanoparticles using bacteria, *Proc. Natl. Acad. Sci. India Sect. B Biol. Sci.* 84 (2014) 331–336, <https://doi.org/10.1007/s40011-013-0230-6>.
- [201] S. He, Z. Guo, Y. Zhang, S. Zhang, J. Wang, N. Gu, Biosynthesis of gold nanoparticles using the bacteria *Rhodopseudomonas capsulata*, *Mater. Lett.* 61 (2007) 3984–3987, <https://doi.org/10.1016/j.matlet.2007.01.018>.
- [202] A. Ahmad, S. Senapati, M.I. Khan, R. Kumar, R. Ramani, V. Srinivas, M. Sastry, Intracellular synthesis of gold nanoparticles by a novel alkalotolerant actinomycete, *Rhodococcus* species, *Nanotechnology* 14 (2003) 824–828, <https://doi.org/10.1088/0957-4484/14/7/323>.
- [203] Y. Nangia, N. Wangoo, S. Sharma, J.-S. Wu, V. Dravid, G.S. Shekhawat, C. Raman Suri, Facile biosynthesis of phosphate capped gold nanoparticles by a bacterial isolate *Stenotrophomonas maltophilia*, *Appl. Phys. Lett.* 94 (2009), <https://doi.org/10.1063/1.3141519>.
- [204] N. Sharma, A.K. Pinnaka, M. Raje, A. Fnu, M.S. Bhattacharyya, A.R. Choudhury, Exploitation of marine bacteria for production of gold nanoparticles, *Microb. Cell Fact.* 11 (2012) 86, <https://doi.org/10.1186/1475-2859-11-86>.
- [205] D.N. Correa-Llantén, S.A. Muñoz-Ibáñez, M.E. Castro, P.A. Muñoz, J.M. Blamey, Gold nanoparticles synthesized by *Geobacillus* sp. strain ID17 a thermophilic bacterium isolated from Deception Island, Antarctica, *Microb. Cell Fact.* 12 (2013) 75, <https://doi.org/10.1186/1475-2859-12-75>.
- [206] P. Singh, H. Singh, Y.J. Kim, R. Mathiyalagan, C. Wang, D.C. Yang, Extracellular synthesis of silver and gold nanoparticles by *Sporosarcina koreensis* DC4 and their biological applications, *Enzyme Microb. Technol.* 86 (2016) 75–83, <https://doi.org/10.1016/j.enzmictec.2016.02.005>.
- [207] J. Li, Q. Li, X. Ma, B. Tian, T. Li, J. Yu, S. Dai, Y. Weng, Y. Hua, Biosynthesis of gold nanoparticles by the extreme bacterium *Deinococcus radiodurans* and an evaluation of their antibacterial properties, *Int. J. Nanomedicine* 11 (2016) 5931–5944, <https://doi.org/10.2147/IJN.S119618>.
- [208] T. Kunoh, M. Takeda, S. Matsumoto, I. Suzuki, M. Takano, H. Kunoh, J. Takada, Green synthesis of gold nanoparticles coupled with Nucleic acid oxidation, *ACS Sustain. Chem. Eng.* 6 (2018) 364–373, <https://doi.org/10.1021/acssuschemeng.7b02610>.
- [209] N.Y. Nadaf, S.S. Kanase, Biosynthesis of gold nanoparticles by *Bacillus marisflavi* and its potential in catalytic dye degradation, *Arab. J. Chem.* 12 (2019) 4806–4814, <https://doi.org/10.1016/j.arabjc.2016.09.020>.
- [210] R. Shunmugam, S. Renukadevi Balusamy, V. Kumar, S. Menon, T. Lakshmi, H. Perumalsamy, Biosynthesis of gold nanoparticles using marine microbe (*Vibrio alginolyticus*) and its anticancer and antioxidant analysis, *J. King Saud Univ. Sci.* 33 (2021) 101260, <https://doi.org/10.1016/j.jksus.2020.101260>.
- [211] R. Qiu, W. Xiong, W. Hua, Y. He, X. Sun, M. Xing, L. Wang, A biosynthesized gold nanoparticle from *Staphylococcus aureus* – as a functional factor in muscle tissue engineering, *Appl. Mater. Today* 22 (2021) 100905, <https://doi.org/10.1016/j.apmt.2020.100905>.
- [212] N. Naimi-Shamel, P. Pourali, S. Dolatabadi, Green synthesis of gold nanoparticles using *Fusarium oxysporum* and antibacterial activity of its tetracycline conjugant, *J. Mycol. Med.* 29 (2019) 7–13, <https://doi.org/10.1016/j.mycmed.2019.01.005>.
- [213] P. Clarance, B. Luvankar, J. Sales, A. Khusro, P. Agastian, J.-C. Tack, M.M. Al Khulaifi, H.A. Al-Shwaiman, A.M. Elgorban, A. Syed, H.-J. Kim, Green synthesis and characterization of gold nanoparticles using endophytic fungi *Fusarium solani* and its in-vitro anticancer and biomedical applications, *Saudi J. Biol. Sci.* 27 (2020) 706–712, <https://doi.org/10.1016/j.sjbs.2019.12.026>.
- [214] M. Owais, A. Chauhan, Sherwani Tufail, M. Sajid, C.R. Suri, M. Owais, Fungus-mediated biological synthesis of gold nanoparticles: potential in detection of liver cancer, *Int. J. Nanomedicine* (2011) 2305, <https://doi.org/10.2147/IJN.S23195>.
- [215] T. Ahmad, I.A. Wani, N. Manzoor, J. Ahmed, A.M. Asiri, Biosynthesis, structural characterization and antimicrobial activity of gold and silver nanoparticles, *Colloids Surfaces B Biointerfaces* 107 (2013) 227–234, <https://doi.org/10.1016/j.colsurfb.2013.02.004>.
- [216] L. Du, L. Xian, J.-X. Feng, Rapid extra-/intracellular biosynthesis of gold nanoparticles by the fungus *Penicillium* sp., *J. Nanoparticle Res.* 13 (2011) 921–930, <https://doi.org/10.1007/s11051-010-0165-2>.
- [217] A. Mishra, S.K. Tripathy, R. Wahab, S.-H. Jeong, I. Hwang, Y.-B. Yang, Y.-S. Kim, H.-S. Shin, S.-I. Yun, Microbial synthesis of gold nanoparticles using the fungus *Penicillium brevicompactum* and their cytotoxic effects against mouse mayo blast cancer C2C12 cells, *Appl. Microbiol. Biotechnol.* 92 (2011) 617–630, <https://doi.org/10.1007/s00253-011-3556-0>.
- [218] M. Kumari, A. Mishra, S. Pandey, S.P. Singh, V. Chaudhry, M.K.R. Mudiam, S. Shukla, P. Kakkar, C.S. Nautilty, Physico-chemical condition optimization during biosynthesis lead to development of improved and Catalytically efficient gold nano particles, *Sci. Rep.* 6 (2016) 27575, <https://doi.org/10.1038/srep27575>.
- [219] M.M. Abd-Kareem, A.A. Zohri, Extracellular mycosynthesis of gold nanoparticles using *Trichoderma hamatum* : optimization, characterization and antimicrobial activity, *Lett. Appl. Microbiol.* 67 (2018) 465–475, <https://doi.org/10.1111/lam.13055>.
- [220] V.C. Verma, S.K. Singh, R. Solanki, S. Prakash, Biofabrication of anisotropic gold nanotriangles using extract of endophytic *Aspergillus clavatus* as a dual functional reductant and stabilizer, *Nanoscale Res. Lett.* 6 (2010) 16, <https://doi.org/10.1007/s11671-010-9743-6>.
- [221] E. Priyadarshini, N. Pradhan, L.B. Sukla, P.K. Panda, Controlled synthesis of gold nanoparticles using *Aspergillus terreus* IF0 and its antibacterial potential against Gram Negative pathogenic bacteria, *J. Nanotechnol.* 2014 (2014) 1–9, <https://doi.org/10.1155/2014/653198>.
- [222] M. Sastry, A. Ahmad, M.I. Khan, R. Kumar, Biosynthesis of metal nanoparticles using fungi and actinomycetes, *Curr. Sci.* (2003) 162–170.
- [223] S.K. Das, A.R. Das, A.K. Guha, Gold nanoparticles: microbial synthesis and application in water Hygiene management, *Langmuir* 25 (2009) 8192–8199, <https://doi.org/10.1021/la900585p>.
- [224] A. Bhargava, N. Jain, M.A. Khan, V. Pareek, R.V. Dilip, J. Panwar, Utilizing metal tolerance potential of soil fungus for efficient synthesis of gold nanoparticles with superior catalytic activity for degradation of rhodamine B, *J. Environ. Manage.* 183 (2016) 22–32, <https://doi.org/10.1016/j.jenvman.2016.08.021>.
- [225] N.N. Dhanasekar, G.R. Rahul, K.B. Narayanan, G. Raman, N. Sakthivel, Green chemistry approach for the synthesis of gold nanoparticles using the fungus

- Alternaria sp, J. Microbiol. Biotechnol. 25 (2015) 1129–1135, <https://doi.org/10.4014/jmb.1410.10036>.
- [226] T.H.A. Nguyen, V.-C. Nguyen, T.N.H. Phan, V.T. Le, Y. Vasseghian, M. A. Trubtysn, A.-T. Nguyen, T.P. Chau, V.-D. Doan, Novel biogenic silver and gold nanoparticles for multifunctional applications: green synthesis, catalytic and antibacterial activity, and colorimetric detection of Fe(III) ions, Chemosphere 287 (2022) 132271, <https://doi.org/10.1016/j.chemosphere.2021.132271>.
- [227] T. Ogi, N. Saitoh, T. Nomura, Y. Konishi, Room-temperature synthesis of gold nanoparticles and nanoplates using *Sewanella* algae cell extract, J. Nanoparticle Res. 12 (2010) 2531–2539.
- [228] A.K. Singh, R. Tiwari, V.K. Singh, P. Singh, S.R. Khadim, U. Singh, V. Srivastava, S.H. Hasan, R.K. Asthana, Green synthesis of gold nanoparticles from *Dunaliella salina*, its characterization and in vitro anticancer activity on breast cancer cell line, J. Drug Deliv. Sci. Technol. 51 (2019) 164–176, <https://doi.org/10.1016/j.jddst.2019.02.023>.
- [229] J. Venkatesan, P. Manivasagan, S.-K. Kim, A.V. Kirthi, S. Marimuthu, A. A. Rahuman, Marine algae-mediated synthesis of gold nanoparticles using a novel *Ecklonia cava*, Bioprocess Biosyst. Eng. 37 (2014) 1591–1597, <https://doi.org/10.1007/s00449-014-1131-7>.
- [230] C. Chellappandian, A. Ramkumar, P. Puja, R. Shammuganathan, A. Pugazhendhi, P. Kumar, Gold nanoparticles using red seaweed *Gracilaria verrucosa*: green synthesis, characterization and biocompatibility studies, Process Biochem. 80 (2019) 58–63.
- [231] A. Mishra, S.K. Tripathy, S.-I. Yun, Bio-synthesis of gold and silver nanoparticles from *Candida guilliermondii* and their antimicrobial effect against pathogenic bacteria, J. Nanosci. Nanotechnol. 11 (2011) 243–248, <https://doi.org/10.1166/jnn.2011.3265>.
- [232] X. Zhang, Y. Qu, W. Shen, J. Wang, H. Li, Z. Zhang, S. Li, J. Zhou, Biogenic synthesis of gold nanoparticles by yeast *Magnusiomyces ingens* LH-F1 for catalytic reduction of nitrophenols, Colloids Surfaces A Physicochem. Eng. Asp. 497 (2016) 280–285, <https://doi.org/10.1016/j.colsurfa.2016.02.033>.
- [233] M.I. Husseiny, M.A. El-Aziz, Y. Badr, M.A. Mahmoud, Biosynthesis of gold nanoparticles using *Pseudomonas aeruginosa*, Spectrochim. Acta Part A Mol. Biomol. Spectrosc. 67 (2007) 1003–1006, <https://doi.org/10.1016/j.saa.2006.09.028>.
- [234] B. Nair, T. Pradeep, Coalescence of nanoclusters and formation of Submicron Crystallites assisted by *Lactobacillus* strains, Cryst. Growth Des. 2 (2002) 293–298, <https://doi.org/10.1021/cg0255164>.
- [235] S. Brown, M. Sarikaya, E. Johnson, A genetic analysis of crystal growth 1 Edited by M. Gottesman, J. Mol. Biol. 299 (2000) 725–735, <https://doi.org/10.1006/jmbi.2000.3682>.
- [236] S. Prakash, N. Soni, Synthesis of gold nanoparticles by the fungus *Aspergillus Niger* and its efficacy against mosquito larvae, Reports Parasitol (2012) 1, <https://doi.org/10.2147/RIP.S29033>.
- [237] Z. Molnár, V. Bódai, G. Szakacs, B. Erdélyi, Z. Fogarassy, G. Sáfrán, T. Varga, Z. Kónya, E. Tóth-Szeles, R. Szűcs, I. Lagzi, Green synthesis of gold nanoparticles by thermophilic filamentous fungi, Sci. Rep. 8 (2018) 3943, <https://doi.org/10.1038/s41598-018-22112-3>.
- [238] L. Castro, M.L. Blázquez, J.A. Muñoz, F. González, A. Ballester, Biological synthesis of metallic nanoparticles using algae, IET Nanobiotechnol. 7 (2013) 109–116, <https://doi.org/10.1049/iet-nbt.2012.0041>.
- [239] M.H. Oueslati, L. Ben Tahar, A.H. Harrath, Synthesis of ultra-small gold nanoparticles by polyphenol extracted from *Salvia officinalis* and efficiency for catalytic reduction of p-nitrophenol and methylene blue, Green Chem. Lett. Rev. 13 (2020) 18–26, <https://doi.org/10.1080/17518253.2019.1711202>.
- [240] N.K.R. Bogireddy, U. Pal, L.M. Gomez, V. Agarwal, Size controlled green synthesis of gold nanoparticles using *Coffee arabica* seed extract and their catalytic performance in 4-nitrophenol reduction, RSC Adv. 8 (2018) 24819–24826, <https://doi.org/10.1039/C8RA04332A>.
- [241] S.S. Shankar, A. Ahmad, R. Pasricha, M. Sastry, Bioreduction of chloroaurate ions by geranium leaves and its endophytic fungus yields gold nanoparticles of different shapes, J. Mater. Chem. 13 (2003) 1822, <https://doi.org/10.1039/b303808b>.
- [242] S.S. Shankar, A. Rai, B. Ankamwar, A. Singh, A. Ahmad, M. Sastry, Biological synthesis of triangular gold nanoprisms, Nat. Mater. 3 (2004) 482–488, <https://doi.org/10.1038/nmat1152>.
- [243] S.S. Shankar, A. Rai, A. Ahmad, M. Sastry, Rapid synthesis of Au, Ag, and bimetallic Au core–Ag shell nanoparticles using *Neem* (*Azadirachta indica*) leaf broth, J. Colloid Interface Sci. 275 (2004) 496–502, <https://doi.org/10.1016/j.jcis.2004.03.003>.
- [244] B. Ankamwar, M. Chaudhary, M. Sastry, Gold nanotriangles biologically synthesized using Tamarind leaf extract and potential application in vapor sensing, Synth. React. Inorganic, Met. Nano-Metal Chem. 35 (2005) 19–26, <https://doi.org/10.1081/SIM-200047527>.
- [245] S.P. Chandran, M. Chaudhary, R. Pasricha, A. Ahmad, M. Sastry, Synthesis of gold nanotriangles and silver nanoparticles using *Aloe vera* plant extract, Biotechnol. Prog. 22 (2006) 577–583, <https://doi.org/10.1021/bp0501423>.
- [246] J. Huang, Q. Li, D. Sun, Y. Lu, Y. Su, X. Yang, H. Wang, Y. Wang, W. Shao, N. He, J. Hong, C. Chen, Biosynthesis of silver and gold nanoparticles by novel sundried *Cinnamomum camphora* leaf, Nanotechnology 18 (2007) 105104, <https://doi.org/10.1088/0957-4484/18/10/105104>.
- [247] K.B. Narayanan, N. Sakthivel, Coriander leaf mediated biosynthesis of gold nanoparticles, Mater. Lett. 62 (2008) 4588–4590, <https://doi.org/10.1016/j.matlet.2008.08.044>.
- [248] A.R. Vilchis-Nestor, V. Sánchez-Mendieta, M.A. Camacho-López, R.M. Gómez-Espinosa, M.A. Camacho-López, J.A. Arenas-Alatorre, Solventless synthesis and optical properties of Au and Ag nanoparticles using *Camellia sinensis* extract, Mater. Lett. 62 (2008) 3103–3105, <https://doi.org/10.1016/j.matlet.2008.01.138>.
- [249] N. Ramezani, Z. Ehsanfar, F. Shamsa, G. Amin, H.R. Shahverdi, H.R.M. Esfahani, A. Shamsaie, R.D. Bazaz, A.R. Shahverdi, Screening of medicinal plant methanol extracts for the synthesis of gold nanoparticles by their reducing potential, Zeitschrift Für Naturforsch. B 63 (2008) 903–908, <https://doi.org/10.1515/znb-2008-0715>.
- [250] Ž. Krpetić, G. Scarl, E. Caneva, G. Speranza, F. Porta, Gold nanoparticles prepared using Cape Aloe active components, Langmuir 25 (2009) 7217–7221, <https://doi.org/10.1021/la9009674>.
- [251] D. Raghunandan, S. Basavaraja, B. Mahesh, S. Balaji, S.Y. Manjunath, A. Venkataraman, Biosynthesis of stable Polyshaped gold nanoparticles from microwave-exposed aqueous extracellular anti-malignant Guava (*Psidium guajava*) leaf extract, NanoBiotechnology 5 (2009) 34–41, <https://doi.org/10.1007/s12030-009-9030-8>.
- [252] S.L. Smitha, D. Philip, K.G. Gopchandran, Green synthesis of gold nanoparticles using *Cinnamomum zeylanicum* leaf broth, Spectrochim. Acta Part A Mol. Biomol. Spectrosc. 74 (2009) 735–739, <https://doi.org/10.1016/j.saa.2009.08.007>.
- [253] J.Y. Song, H.-K. Jang, B.S. Kim, Biological synthesis of gold nanoparticles using *Magnolia kobus* and *Diopyros kaki* leaf extracts, Process Biochem 44 (2009) 1133–1138, <https://doi.org/10.1016/j.procbio.2009.06.005>.
- [254] J. Kasthuri, K. Kathiravan, N. Rajendiran, Phyllanthin-assisted biosynthesis of silver and gold nanoparticles: a novel biological approach, J. Nanoparticle Res. 11 (2009) 1075–1085, <https://doi.org/10.1007/s11051-008-9494-9>.
- [255] J. Kasthuri, S. Veerapandian, N. Rajendiran, Biological synthesis of silver and gold nanoparticles using apigenin as reducing agent, Colloids Surfaces B Biointerfaces 68 (2009) 55–60, <https://doi.org/10.1016/j.colsurfb.2008.09.021>.
- [256] K.B. Narayanan, N. Sakthivel, Phytosynthesis of gold nanoparticles using leaf extract of *Coleus amboinicus* Lour, Mater. Charact. 61 (2010) 1232–1238, <https://doi.org/10.1016/j.matchar.2010.08.003>.
- [257] R.K. Das, B.B. Borthakur, U. Bora, Green synthesis of gold nanoparticles using ethanolic leaf extract of *Centella asiatica*, Mater. Lett. 64 (2010) 1445–1447, <https://doi.org/10.1016/j.matlet.2010.03.051>.
- [258] N. Gupta, H.P. Singh, R.K. Sharma, Single-pot synthesis: plant mediated gold nanoparticles catalyzed reduction of methylene blue in presence of stannous chloride, Colloids Surfaces A Physicochem. Eng. Asp. 367 (2010) 102–107, <https://doi.org/10.1016/j.colsurfa.2010.06.022>.
- [259] B. Ankamwar, Biosynthesis of gold nanoparticles (Green-gold) using leaf extract of Terminalia Catappa, J. Chem. 7 (2010) 1334–1339, <https://doi.org/10.1155/2010/745120>.
- [260] A.N. Mishra, S. Bhaduria, M.S. Gaur, R. Pasricha, B.S. Kushwah, Synthesis of gold nanoparticles by leaves of Zero-Calorie Sweetener Herb (*Stevia rebaudiana*) and their Nanoscopic characterization by spectroscopy and microscopy, Int. J. Green Nanotechnol. Phys. Chem. 1 (2010) P118–P124, <https://doi.org/10.1080/19430871003684705>.
- [261] D. Philip, Rapid green synthesis of spherical gold nanoparticles using *Mangifera indica* leaf, Spectrochim. Acta Part A Mol. Biomol. Spectrosc. 77 (2010) 807–810, <https://doi.org/10.1016/j.saa.2010.08.008>.
- [262] S.P. Dubey, M. Lahtinen, H. Särkkä, M. Sillanpää, Bioprospective of *Sorbus aucuparia* leaf extract in development of silver and gold nanocolloids, Colloids Surfaces B Biointerfaces 80 (2010) 26–33, <https://doi.org/10.1016/j.colsurfb.2010.05.024>.
- [263] S.P. Dubey, M. Lahtinen, M. Sillanpää, Green synthesis and characterizations of silver and gold nanoparticles using leaf extract of *Rosa rugosa*, Colloids Surfaces A Physicochem. Eng. Asp. 364 (2010) 34–41, <https://doi.org/10.1016/j.colsurfa.2010.04.023>.
- [264] A.D. Dwivedi, K. Gopal, Plant-mediated biosynthesis of silver and gold nanoparticles, J. Biomed. Nanotechnol. 7 (2011) 163–164, <https://doi.org/10.1166/jbn.2011.1250>.
- [265] P. Kumar, P. Singh, K. Kumari, S. Mozumdar, R. Chandra, A green approach for the synthesis of gold nanotriangles using aqueous leaf extract of *Callistemon viminalis*, Mater. Lett. 65 (2011) 595–597, <https://doi.org/10.1016/j.matlet.2010.11.025>.
- [266] D. Philip, C. Unni, Extracellular biosynthesis of gold and silver nanoparticles using *Krishna tulsi* (*Ocimum sanctum*) leaf, Phys. E Low-Dimensional Syst. Nanostructures 43 (2011) 1318–1322, <https://doi.org/10.1016/j.physe.2010.10.006>.
- [267] D. Philip, C. Unni, S.A. Aromal, V.K. Vidhu, *Murraya koenigii* leaf-assisted rapid green synthesis of silver and gold nanoparticles, Spectrochim. Acta Part A Mol. Biomol. Spectrosc. 78 (2011) 899–904, <https://doi.org/10.1016/j.saa.2010.12.060>.
- [268] D.S. Sheny, J. Mathew, D. Philip, Phytosynthesis of Au, Ag and Au–Ag bimetallic nanoparticles using aqueous extract and dried leaf of *Anacardium occidentale*, Spectrochim. Acta Part A Mol. Biomol. Spectrosc. 79 (2011) 254–262, <https://doi.org/10.1016/j.saa.2011.02.051>.
- [269] D. Raju, U.J. Mehta, S. Hazra, Synthesis of gold nanoparticles by various leaf fractions of *Semecarpus anacardium* L. tree, Trees (Berl.) 25 (2011) 145–151, <https://doi.org/10.1007/s00468-010-0493-y>.
- [270] M.M.H. Khalil, E.H. Ismail, F. El-Magdoub, Biosynthesis of Au nanoparticles using olive leaf extract, Arab. J. Chem. 5 (2012) 431–437, <https://doi.org/10.1016/j.arabjc.2010.11.011>.
- [271] S. Konwar Boruah, C. Medhi, Okhil Kumar Medhi, P. Kumar Boruah, P. Sarma, Green synthesis of gold nanoparticles using *Camellia sinensis* and kinetics of the

- reaction, *Adv. Mater. Lett.* 3 (2012) 481–486, <https://doi.org/10.5185/amlett.2012.icnano.103>.
- [272] S. Mukherjee, V. B. S. Prashanthi, P.R. Bangal, B. Sreedhar, C.R. Patra, Potential therapeutic and diagnostic applications of one-step *in situ* biosynthesized gold nanoconjugates (2-in-1 system) in cancer treatment, *RSC Adv.* 3 (2013) 2318, <https://doi.org/10.1039/c2ra22299j>.
- [273] M. Jeyaraj, R. Arun, G. Sathishkumar, D. MubarakAli, M. Rajesh, G. Sivanandhan, G. Kapildev, M. Manickavasagam, N. Thajuddin, A. Ganapathi, An evidence on G2/M arrest, DNA damage and caspase mediated apoptotic effect of biosynthesized gold nanoparticles on human cervical carcinoma cells (HeLa), *Mater. Res. Bull.* 52 (2014) 15–24, <https://doi.org/10.1016/j.materresbull.2013.12.060>.
- [274] M. Klekotko, K. Matczyszyn, J. Siednienko, J. Olesiak-Banska, K. Pawlik, M. Samoc, Bio-mediated synthesis, characterization and cytotoxicity of gold nanoparticles, *Phys. Chem. Chem. Phys.* 17 (2015) 29014–29019, <https://doi.org/10.1039/C5CP01619C>.
- [275] S. Mukherjee, M. Dasari, S. Priyamvada, R. Kotcherlakota, V.S. Bollu, C.R. Patra, A green chemistry approach for the synthesis of gold nanoconjugates that induce the inhibition of cancer cell proliferation through induction of oxidative stress and their *in vivo* toxicity study, *J. Mater. Chem. B* 3 (2015) 3820–3830, <https://doi.org/10.1039/C5TB00244C>.
- [276] K. Tahir, S. Nazir, B. Li, A.U. Khan, Z.U.H. Khan, P.Y. Gong, S.U. Khan, A. Ahmad, Nerium oleander leaves extract mediated synthesis of gold nanoparticles and its antioxidant activity, *Mater. Lett.* 156 (2015) 198–201, <https://doi.org/10.1016/j.matlet.2015.05.062>.
- [277] B. Paul, B. Bhuyan, D.D. Purkayastha, S. Vadivel, S.S. Dhar, One-pot green synthesis of gold nanoparticles and studies of their anticoagulative and photocatalytic activities, *Mater. Lett.* 185 (2016) 143–147, <https://doi.org/10.1016/j.matlet.2016.08.121>.
- [278] S. Francis, S. Joseph, E.P. Koshy, B. Mathew, Synthesis and characterization of multifunctional gold and silver nanoparticles using leaf extract of *Naregamia alata* and their applications in the catalysis and control of mastitis, *New J. Chem.* 41 (2017) 14288–14298, <https://doi.org/10.1039/C7NJ02453C>.
- [279] P.P. Dutta, M. Bordoloi, K. Gogoi, S. Roy, B. Narzary, D.R. Bhattacharyya, P. K. Mohapatra, B. Mazumder, Antimalarial silver and gold nanoparticles: green synthesis, characterization and *in vitro* study, *Biomed. Pharmacother.* 91 (2017) 567–580, <https://doi.org/10.1016/j.biopha.2017.04.032>.
- [280] B. Sundararajan, B.D. Ranjitha Kumari, Novel synthesis of gold nanoparticles using *Artemisia vulgaris L.* leaf extract and their efficacy of larvicidal activity against dengue fever vector *Aedes aegypti L.*, *J. Trace Elem. Med. Biol.* 43 (2017) 187–196, <https://doi.org/10.1016/j.jtemb.2017.03.008>.
- [281] A. Chahardoli, N. Karimi, F. Sadeghi, A. Fattahi, Green approach for synthesis of gold nanoparticles from *Nigella arvensis* leaf extract and evaluation of their antibacterial, antioxidant, cytotoxicity and catalytic activities, *Artif. Cells, Nanomedicine, Biotechnol.* 46 (2018) 579–588, <https://doi.org/10.1080/21691401.2017.1332634>.
- [282] D. Baruah, M. Goswami, R.N.S. Yadav, A. Yadav, A.M. Das, Biogenic synthesis of gold nanoparticles and their application in photocatalytic degradation of toxic dyes, *J. Photochem. Photobiol. B* 186 (2018) 51–58, <https://doi.org/10.1016/j.jphotobiol.2018.07.002>.
- [283] N.U. Islam, K. Jalil, M. Shahid, A. Rauf, N. Muhammad, A. Khan, M.R. Shah, M. A. Khan, Green synthesis and biological activities of gold nanoparticles functionalized with *Salix alba*, *Arab. J. Chem.* 12 (2019) 2914–2925, <https://doi.org/10.1016/j.arabjc.2015.06.025>.
- [284] M. Khoshnamvand, S. Ashtiani, C. Huo, S.P. Saeb, J. Liu, Use of *Alcea rosea* leaf extract for biomimetic synthesis of gold nanoparticles with innate free radical scavenging and catalytic activities, *J. Mol. Struct.* 1179 (2019) 749–755, <https://doi.org/10.1016/j.molstruc.2018.11.079>.
- [285] N. Thangamani, N. Bhuvaneshwari, Green synthesis of gold nanoparticles using *Simarouba glauca* leaf extract and their biological activity of micro-organism, *Chem. Phys. Lett.* 732 (2019) 136587, <https://doi.org/10.1016/j.cplett.2019.07.015>.
- [286] S. Balasubramanian, S.M.J. Kala, T.L. Pushparaj, Biogenic synthesis of gold nanoparticles using *Jasminum auriculatum* leaf extract and their catalytic, antimicrobial and anticancer activities, *J. Drug Deliv. Sci. Technol.* 57 (2020) 101620, <https://doi.org/10.1016/j.jddst.2020.101620>.
- [287] O.M. El-Brady, M.S. Ayat, M.A. Shabrawy, P. Millet, Green synthesis of gold nanoparticles using Parsley leaves extract and their applications as an alternative catalytic, antioxidant, anticancer, and antibacterial agents, *Adv. Powder Technol.* 31 (2020) 4390–4400, <https://doi.org/10.1016/j.apert.2020.09.017>.
- [288] J. Chen, Y. Li, G. Fang, Z. Cao, Y. Shang, S. Alfarraj, S. Ali Alharbi, J. Li, S. Yang, X. Duan, Green synthesis, characterization, cytotoxicity, antioxidant, and anti-human ovarian cancer activities of *Curcumae kwangsiensis* leaf aqueous extract green-synthesized gold nanoparticles, *Arab. J. Chem.* 14 (2021) 103000, <https://doi.org/10.1016/j.arabjc.2021.103000>.
- [289] A. Rauf, T. Ahmad, A. Khan, Maryam, G. Uddin, B. Ahmad, Y.N. Mabkhot, S. Bawazeer, N. Riaz, B.K. Malikovna, Z.M. Almarhoon, A. Al-Harrasi, Green synthesis and biomedical applications of silver and gold nanoparticles functionalized with methanolic extract of *Mentha longifolia*, *Artif. Cells, Nanomedicine, Biotechnol.* 49 (2021) 194–203, <https://doi.org/10.1080/21691401.2021.1890099>.
- [290] A. Guliani, A. Kumari, A. Acharya, Green synthesis of gold nanoparticles using aqueous leaf extract of *Populus alba*: characterization, antibacterial and dye degradation activity, *Int. J. Environ. Sci. Technol.* 18 (2021) 4007–4018, <https://doi.org/10.1007/s13762-020-03065-5>.
- [291] B. Ankamwar, C. Damle, A. Ahmad, M. Sastry, Biosynthesis of gold and silver nanoparticles using *Embelica officinalis* fruit extract, their phase transfer and Transmetallation in an organic solution, *J. Nanosci. Nanotechnol.* 5 (2005) 1665–1671, <https://doi.org/10.1166/jnn.2005.184>.
- [292] G.S. Ghodake, N.G. Deshpande, Y.P. Lee, E.S. Jin, Pear fruit extract-assisted room-temperature biosynthesis of gold nanoplates, *Colloids Surfaces B Biointerfaces* 75 (2010) 584–589, <https://doi.org/10.1016/j.colsurfb.2009.09.040>.
- [293] S.P. Dubey, M. Lahtinen, M. Sillanpää, Tansy fruit mediated greener synthesis of silver and gold nanoparticles, *Process Biochem.* 45 (2010) 1065–1071, <https://doi.org/10.1016/j.procbio.2010.03.024>.
- [294] G. S. P.K. Jha, V. V. C.J.M.S.M. R, R. Jha, Cannonball fruit (*Couroupita guianensis*, Aubl.) extract mediated synthesis of gold nanoparticles and evaluation of its antioxidant activity, *J. Mol. Liq.* 215 (2016) 229–236, <https://doi.org/10.1016/j.molliq.2015.12.043>.
- [295] A. Sett, M. Gadewar, P. Sharma, M. Deka, U. Bora, Green synthesis of gold nanoparticles using aqueous extract of *Dillenia indica*, *Adv. Nat. Sci. Nanosci. Nanotechnol.* 7 (2016) 025005, <https://doi.org/10.1088/2043-6262/7/2/025005>.
- [296] M.P. Desai, G.M. Sangaokar, K.D. Pawar, Kokum fruit mediated biogenic gold nanoparticles with photoluminescent, photocatalytic and antioxidant activities, *Process Biochem.* 70 (2018) 188–197, <https://doi.org/10.1016/j.procbio.2018.03.027>.
- [297] P.S. Kumar, M.V. Jeyalatha, J. Malathi, S. Ignacimuthu, Anticancer effects of one-pot synthesized biogenic gold nanoparticles (Mc-AuNPs) against laryngeal carcinoma, *J. Drug Deliv. Sci. Technol.* 44 (2018) 118–128, <https://doi.org/10.1016/j.jddst.2017.12.008>.
- [298] Nr. Ms, S. J.P. Pp, Green synthesis and characterization of bioinspired silver, gold and platinum nanoparticles and evaluation of their synergistic antibacterial activity after combining with different classes of antibiotics, *Mater. Sci. Eng. C* 96 (2019) 693–707, <https://doi.org/10.1016/j.msec.2018.11.050>.
- [299] G.A. Filip, B. Moldovan, I. Baldea, D. Olteanu, R. Suharoschi, N. Decea, C. M. Cismaru, E. Gal, M. Cenariu, S. Clichici, L. David, UV-light mediated green synthesis of silver and gold nanoparticles using Cornelian cherry fruit extract and their comparative effects in experimental inflammation, *J. Photochem. Photobiol. B Biol.* 191 (2019) 26–37, <https://doi.org/10.1016/j.jphotobiol.2018.12.006>.
- [300] M.A. Mahdi, M.T. Mohammed, A.N. Jassim, Y.M. Taay, Green synthesis of gold NPs by using dragon fruit: toxicity and wound healing, *J. Phys. Conf. Ser.* 1853 (2021) 012039, <https://doi.org/10.1088/1742-6596/1853/1/012039>.
- [301] K. Ghule, A.V. Ghule, J.-Y. Liu, Y.-C. Ling, Microscale size triangular gold Prisms synthesized using Bengal Gram Beans (*Cicer arietinum L.*) extract and H<sub>4</sub>CU4·3H<sub>2</sub>O: a green biogenic approach, *J. Nanosci. Nanotechnol.* 6 (2006) 3746–3751, <https://doi.org/10.1166/jnn.2006.608>.
- [302] S. Arulkumar, M. Sabesan, Biosynthesis and characterization of gold nanoparticle using antiparkinsonian drug *Mucuna pruriens* plant extract, *Int. J. Res. Pharm. Sci.* 4 (2010) 417–420.
- [303] J.G. Nirmala, S. Akila, M.S.A.M. Nadar, R.T. Narendhirakannan, S. Chatterjee, Biosynthesized *Vitis vinifera* seed gold nanoparticles induce apoptotic cell death in A431 skin cancer cells, *RSC Adv.* 6 (2016) 82205–82218, <https://doi.org/10.1039/C6RA16310F>.
- [304] N. Verma, A green synthetic approach for size tunable nanoporous gold nanoparticles and its glucose sensing application, *Appl. Surf. Sci.* 462 (2018) 753–759, <https://doi.org/10.1016/j.apsusc.2018.08.175>.
- [305] S. Vimalraj, T. Ashokkumar, S. Saravanan, Biogenic gold nanoparticles synthesis mediated by *Mangifera indica* seed aqueous extracts exhibits antibacterial, anticancer and anti-angiogenic properties, *Biomed. Pharmacother.* 105 (2018) 440–448, <https://doi.org/10.1016/j.biopha.2018.05.151>.
- [306] K. Perveen, F.M. Husain, F.A. Qais, A. Khan, S. Razak, T. Afzar, P. Alam, A. M. Almajwal, M.M.A. Abulmeaty, Microwave-assisted rapid green synthesis of gold nanoparticles using seed extract of *Trachyspermum ammi*: ROS mediated Biofilm inhibition and anticancer activity, *Biomolecules* 11 (2021) 197, <https://doi.org/10.3390/biom1120197>.
- [307] U. Ullah, A. Rauf, E. El-Sharkawy, F.A. Khan, A. Khan, S.M. Buhkari, S. Bawazeer, Y.N. Mabkhot, B.K. Malikovna, G. Kazhybayeva, M.A. Sharifiati, M. Thiruvengadam, Green synthesis, *in vivo* and *in vitro* pharmacological studies of *Tamarindus indica* based gold nanoparticles, *Bioprocess Biosyst. Eng.* 44 (2021) 1185–1192, <https://doi.org/10.1007/s00449-020-02500-8>.
- [308] K. Leonard, B. Ahmad, H. Okamura, J. Kurawaki, In situ green synthesis of biocompatible ginseng capped gold nanoparticles with remarkable stability, *Colloids Surfaces B Biointerfaces* 82 (2011) 391–396, <https://doi.org/10.1016/j.colsurfb.2010.09.020>.
- [309] M. Dhayalan, M.I.J. Denison, M. Ayyar, N.N. Gandhi, K. Krishnan, B. Abdulhadi, Biogenic synthesis, characterization of gold and silver nanoparticles from *Coleus forskohlii* and their clinical importance, *J. Photochem. Photobiol. B Biol.* 183 (2018) 251–257, <https://doi.org/10.1016/j.jphotobiol.2018.04.042>.
- [310] C. Umamaheswari, A. Lakshmanan, N.S. Nagarajan, Green synthesis, characterization and catalytic degradation studies of gold nanoparticles against Congo red and methyl orange, *J. Photochem. Photobiol. B Biol.* 178 (2018) 33–39, <https://doi.org/10.1016/j.jphotobiol.2017.10.017>.
- [311] N.S. Al-Radadi, Facile one-step green synthesis of gold nanoparticles (AuNp) using licorice root extract: antimicrobial and anticancer study against HepG2 cell line, *Arab. J. Chem.* 14 (2021) 102956, <https://doi.org/10.1016/j.arabjc.2020.102956>.
- [312] A. Bankar, B. Joshi, A. Ravi Kumar, S. Zinjarde, Banana peel extract mediated synthesis of gold nanoparticles, *Colloids Surfaces B Biointerfaces* 80 (2010) 45–50, <https://doi.org/10.1016/j.colsurfb.2010.05.029>.

- [313] K. Xin Lee, K. Shamel, M. Miyake, N. Kuwano, N.B. Bt Ahmad Khairudin, S.E. Bt Mohamad, Y.P. Yew, Green synthesis of gold nanoparticles using aqueous extract of *Garcinia mangostana* fruit peels, *J. Nanomater.* 2016 (2016) 1–7, <https://doi.org/10.1155/2016/8489094>.
- [314] B.R. Gangapuram, R. Bandi, M. Alle, R. Dadigala, G.M. Kotu, V. Guttina, Microwave assisted rapid green synthesis of gold nanoparticles using *Annona squamosa* L peel extract for the efficient catalytic reduction of organic pollutants, *J. Mol. Struct. Molstruc.* 2018 (2018) 305–315, <https://doi.org/10.1016/j.molstruc.2018.05.004>.
- [315] M. Bahram, E. Mohammadzadeh, Green synthesis of gold nanoparticles with willow tree bark extract: a sensitive colourimetric sensor for cysteine detection, *Anal. Methods* 6 (2014) 6916–6924, <https://doi.org/10.1039/C4AY01362J>.
- [316] K. Jadhav, R. Hr, S. Deshpande, S. Jagwani, D. Dhamecha, S. Jalalpur, K. Subburayam, D. Baheti, Phytosynthesis of gold nanoparticles: characterization, biocompatibility, and evaluation of its osteoinductive potential for application in implant dentistry, *Mater. Sci. Eng. C* 93 (2018) 664–670, <https://doi.org/10.1016/j.msec.2018.08.028>.
- [317] E. Rodríguez-León, B.E. Rodríguez-Vázquez, A. Martínez-Higuera, C. Rodríguez-Beas, E. Larios-Rodríguez, R.E. Navarro, R. López-Espárza, R.A. Iñiguez-Palomares, Synthesis of gold nanoparticles using *Mimosa tenuiflora* extract, assessments of cytotoxicity, cellular uptake, and catalysis, *Nanoscale Res. Lett.* 14 (2019) 334, <https://doi.org/10.1186/s11671-019-3158-9>.
- [318] O.S. ElMitwalli, O.A. Barakat, R.M. Daoud, S. Akhtar, F.Z. Henari, Green synthesis of gold nanoparticles using cinnamon bark extract, characterization, and fluorescence activity in Au/eosin Y assemblies, *J. Nanoparticle Res.* 22 (2020) 309, <https://doi.org/10.1007/s11051-020-04983-8>.
- [319] M.O. Montes, A. Mayoral, F.L. Deepak, J.G. Parsons, M. Jose-Yacamán, J. R. Peralta-Videa, J.L. Gardea-Torresdey, Anisotropic gold nanoparticles and gold plates biosynthesis using alfalfa extracts, *J. Nanoparticle Res.* 13 (2011) 3113–3121, <https://doi.org/10.1007/s11051-011-0230-5>.
- [320] Y. Zeiri, P. Elia, R. Zach, S. Hazan, S. Kolusheva, Z. Porat, Green synthesis of gold nanoparticles using plant extracts as reducing agents, *Int. J. Nanomedicine* (2014) 4007, <https://doi.org/10.2147/IJN.S57343>.
- [321] S. Kalita, R. Kandimalla, K.K. Sharma, A.C. Kataki, M. Deka, J. Kotoky, Amoxicillin functionalized gold nanoparticles reverts MRSA resistance, *Mater. Sci. Eng. C* 61 (2016) 720–727, <https://doi.org/10.1016/j.msec.2015.12.078>.
- [322] L. Castro, M.L. Blázquez, F. González, J.A. Muñoz, A. Ballester, Extracellular biosynthesis of gold nanoparticles using sugar beet pulp, *Chem. Eng. J.* 164 (2010) 92–97, <https://doi.org/10.1016/j.cej.2010.08.034>.
- [323] L. Castro, M.L. Blázquez, J.A. Muñoz, F. González, C. García-Balboa, A. Ballester, Biosynthesis of gold nanowires using sugar beet pulp, *Process Biochem.* 46 (2011) 1076–1082, <https://doi.org/10.1016/j.procbio.2011.01.025>.
- [324] M. Noruzi, D. Zare, K. Khoshnevisan, D. Davoodi, Rapid green synthesis of gold nanoparticles using Rosa hybrida petal extract at room temperature, *Spectrochim. Acta Part A Mol. Biomol. Spectrosc.* 79 (2011) 1461–1465, <https://doi.org/10.1016/j.saa.2011.05.001>.
- [325] M. Venkatachalam, K. Govindaraju, A. Mohamed Sadiq, S. Tamiselvan, V. Ganesh Kumar, G. Singaravelu, Functionalization of gold nanoparticles as antidiabetic nanomaterial, *Spectrochim. Acta Part A Mol. Biomol. Spectrosc.* 116 (2013) 331–338, <https://doi.org/10.1016/j.saa.2013.07.038>.
- [326] P. Anbu, S.C. Gopinath, S. Jayanthi, Synthesis of gold nanoparticles using Platycodon grandiflorum extract and its antipathogenic activity under optimal conditions, *Nanomater. Nanotechnol.* 10 (2020) 184798042096169, <https://doi.org/10.1177/1847980420961697>.
- [327] A.K. Singh, M. Talat, D.P. Singh, O.N. Srivastava, Biosynthesis of gold and silver nanoparticles by natural precursor clove and their functionalization with amine group, *J. Nanoparticle Res.* 12 (2010) 1667–1675, <https://doi.org/10.1007/s11051-009-9835-3>.
- [328] S. Ahn, P. Singh, M. Jang, Y.-J. Kim, V. Castro-Aceituno, S.Y. Simu, Y.J. Kim, D.-C. Yang, Gold nanoflowers synthesized using *Acanthopanax cortex* extract inhibit inflammatory mediators in LPS-induced RAW264.7 macrophages via NF- $\kappa$ B and AP-1 pathways, *Colloids Surfaces B Biointerfaces* 162 (2018) 398–404, <https://doi.org/10.1016/j.colsurfb.2017.11.037>.
- [329] U.K. Parida, B.K. Bindhani, P. Nayak, Green synthesis and characterization of gold nanoparticles using onion extract, *World J. Nano Sci. Eng.* 1 (2011) 93–98, <https://doi.org/10.4236/wjnse.2011.14015>.
- [330] M.M. Rahaman Mollick, B. Bhowmick, D. Mondal, D. Maity, D. Rana, S.K. Dash, S. Chattopadhyay, S. Roy, J. Sarkar, K. Acharya, M. Chakraborty, D. Chattpadhyay, Anticancer (in vitro) and antimicrobial effect of gold nanoparticles synthesized using *Abelmoschus esculentus* (L.) pulp extract via a green route, *RSC Adv.* 4 (2014) 37838, <https://doi.org/10.1039/C4RA07285E>.
- [331] A. Ahmad, F. Syed, A. Shah, Z. Khan, K. Tahir, A.U. Khan, Q. Yuan, Silver and gold nanoparticles from *Sargentodoxa cuneata*: synthesis, characterization and antileishmanial activity, *RSC Adv.* 5 (2015) 73793–73806, <https://doi.org/10.1039/C5RA13206A>.
- [332] A. Ahmad, Y. Wei, F. Syed, M. Imran, Z.U.H. Khan, K. Tahir, A.U. Khan, M. Raza, Q. Khan, Q. Yuan, Size dependent catalytic activities of green synthesized gold nanoparticles and electro-catalytic oxidation of catechol on gold nanoparticles modified electrode, *RSC Adv.* 5 (2015) 99364–99377, <https://doi.org/10.1039/C5RA20096B>.
- [333] A.A. Kajani, A.-K. Bordbar, S.H. Zarkesh Esfahani, A. Razmjou, Gold nanoparticles as potent anticancer agent: green synthesis, characterization, and in vitro study, *RSC Adv.* 6 (2016) 63973–63983, <https://doi.org/10.1039/C6RA09050H>.
- [334] P. Roy, S.K. Saha, P. Gayen, P. Chowdhury, S.P. Sinha Babu, Exploration of antifilarial activity of gold nanoparticle against human and bovine filarial parasites: a nanomedicinal mechanistic approach, *Colloids Surfaces B Biointerfaces* 161 (2018) 236–243, <https://doi.org/10.1016/j.colsurfb.2017.10.057>.
- [335] P. Deepak, R. Sowmiya, G. Balasubramani, D. Aiswarya, D. Arul, M.P.D. Josebin, P. Perumal, Mosquito-larvicidal efficacy of gold nanoparticles synthesized from the seaweed, *Turbinaria ornata* (Turner) J.Agardh 1848, Part. Sci. Technol. 36 (2018) 974–980, <https://doi.org/10.1080/02726351.2017.1331286>.
- [336] Y. Rao, G.K. Inwati, M. Singh, Green synthesis of capped gold nanoparticles and their effect on Gram-Positive and Gram-Negative bacteria, *Futur. Sci. OA* 3 (2017), <https://doi.org/10.4155/fsoa-2017-0062>.
- [337] T. Dinh, H. Kovács, Z. Dobó, The fate of noble metals and rare earth elements during pelletized biomass combustion, *Heliyon* 10 (2024) e23546, <https://doi.org/10.1016/j.heliyon.2023.e23546>.
- [338] T. Dinh, H. Kovács, Z. Dobó, The formation of gold in woody biomass combustion ashes, *Heliyon* 10 (2024) e32425, <https://doi.org/10.1016/j.heliyon.2024.e32425>.
- [339] T. Dinh, Z. Dobó, H. Kovács, Phytomining of rare earth elements – a review, *Chemosphere* 297 (2022) 134259, <https://doi.org/10.1016/j.chemosphere.2022.134259>.
- [340] R.G. Haverkamp, A.T. Marshall, D. van Agterveld, Pick your carats: nanoparticles of gold–silver–copper alloy produced in vivo, *J. Nanoparticle Res.* 9 (2007) 697–700, <https://doi.org/10.1007/s11051-006-9198-y>.
- [341] P. Dang, C. Li, A mini-review of phytomining, *Int. J. Environ. Sci. Technol.* 19 (2022) 12825–12838, <https://doi.org/10.1007/s13762-021-03807-z>.
- [342] P.J. Babu, A. Tirkey, Green synthesis of gold nanoparticles and their biomedical and healthcare applications, in: *Nanotechnol. Hum. Heal.*, Elsevier, 2023, pp. 191–229, <https://doi.org/10.1016/B978-0-323-90750-7.00006-5>.
- [343] C.W.N. Anderson, S.M. Bhatti, J. Gardea-Torresdey, J. Parsons, In vivo effect of copper and silver on synthesis of gold nanoparticles inside living plants, *ACS Sustain. Chem. Eng.* 1 (2013) 640–648, <https://doi.org/10.1021/sc400011s>.
- [344] A.T. Marshall, R.G. Haverkamp, C.E. Davies, J.G. Parsons, J.L. Gardea-Torresdey, D. van Agterveld, Accumulation of gold nanoparticles in *Brassica juncea*, *Int. J. Phytoremediation* 9 (2007) 197–206, <https://doi.org/10.1080/15226510701376026>.
- [345] I.R. Beattie, R.G. Haverkamp, Silver and gold nanoparticles in plants: sites for the reduction to metal, *Metalomics* 3 (2011) 628, <https://doi.org/10.1039/c1mt00044f>.
- [346] R. Bali, A.T. Harris, Biogenic synthesis of Au nanoparticles using vascular plants, *Ind. Eng. Chem. Res.* 49 (2010) 12762–12772, <https://doi.org/10.1021/ie101600m>.
- [347] J.L. Gardea-Torresdey, J.G. Parsons, E. Gomez, J. Peralta-Videa, H.E. Troiani, P. Santiago, M.J. Yacaman, Formation and growth of Au nanoparticles inside live alfalfa plants, *Nano Lett.* 2 (2002) 397–401.
- [348] D.L. Starnes, A. Jain, S.V. Saha, In planta engineering of gold nanoparticles of desirable geometries by Modulating growth conditions: an environment-friendly approach, *Environ. Sci. Technol.* 44 (2010) 7110–7115, <https://doi.org/10.1021/es101136q>.
- [349] A.F. Taylor, E.L. Rylott, C.W.N. Anderson, N.C. Bruce, Investigating the toxicity, uptake, nanoparticle formation and genetic response of plants to gold, *PLoS One* 9 (2014) e93793, <https://doi.org/10.1371/journal.pone.0093793>.
- [350] A. Jain, B. Sinil, D.L. Starnes, R. Sanagala, S. Krishnamurthy, S.V. Saha, Role of Fe-responsive genes in bioreduction and transport of ionic gold to roots of *Arabidopsis thaliana* during synthesis of gold nanoparticles, *Plant Physiol. Biochem.* 84 (2014) 189–196, <https://doi.org/10.1016/j.plaphy.2014.09.013>.
- [351] J.L. Gardea-Torresdey, E. Rodriguez, J.G. Parsons, J.R. Peralta-Videa, G. Meitzner, G. Cruz-Jimenez, Use of ICP and XAS to determine the enhancement of gold phytoextraction by *Chilopsis linearis* using thiocyanate as a complexing agent, *Anal. Bioanal. Chem.* 382 (2005) 347–352, <https://doi.org/10.1007/s0016-004-2966-6>.
- [352] E. Rodriguez, J.G. Parsons, J.R. Peralta-Videa, G. Cruz-Jimenez, J. Romero-Gonzalez, B.E. Sanchez-Salcido, G.B. Saupe, M. Duarte-Gardea, J.L. Gardea-Torresdey, Potential of *Chilopsis linearis* for gold phytomining: using Xas to determine gold reduction and nanoparticle formation within plant tissues, *Int. J. Phytoremediation* 9 (2007) 133–147, <https://doi.org/10.1080/15226510701232807>.
- [353] N.C. Sharma, S.V. Saha, S. Nath, J.G. Parsons, J.L. Gardea-Torresdey, T. Pal, Synthesis of plant-mediated gold nanoparticles and catalytic role of biomatrix-embedded nanomaterials, *Environ. Sci. Technol.* 41 (2007) 5137–5142, <https://doi.org/10.1021/es062929a>.
- [354] X. Luo, J. Cao, Discovery of nano-sized gold particles in natural plant tissues, *Environ. Chem. Lett.* 16 (2018) 1441–1448, <https://doi.org/10.1007/s10311-018-0749-0>.
- [355] D. Raju, U.J. Mehta, A. Ahmad, Phytosynthesis of intracellular and extracellular gold nanoparticles by living peanut plant (*Araucaria hypogaea* L.), *Biotechnol. Appl. Biochem.* 59 (2012) 471–478, <https://doi.org/10.1002/bab.1049>.
- [356] O.C. Mukhorro, W.D. Roos, M. Jaffer, J.J. Bolton, M.J. Stillman, D.R. Beukes, E. Antunes, Very green Photosynthesis of gold nanoparticles by a living aquatic plant: Photoreduction of Au III by the seaweed *Ulva armoricana*, *Chem. Eur. J.* 24 (2018) 1657–1666, <https://doi.org/10.1002/chem.201704448>.